NEW MEASUREMENTS OF FLUORESCENCE YIELDS

by

W. GELLETLY, B.Sc.

Thesis submitted

For the Degree of

DOCTOR OF PHILOSOPHY

University of Edinburgh,

September, 1965.

The measurements described in Chapter 7 of this thesis were made in collaboration with Mr. F. Shaikh of the Department of Natural Philosophy. The present author is solely responsible for the description, interpretation, and discussion of these results given here.

C O N T E N T S

C O N T E N T S (Contd.)

C O N T E N T S (Contd.)

C O N T E N T S (Contd.)

CHAPTER I

THE AUGER EFFECT AND OTHER RADIATIONLESS TRANSITIONS

The Auger Effect

When an atom has been ionised in an inner electron shell, leaving a vacancy in such a shell, it may reorganise in one of two ways. Within 10^{-14} to 10^{-17} seconds the vacancy is filled by an electron transition from a higher shell. The excess energy, equal to the difference in ionisation energy of the two levels concerned in the transition, may then be emitted in the form of electromagnetic radiation, the characteristic X-radiation. Alternatively, this energy may be communicated to another electron in a higher shell, which is ejected from the atom. The latter process of reorganisation, without the emission of electromagnetic radiation, is known as the Auger effect in recognition of the work of Pierre Auger (1925). He was the first to interpret, in terms of this process, the paired photoelectron and Auger electron tracks observed in a Wilson cloud chamber containing an inert gas exposed to a beam of ionising X-rays.

The importance of the role of the Auger effect in determining intensity relations in X-ray spectra is self evident. But before about 1950 the fundamental nature of the Auger effect does not appear to have been generally appreciated. This neglect stemmed from the fact that whereas X-ray line spectra had been studied in great

detail, low energy β-ray spectroscopy was relatively crude and undeveloped. Many well known texts on Atomic Physics did not even discuss the Auger effect, and those that did gave it only a cursory treatment. After 1950, β-ray spectrometers were developed rapidly until today instruments are available (Graham et al. (1960)) whose resolution is in some cases limited only by the natural widths of the atomic energy levels themselves. It has thus become possible to examine low energy electron spectra in detail.

At the same time, interest in the Auger effect has been stimulated by the increasing study of processes involving the interaction of the nucleus and the surrounding orbital electrons, such as electron capture and the internal conversion of nuclear gamma radiation. Since such processes lead to the inner shell ionisation of the atom they are always accompanied by the emission of X-rays or Auger electrons. Hence measurements of the resulting X-ray or Auger electron intensities may yield a great deal of information concerning the initial nuclear processes of internal conversion and electron capture.

In this connection the most important measure of the effect of Auger transitions is the fluorescence yield of an atomic shell, which is defined for the atomic P shell as

$$\omega_P = \frac{\text{Number of P X-rays emitted}}{\text{Number of primary P vacancies}} \qquad (1.1)$$

The corresponding Auger yield a_P is defined as

$$a_P = (1 - \omega_P) = \frac{\text{Number of P Auger electrons emitted}}{\text{Number of primary P vacancies}} \quad (1.2)$$

Burhop (1952) and Bergström and Nördling (1965) have both discussed at length the many types of measurement in nuclear spectroscopy which require an accurate quantitative knowledge of fluorescence and Auger yields, and of Auger transition probabilities, for the derivation of nuclear quantities associated with internal conversion and electron capture. One example of this is the measurement of the relative probability of K electron capture and positron emission. Bouchez (1952) gives this ratio as

$$\frac{P_{Kc}}{P_{\beta+}} = \frac{\text{K X-ray Intensity}}{\omega_K \cdot \beta+ \text{ Intensity}} = \frac{\text{K Auger Intensity}}{a_K \cdot \beta+ \text{ Intensity}} \quad (1.3)$$

where P_{Kc} and $P_{\beta+}$ are the probabilities of K electron capture and positron emission, respectively. Bouchez reviews the various methods which can be used to determine the intensity of the K X-rays or K Auger electrons relative to the intensity of positron emission.

A second instance of the need for measurements of fluorescence yields is the measurement of the ratio of L- to K-electron capture, a quantity of importance in the theory of electron capture. The relative probabilities of the two processes are related to the relative intensities of K- and L- X-rays (I_K and I_L respectively) by the relation

$$\frac{I_L}{I_K} = \frac{P_{LC}}{P_{KC}} + f_{KL} \frac{\omega_L}{\omega_K} \qquad (1.4)$$

where P_{LC} and P_{KC} are the probabilities of L- and K-electron capture respectively, and f_{KL} is the fraction of emitted K X-rays which leave a vacancy in the L shell. Robinson and Fink (1960) have discussed the experimental measurements, and how the quantity P_{LC}/P_{KC} is related to the Q value of the electron capture process.

A knowledge of the Auger effect and of Auger transition probabilities is also extremely useful in β-ray spectroscopy. Since Auger electron lines appear in many conversion electron spectra, and the energies of several KLL Auger electron lines are known with great accuracy, they can be used as low energy calibration lines. Many low energy conversion lines overlap with Auger electron lines and the assignment of these conversion lines is greatly simplified by a knowledge of Auger transition probabilities.

Yet another simple application requiring a knowledge of fluorescence yields is the determination of the K conversion coefficient (α_K) of a gamma transition from the measurement with a scintillation counter of the intensity (I_{KX}) of the K X-rays following internal conversion, and the intensity (I_γ) of the gamma ray. The conversion coefficient can then be written as

$$\alpha_K = \frac{I_{KX}}{I_\gamma} \cdot \frac{\varepsilon_\gamma}{\varepsilon_{KX}\omega_K} \qquad (1.5),$$

where ε_γ and ε_{KX} are the efficiencies of detection of the gamma ray and of the K X-rays in the counter.

A knowledge of the Auger effect, and of the fluorescence and Auger yields which characterise it, is obviously important in the experimental situations described above. It is important in many other experimental situations as well.

The Nature of the Auger Effect

Up to this point we have ignored the question of the true nature of the Auger effect. Originally it was regarded as a process in which a real X-ray photon is emitted and then reabsorbed by another electron of the same atom. The probability of such an "internal photoelectric effect" might be expected to be larger than the probability of the same effect in a neighbouring atom, due to the concentration of the radiation field about the point of production of the X-ray. The alternative approach was to regard it as being due to the direct interaction of the two electrons concerned. From the standpoint of the nonrelativistic theory both approaches are equally valid. In the relativistic theory on the other hand no method exists for handling the perturbation problem as being due to the direct interaction of the two electrons.

Taylor and Mott (1933) and later Tralli and Goertzel (1951) examined this point. As in the similar case of the internal conversion of nuclear gamma radiation, they were able to show that the rate of emission of electromagnetic radiation is virtually unaffected by the

radiationless transitions occurring at the same time. Again Auger electron transitions are observed which are forbidden by the selection rules for the corresponding radiative transitions. In the light of this it is very difficult to maintain the interpretation of the Auger effect as the "internal conversion" of real X-ray photons. Almost all of the ejected electrons are now regarded as being due to the direct interaction of the two electrons, with a small fraction, of order 1/137, arising from the internal absorption of X-rays.

Other Radiationless Transitions

Radiationless transitions similar to the Auger effect play an important part in other domains of atomic and molecular physics. They are not our proper concern, but they are mentioned briefly here to complete our picture of the role of radiationless transitions in the atom.

Radiationless transitions have been observed in the outer levels of the atom, where the phenomenon is known as auto-ionisation. It is commonly observed in cases where an excited state has an energy greater than the ionisation energy. An example of this, cited by Burhop (1952), occurs in the arc spectrum of Copper. The normal configuration of the outer electron of Copper is $3d^{10}4s$. The 4s electron is the first in a new shell and it is not very strongly bound as a result. The excited state

$3d^9 4s5s$ also exists, and has an excitation energy greater than the energy required to remove the electron from the normal atom. A radiationless process is possible in which the 5s electron makes the transition to 3d to complete the shell and the 4s electron is ejected from the atom. The possibility of such a transition greatly reduces the half life of such a $3d^9 4s5s$ state and increases its breadth. Observations of emission lines having such a state as an initial state reveal that they are unusually wide. Burhop (1952) discusses the effects of this type of transition in both atomic and molecular spectra.

After a vacancy in an inner electron shell has been filled by an Auger transition the atom is left doubly ionised. The two vacancies which are left may also be filled by Auger transitions. Since the probability of radiationless transitions increases for higher shells, it is obvious that this process may continue and a vacancy cascade may occur, leaving the atom multiply ionised. The consequences of this vacancy cascade are important in molecular physics, and in the production of radiation damage in solids. Krause et al. (1964) have observed Neon ions with five units of positive charge following ionisation of the K shell by K X-rays. The interpretation of such an experiment is complicated by the presence of other mechanisms, such as 'nuclear shake-off', which also produce ionisation, but the effect of vacancy cascades has been observed many times. A short discussion of this effect

is given by Snell (1965).

The Auger effect is also important in the mesic atom. μ^- - mesic atoms are produced when a slow μ^--meson is captured by an atom into an orbit of high total and azimuthal quantum number. The μ^--meson then makes a series of transitions down to a level of low total quantum number before it is eventually captured by the nucleus. Each transition from a higher to a lower level is accompanied by the emission of characteristic X-rays or Auger electrons. Since the energy levels in the mesic atom are more widely spaced than in the normal atom, both the X-rays and the Auger electrons are of higher energy than normal. The fluorescence yield of an orbit in a mesic atom is as important a constant as in the normal electronic atom, and many measurements of K- and L-shell fluorescence yields in mesic atoms have been made. These measurements and the results obtained from them have been fully described by Stearns (1957).

References - Chapter 1

(1) Auger, P. (1925), J. Phys. Rad. 6, 205.

(2) Bergström, I. and Nördling, C. (1965), "The Auger Effect" in α-, β-, and γ-ray spectroscopy, Edited by K. Siegbahn. (North-Holland Publishing Co., Amsterdam).

(3) Bouchez, R. (1952), Physica 18, 1171.

(4) Burhop, E.S. (1952), The Auger Effect and Other Radiationless Transitions (Cambridge University Press, Cambridge).

(5) Graham, R.L., Ewan, G.T. and Geiger, J.S. (1960), Nuc. Inst. & Methods 9, 245.

(6) Krause, M.O., Vestal, M.L. and Johnston, W.H. (1964), Phys. Rev. 133A, 385.

(7) Robinson, B.L. and Fink, R.W. (1960), Rev. Mod. Phys. 32, 1171.

(8) Snell, A.H. (1965), 'The Atomic and Molecular Consequences of Decay' in α-, β- and γ-ray Spectroscopy, Edited by K. Siegbahn (North-Holland Publishing Co., Amsterdam).

(9) Stearns, M.B. (1957), Prog. in Nucl. Phys. 6, 108.

(10) Taylor, H.M. and Mott, N.F. (1933), Proc. Roy. Soc. A138, 665.

(11) Tralli, N. and Goertzel, G.A. (1951), Phys. Rev. 83, 399.

CHAPTER 2

PREVIOUS WORK ON FLUORESCENCE YIELDS

Elements of the Theory

Before going on to discuss the measurements and calculations of Fluorescence yields which have been made up to the present, a short account of the elements of the theory of the Auger effect will be given.

The theory of the Auger effect was first given by Wentzel (1927). In the nonrelativistic approximation which Wentzel used, one assumes that the two electrons initially move in the field due to the nucleus and the average effect of the other atomic electrons. The Auger electron is then ejected because of the perturbation caused by the electrostatic interaction between the two electrons. This perturbation causes a transition in which the Auger electron is ejected into the continuum and the other electron goes to a discrete state of lower energy.

Let $\psi_i(r_1)$ and $\phi_i(r_2)$ be the Schrödinger wave functions describing the two electrons in the initial state, where the atom has a vacancy in an inner electron shell. Let $\psi_f(r_1)$ be the final state wave function of one of the electrons in the originally unoccupied level, and $\phi_f(r_2)$ be the final state wave function of the electron ejected from the atom into the continuum. Then the probability W_a of the Auger transition is

$$W_a = \frac{2\pi}{\hbar}\left|\iint \phi_f^*(r_2)\psi_f^*(r_1)\, V_{12}\, \psi_i(r_1)\,\phi_i(r_2)\, dt_1\, dt_2\right|^2 \qquad (2.1)$$

where the perturbation energy $V_{12} = \dfrac{e^2}{4\pi\varepsilon_0 |r_1 - r_2|}$.

Now in any two electron problem we must take account of the Pauli Principle. Because the two electrons are indistinguishable, the first electron (r_1) may be the Auger electron and the second (r_2) may make the transition to fill the initial vacancy. This is correctly accounted for if we replace the product of wave functions in (2.1) by antisymmetric combinations of the single electron wave functions. Thus $\psi_i(r_1)\phi_i(r_2)$ would become

$$\frac{1}{\sqrt{2}}\left(\psi_i(r_1)\,\phi_i(r_2) - \psi_i(r_2)\phi(r_1)\right)$$

Hence the corrected Auger transition probability becomes

$$W_a = \frac{2\pi}{\hbar}\left|\iint\left[\phi_f^*(r_2)\psi_f^*(r_1)\, V_{12}\, \psi_i(r_1)\phi_i(r_2) - \phi_f^*(r_1)\psi_f(r_2)\, V_{12}\, \psi_i(r_2)\phi_i(r_1)\right] dt_1\, dt_2\right|^2 \qquad (2.2)$$

This represents the combination of the two experimentally indistinguishable transitions.

In the relativistic case there is no mechanism for dealing with the process as a direct interaction of the two electrons. Here the Auger transition must be induced by the interaction of the Auger electron in its initial bound state with the electromagnetic radiation emitted

when the other electron fills the hole. The vector and scalar potentials of the radiation field A_{if} and Θ_{if} are related to the wave functions of the electron filling the vacancy by the equations,

$$A_{if} = -e\int\left[\frac{(\exp. iK|t_1 - t_2|)}{|t_1 - t_2|}\right]\psi_f^*(t_1)\vec{\alpha}\,\psi_i(t_1)\,dt_1 \tag{2.3}$$

and $$\Theta_{if} = -e\int\left[\frac{(\exp iK|t_1 - t_2|)}{|t_1 - t_2|}\right]\psi_f^*(t_1)\,\psi_i(t_1)\,dt_1 \tag{2.4}$$

This gives a transition probability

$$W_a = \frac{2\pi}{\hbar}\sum_{if}\left|e\int\phi_f^*(t_2)(\vec{\alpha}A_{if} - \Theta_{if})\,\phi_i(t_2)\,dt_2\right| \tag{2.5}$$

where $K = (E_i - E_f)/hc$ and $(E_i - E_f)$ is the energy released by the electron which fills the initial vacancy and $\vec{\alpha}$ represents the set of Dirac matrices.

The expression (2.5) has exactly the same form as the corresponding expression for the transition probability in the internal conversion of gamma radiation. In the latter case the electromagnetic field causing the transition is due to a nucleon transition, and no account need be taken of the Pauli principle.

K Shell Yields

Non relativistic calculations of the K shell fluorescence yield of the atom have been made by Burhop (1935) and Pincherle (1935) using Hydrogen-like single

electron wave functions with an effective nuclear charge given by Slater's rules. Their calculations show that the Auger transition rate is almost independent of Atomic number (Z), while the transition rate for radiation increases approximately with the fourth power of Z. This leads to a relation of the form

$$\omega_K = \frac{1}{1 + A/Z^4} \quad \text{or} \quad \left(\frac{\omega_K}{(1 - \omega_K)}\right)^{1/4} = BZ \qquad (2.6)$$

where A and B are constants.

On taking screening into account, Z is replaced by $(Z - \sigma)$ and we obtain

$$\left(\frac{\omega_K}{1 - \omega_K}\right)^{1/4} = -A + BZ \qquad (2.7)$$

where $A = \sigma B$. In addition we can take relativistic effects into account to a first approximation by replacing Z by $Z(1 - \alpha Z^2)$, and we arrive finally at

$$\left(\frac{\omega_K}{1 - \omega_K}\right)^{1/4} = -A + BZ - CZ^3 \qquad (2.8)$$

where $C = \alpha A$ and α is the fine structure constant. The constants A, B and C can be obtained from experiment by a least squares fit with the existing data.

Although there are marked disagreements between the results of various workers, the available data on K shell yields shows a reasonable agreement with an expression of the form (2.8). Several authors have published empirical and semi-emprical curves for the K fluorescence yield and Listengarten (1961) gives a list

of references to these papers. The experimental techniques available for the measurement of ω_K and the results obtained using these techniques have been summarised by Burhop (1952), and later measurements have been summarised by Burhop (1955), Laberrigue-Frolov and Radvanyi (1956), Wapstra, Njigh and van Lieshout (1959) and by Listengarten (1961). Values of the constants A, B and C, found by various authors, are shown in Table I.

Table I

Constant	Burhop (1955)	Laberrigue-Frolov et al. (1956)	Wapstra et al. (1959)
$A.10^2$	4.4	2.17	6.4
$B.10^2$	3.46	3.318	3.40
$C.10^6$	1.35	1.14	1.03

The 1959 values do not appear to be in significantly better agreement with the new values listed by Listengarten than Burhop's 1955 values.

Further measurements are required in the regions of high and low Atomic numbers. In the latter case the measurements available are subject to large errors because of the experimental difficulties involved. In the former, the region of high Z, more precise observations are required in order to differentiate between the predictions of the nonrelativistic theory and the

relativistic calculations of Massey and Burhop (1936). Their calculations have been recently extended by Asaad (1959) and by Listengarten (1961). Their results indicate that the effect of introducing relativistic wave functions is to lower ω_K by a significant amount for large atomic numbers. E.g. For $Z = 80$ they give $\omega_K = 0.94$ compared with a value of $\omega_K = 0.97$ predicted by the non-relativistic theory. As yet the experiments are not precise enough to decide between the two forms of the theory.

L Shell Yields

Present knowledge of the L shell fluorescence yields is less satisfactory. Most authors have been content to measure the mean L shell fluorescence yield $\bar{\omega}_L$ which is a weighted mean of the individual L subshell yields. Measurements of this quantity are of limited significance and they must be interpreted with great care, since the fluorescence yields of the individual subshells are in general different. In addition, the initial distribution of vacancies amongst the three L subshells varies markedly with the mode of excitation. For example the distribution of vacancies amongst the LI, LII, and LIII subshells is approximately 1 : 2 : 3 following fluorescence excitation, and 0.03 : 1.0 : 1.0 following the internal conversion of Electric Quadrupole gamma radiation. It is immediately obvious that the mean L shell fluorescence yield applies strictly only to a single element and to a

particular method of producing vacancies. Many authors appear to be unaware of this and indiscriminately apply measured values of $\bar{\omega}_L$ in situations where they are not relevant.

A few authors have measured the separate L sub-shell yields which are dependent on Atomic number alone. In general their results do not agree well with one another, and are limited in precision. LII shell yields in particular are not yet known with sufficient accuracy. Salguiero et al. (1961) have pointed out that even in the best studied case of Bismuth (Z = 83), the measured values of the LII shell fluorescence yield vary from 0.32 to 0.66. (Kinsey (1948a), Ross et al. (1955), Burde and Cohen (1956), Tousset and Moussa (1958), Risch (1958) and Jopson et al. (1963)).

Coster-Krönig Transitions

An additional complication in dealing with measurements of L shell yields is the possibility of Auger transitions which transfer ionisation from one L sub-shell to another. The importance of this class of transitions was first pointed out by Coster and Krönig (1935), and in consequence such transitions are known as Coster-Krönig transitions. An example of a Coster-Krönig transfer in the L shell is LI — LIII MV in which an initial vacancy in the LI shell is filled by an electron from the LIII shell and the excess energy is communicated

to an electron in the MV subshell which is ejected from the atom. Such a transition is only possible when the difference in energy of the two L subshells is greater than the binding energy of the electron in the MV subshell of the atom with Atomic number (Z + 1). Coster and Krönig noticed this and suggested that it is transitions of this kind which produce the so called 'anomalies' in L X-ray satellite intensities.

L X-ray satellites exhibit several important differences in behaviour from K series satellites. Their intensity relative to the parent line varies irregularly with Atomic number and they can be much more intense relative to the parent line than K satellites. Typical behaviour is revealed by the X-ray satellites of the $L\alpha_1$(LIII — MV) and $L\beta_2$(LIII - NV) transitions. In the range Z = 50 to Z = 74 they are too weak to be observed and it is in just this region that Coster-Krönig transfers of the type LI - LIII MIV, MV are energetically forbidden. Outside this range of Atomic number these lines have intensities up to half that of the parent line. Similar behaviour is displayed by many other satellite lines and the corresponding Coster-Krönig transitions. Coster and Krönig have shown that the intensity relative to the parent line depends on the Coster-Krönig transition rate which in turn is dependent on the energy of the ejected electron. Their description of the effect is briefly as follows.

Let us consider the Coster-Krönig transfer LI - LIII MV. As with any other Auger transition we can write the transition probability in the form (2.2). We can rewrite this expression in the form

$$W_a = \frac{2\pi}{\hbar}\left|\iint \chi_f V_{12} \chi_i \, (dr_1)(dr_2)\right|^2 \qquad (2.9)$$

where $\chi_i = \frac{1}{\sqrt{2}}\left[\phi_i(r_2)\psi_i(r_1) - \phi_i(r_1)\psi_i(r_2)\right]$, and χ_f has a similar form. For the LI - LIII MV transition which we are considering, the first product in the bracket describes the transition in which the original 2s vacancy is filled by an electron from the 2p shell and the 3d electron is ejected from the atom with finite kinetic energy W. This is the direct transition and the corresponding integral is known as the direct integral. The second product leads to an exchange term in which the 2s vacancy is filled by the 3d electron and the 2p electron is ejected. The small overlap of the 2s and 3d wave functions means that the exchange term is small and we may neglect it. The direct integral can now be written as

$$W_{CK} = \frac{2\pi}{\hbar}\left|\iint \phi_f^*(t_2)\,\phi_i(t_2)\,\psi_f^*(t_1)\,\psi_i(t_1)\,\frac{e^2}{4\pi\varepsilon_0|t_1-t_2|}\,dt_1\,dt_2\right|^2 \qquad (2.10)$$

$$\text{i.e. } W_{CK} = \frac{2\pi}{\hbar}\left|\iint \frac{p_1\,dt_1 \cdot p_2\,dt_2}{4\pi\varepsilon_0|t_1-t_2|}\right|^2 \qquad (2.11)$$

where $p_1 = e\,\phi_f^*(r_2)\phi_i(r_2)$ and $p_2 = e\,\psi_f^*(r_1)\psi_i(r_1)$ may be regarded as charge densities due to the two electrons.

If the Coster-Krönig transition probability is to be large, then p_1 and p_2 must be large and $|r_1 - r_2|$ must be small. In the case we are considering, LI - LIII MV, if p_1 is to be large then the wave-function of the ejected electron $\phi_f(r_2)$ and the 3d wave function $\phi_i(r_2)$ must overlap strongly. Similarly if p_2 is to be large, then $\psi_f(r_1)$ and $\psi_i(r_1)$, the 2s and 2p electron wave functions must also overlap strongly. The nature of the transition means that $|r_1 - r_2|$ must be small.

The angular momentum "ℓ_2" of the ejected electron must have one of the values one, two, or three in units of h ; for before the Coster-Krönig transition takes place the two interacting electrons have angular momenta $\ell_1' = 1$ and $\ell_2' = 2$ with vector resultants L = 1, 2 or 3, while after the transition $\ell_1'' = 0$, so that $\ell_2'' = L = 1$, 2 or 3. The required result follows from the conservation of angular momentum.

Figure 1 gives some indication of the approximate size and position of the normalised radial parts P of the various wave functions concerned in the transition LI - LIII MV. P is the ordinary radial wave function multiplied by r. The wave functions P(2s) and P(2p) have a very large overlap in the region where they have their largest numerical values.

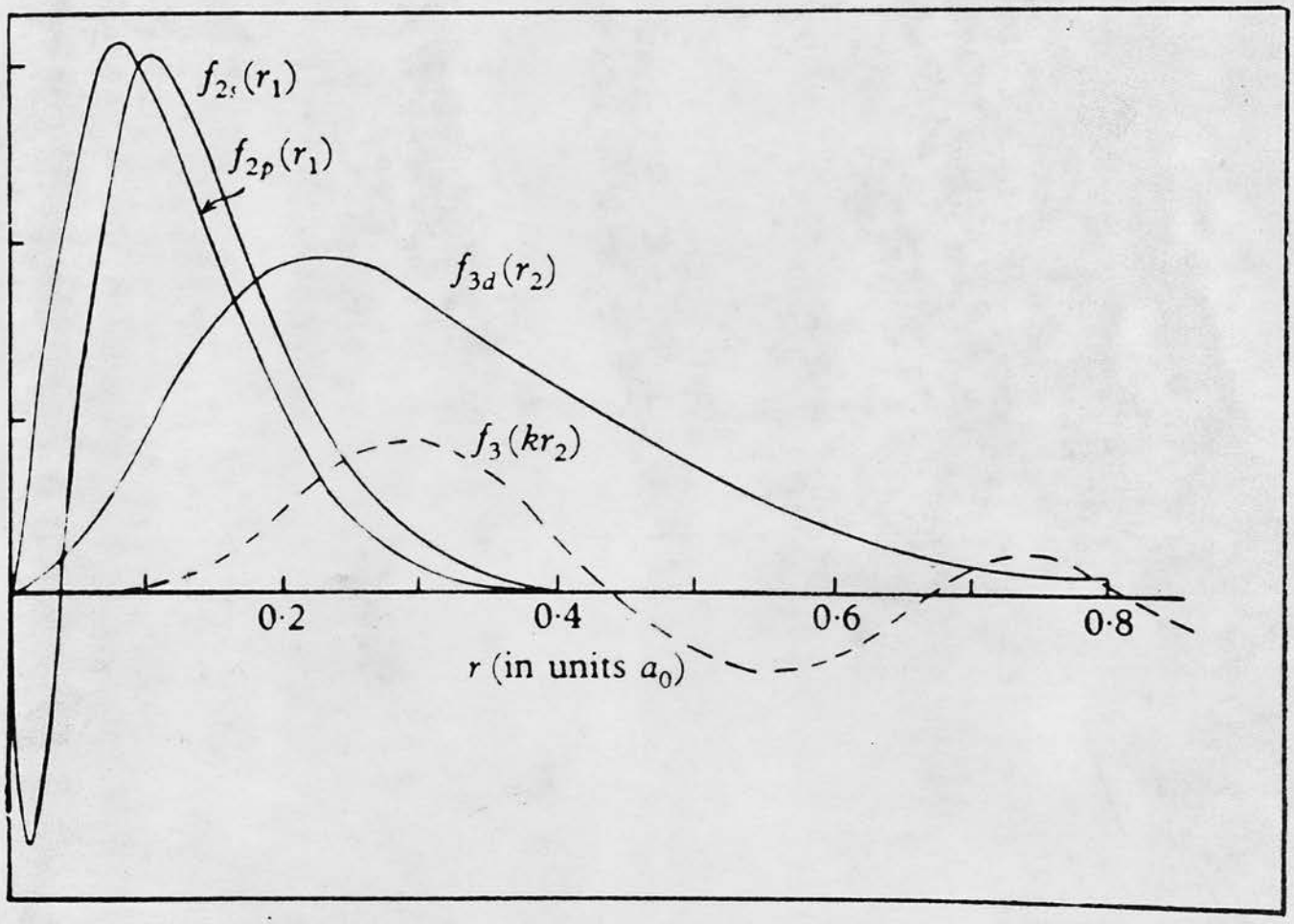

Fig. 13. Form of the radial functions $f_{2s}(r_1)$, $f_{2p}(r_1)$, $f_{3d}(r_2)$, $f_3(kr)$ important in the calculation of the Coster-Kronig transition probability for the transition $(L_1 - L_{III} M_{IV,V})$.

Figure 1

Coster and Krönig's illustration of typical radial wave functions for 2s, 2p, 3d and P(W).

The radial part of the wave function P(W) of the ejected electron is a solution of the one dimensional wave equation of an electron moving in the field,

$$V''(r) = V(r) + \frac{\ell_2''(\ell_2''+1)}{2r^2} ,$$

where V(r) is the Hartree field of the atom. For ℓ_2'' equal to one and two, P(W) is always oscillatory in the region where P(3d) has its largest numerical value. The charge density p_2 will change sign and will keep the transition rate low. For ℓ_2'' equal to three the situation is different. If W is small, then the first maximum of P(W) lies to the right of P(3d) and the overlapping is slight. As W increases this maximum moves to the left until it coincides with the first maximum of P(3d). This is the situation which gives the maximum transition rate and which is shown in Figure 1. For larger values of W the overlapping is less complete and the transition rate decreases again.

This explanation fits the observed behaviour of the satellite lines of the LIII transitions in the region below Z = 53 extremely well. They appear faintly at first, rise to a maximum and finally fade away again, as the energy of the ejected electron increases slowly from zero for Z = 53 to larger values as Z decreases. This behaviour is shown graphically in Figure 3.

Three groups of Coster-Krönig transitions are possible in the L shell. They transfer ionisation from the

LI — LII, LI — LIII, and LII — LIII subshells respectively. Burhop (1952) gives a table of the possible Coster-Krönig transitions and the ranges of Atomic number for which they may occur. The associated Coster-Krönig transfer yield, the probability of the transfer of ionisation from subshell i to subshell j per vacancy created in the subshell i, will be designated f_{ij} throughout the present work. The possibility of these transitions further complicates the problem of determining the L subshell yields, since there are now nine individual fluorescence, Auger and Coster-Krönig transfer yields associated with the three L subshells.

Previous Measurements of L Shell Yields

All of the measured values of fluorescence and other yields of the L subshells known to the author have been collected in Appendix A. A brief description of the more important experiments will be given here.

A measurement of the mean L shell fluorescence yield $\bar{\omega}_L$ has been made by Lay (1934) for some twenty-one elements in the range $Z = 40$ to $Z = 92$. His method was to compare directly on a photographic plate the intensity of 'blackening' due to an X-ray beam from an X-ray tube and the intensity of 'blackening' due to the induced L fluorescent radiation from a target of the element studied, which had been exposed to the X-ray beam. His work was carefully carried out but suffers

from the difficulties inherent in the comparison of two very different exposures on a photographic plate. In this method, the relative numbers of primary vacancies in the three L subshells depend on the frequency of the primary radiation, but for frequencies well above the critical frequency the initial vacancy distribution is approximately $n_1 : n_2 : n_3 = 1 : 2 : 3$.

Measurements of $\bar{\omega}_L$ for the fluorescent excitation of Krypton and Xenon using a Wilson Cloud Chamber were made by Auger (1926) and Bower (1936). In principle their method was very simple. A homogeneous X-ray beam was incident on the chamber, and a measure of the fluorescence yield of the gas inside was obtained by counting the numbers of photoelectron tracks with and without accompanying Auger electrons. The ratios, of the number of photoelectron tracks with Auger electron tracks to the number without, observed by the two experimenters agreed well, but considerable doubt existed as to the correct value of the L jump, which determines the fraction of photoelectron tracks which originate in the L shell. This method is confined to those elements available in gaseous form.

During the last four or five years an extensive series of measurements of $\bar{\omega}_L$ has been carried out by a group at the Lawrence Radiation Laboratory. In a series of papers, Jopson et al. (1961, 1962, 1963 and 1964(a+b)) have described the measurement of $\bar{\omega}_L$ for thirty one elements after the production of L shell vacancies

following K_α X-ray emission. The techniques employed in these measurements were varied, but they all depended on the counting of coincidences between K- and L-X-rays. Initially vacancies were produced in the K shell by electron capture, or by the photoelectric absorption of X-rays or gamma rays. The resulting KX-rays were detected in a scintillation counter. The L X-rays were detected either in a thin window scintillation counter or in a proportional counter. Corrections were applied for the detection of K_β X-rays which were not resolved from the K_α group, the absorption of L X-rays between the source and the counter, etc. The large correction required for the absorption of the L X-rays introduced a considerable uncertainty into their results.

Recently (Jopson et al. (1964a)) they have extended their method to give a measure of the individual LII and LIII subshell yields. The method was as before but a secondary target was introduced which was of a material whose K absorption edge energy is straddled by the energies of the $K\alpha_1$ and $K\alpha_2$ X-rays of the element studied. Coincidences were recorded between L X-rays and K X-rays from the secondary radiator. Since the $K\alpha_2$ X-rays cannot ionise the K shell of the atoms of the secondary target, the secondary K X-rays effectively marked the production of LIII shell vacancies in the primary target. Twelve elements between Holmium (Z = 67) and Bismuth (Z = 83) were studied in this way. The values of ω_3 obtained were then combined with their

previous neasurements of $\bar{\omega}_L$ and a knowledge of the initial distribution of L shell vacancies, to give values of ω_2. Again the corrections for L X-ray absorption were large and difficult to carry out. The solid angles subtended at the source by the L X-ray counter were also small and consequently subject to large errors.

Measurements of the three separate L subshell yields were made by Kustner and Arends (1937). L shell vacancies were produced by fluorescent excitation with a homogeneous X-ray beam. The intensities of the primary and secondary beams of radiation were compared using gas ionisation chambers. The wavelength of the primary radiation was progressively increased to cause ionisation, in the LIII shell alone, then in the LII and LIII shells, and finally in all three subshells. From these measurements they could then deduce the fluorescence yields of each of the three subshells. Unfortunately Kustner and Arends were unaware of the possibility of Coster-Krönig transfers and did not allow for them in their calculations. This should not affect their values of ω_3, or their values of ω_2 in the region where f_{23} is small. Their results show ω_2 decreasing with increasing Atomic number, a trend which disagrees with all other measurements except those of Roos (1960), and also disagrees with the expected theoretical variation. If we attempt to correct their results for ω_2 to allow for the possibility of Coster-Krönig transfers we find that we are also required to make entirely unrealistic assumptions

about the values of the other L shell yields. This suggests that their values for ω_2 not only require correction for the occurrence of Coster-Krönig transfers, but are genuinely in error.

Careful measurements of the LIII shell fluorescence yields of Lead (Z = 82), Thorium (Z = 90), and Uranium (Z = 92) were made by Stephenson (1937). Stephenson's method was in principle the same as that of Kustner and Arends. A homogeneous X-ray beam, of wavelength such that the LIII shell alone was ionised, was directed on to a target of the element studied and the fluorescent radiation from this target was detected in a current ionisation chamber. This chamber could be rotated into the path of the primary beam and it was used to measure the intensity of the primary beam as well. After some manipulation of the data a value of ω_3 was obtained from a comparison of the two intensities. Stephenson's measurements are in reasonable agreement with those of Kustner and Arends, but are somewhat lower than the extrapolated values of Jopson et al.

Experiments employing a method similar to that of the present author were carried out by Salguiero et al. (1961) and by Woods Halley and Engelkeimer (1964). In the latter case $\bar{\omega}_L$ was determined for the five elements Radium, Thorium, Uranium, Plutonium and Curium. In the former, the LII shell yields of Plutonium were measured as well as $\bar{\omega}_L$. In both experiments the L shell vacancies were produced by the internal conversion of an

electric quadrupole transition de-exciting the first excited level of the daughter nucleus. The primary distribution of vacancies between the three subshells was approximately $n_1 : n_2 : n_3 \approx 0.03 : 1.0 : 1.0$. A measure of $\bar{\omega}_L$ was obtained from a determination of the number of L X-rays emitted per alpha particle emitted by the parent source, the total conversion coefficient of the gamma ray, and the intensity of the alpha particle transition to the first excited state. Salguiero et al. also measured the relative intensities of the Plutonium L X-ray lines, and were able to obtain the LII fluorescence, Auger and Coster-Krönig yields. Both of these experiments will be discussed at greater length later.

The fluorescence yields of the L subshells of the elements between Z = 73 and Z = 92 were computed by Kinsey (1948a) using the calculated radiation widths of Massey and Burhop (1936a), the measured radiation widths of Cooper (1942), and the measured level widths of a number of authors. His method was based on the fact that the total width Γ of an atomic shell is proportional to the total probability per unit time that a vacancy in the shell is destroyed, and the radiation width Γ_R is proportional to the total transition probability per unit time for radiative transitions. Thus $\omega = \Gamma_R / \Gamma$. In a further paper, Kinsey (1948b) measured the L X-ray intensities per disintegration of ThB, ThC, and RaD and compared his results with a value obtained from his semi-empirical calculation of the fluorescence yields. He found that his values of ω_2 and ω_3 were in general too

low by at least ten per cent and he arbitrarily increased them all by this amount. Even with this correction they are somewhat lower than the experimental values available.

Listengarten (1961) has criticised Kinsey's values as too low on the grounds that Massey and Burhop's calculated radiation widths, on which they are based, are too low. As evidence he cites their values for the widths of the K level for Z = 79 and Z = 51, which are approximately ten to fifteen per cent lower than the average experimental value given by Sachenko (1957). Measured values of ω_3 are also fifteen to twenty per cent higher than Kinsey's calculated yields. Massey and Burhop used a Slater screening constant in their calculations, which also leads to low values for calculated L shell internal conversion coefficients accord- to Sliv and Listengarten (1952). Listengarten has used Kinsey's method of calculation to obtain values for the fluorescence and other yields in the range Z = 47 to Z = 97. He based his calculations on the same data as Kinsey, but on the basis of the evidence discussed above he multiplied Massey and Burhop's values of the radiation widths by approximately 1.4. His method varied from that of Kinsey in that for Z = 47, 54 and 56 he included experimental measurements of the fluorescence yields. He also used the experimental yields for Z = 55 and Z = 82 as a check on his calculations. Figure 2 shows a reproduction of Listengarten's graph of the variation of the L shell yields with Z. He assumed that the

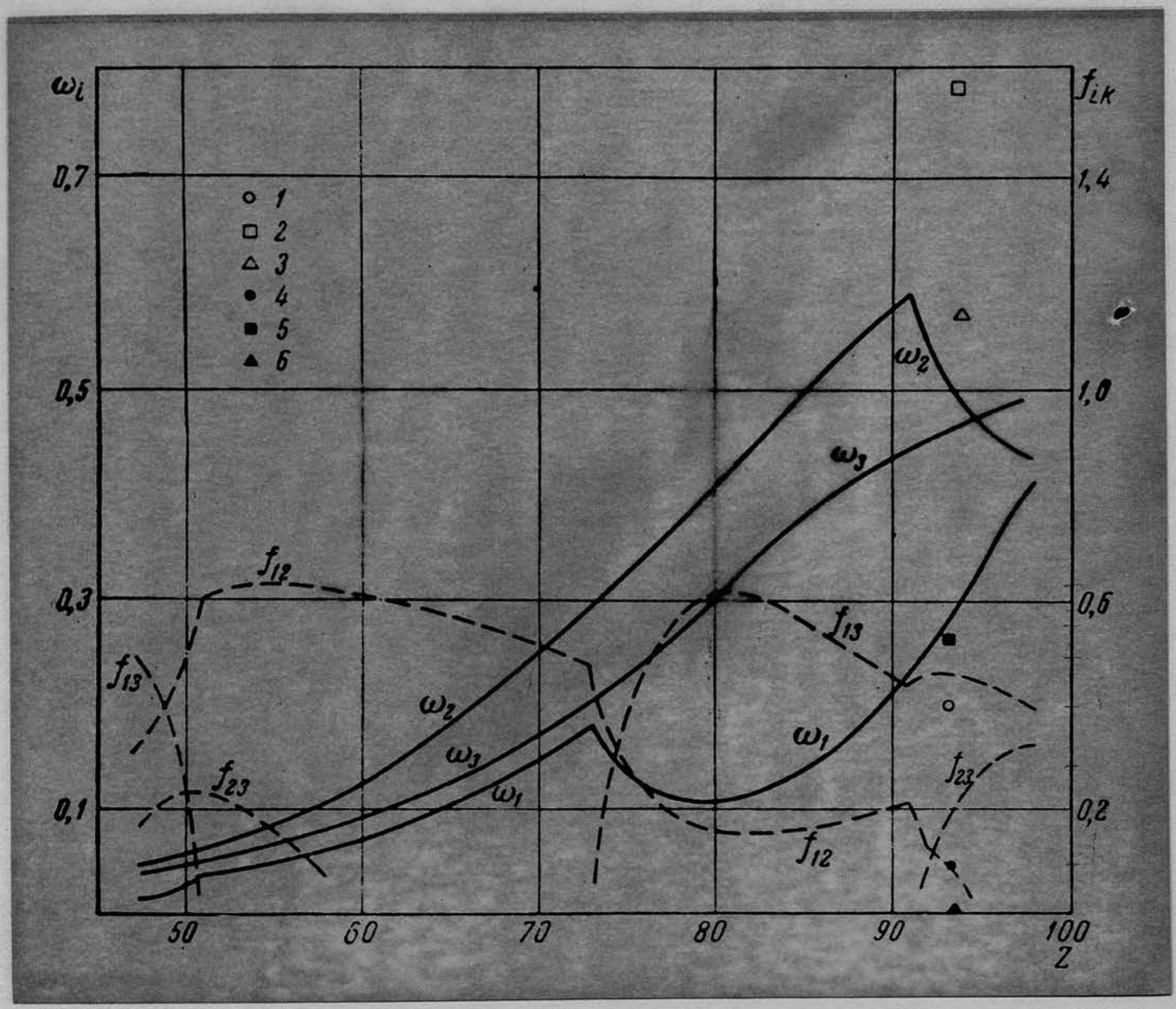

Figure 2

Listengarten's graphs of the L shell fluorescence and Cöster-Kronig yields in the range Z = 47 to Z = 97.

Auger widths increase linearly with Atomic number up to element 82 and more rapidly for $Z > 82$. He also assumed that the Coster-Krönig widths, $\Gamma_{CK'}$ increase sharply at $Z = 51$, 73, 91 and 92. For other ranges of Z he has altered the values of Γ_{CK} to take account of the varying energies of the Coster-Kronig electrons. Finally he has assumed that the LII — LIII MIV, V transitions which become energetically possible at $Z = 91$ and $Z = 94$ respectively cause f_{23} to increase in the same way as f_{13} varies for $Z > 73$. Graphs of the Coster-Krönig electron energies for the LI - LIII, MIV, MV transition in the ranges $Z > 73$ and $Z < 51$ and for the LII - LIII MIV, V transition in the range $Z > 90$ are shown in Figure 3. Figure 3 also shows the variation of the L_{α_1} (LIII - MV) X-ray satellite intensity relative to the parent line in the two lower ranges of Z. An examination of the variation of the ejected electron energies in the two cases suggests that Listengarten's last assumption is not a very sound one. The ejected electron energy increases much more rapidly for the LII - LIII MIV, MV transition, and we might expect that f_{23} would reach its maximum value much more quickly than f_{13} does above $Z = 73$.

An interesting feature of Listengarten's curves is the prediction of a cusp in the graph of ω_2 versus Z at $Z = 91$, which is due to the abrupt change in f_{23} at $Z = 91$. If Listengarten is correct, then ω_2 for Uranium should be greater than ω_2 for Plutonium.

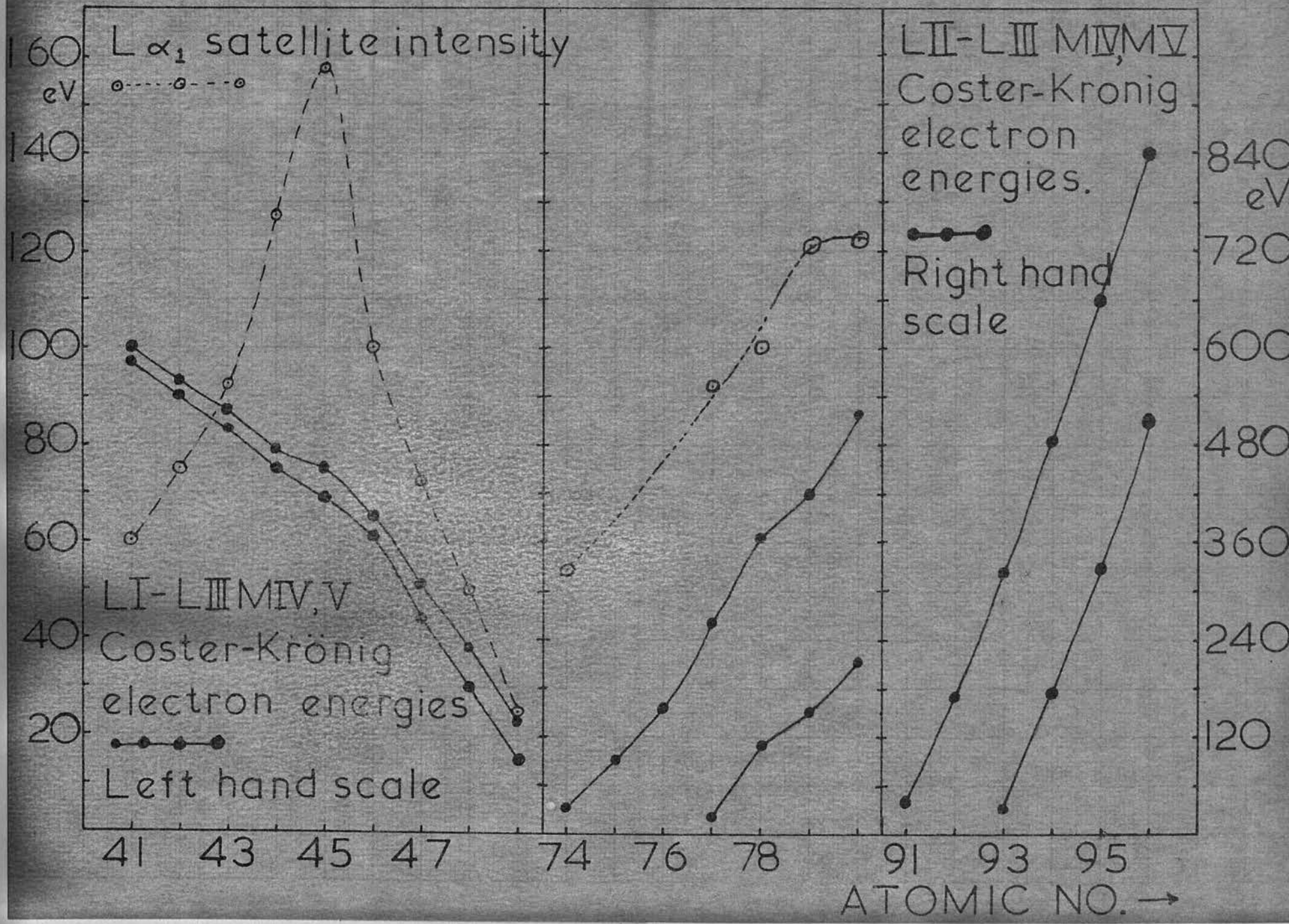
Lα1 satellite intensity
LI-LIIIMIV,V
Coster-Krönig
electron energies
Left hand scale
LII-LIIIMIV,MV
Coster-Kronig
electron
energies.
Right hand
scale
160
eV
140
120
100
80
60
40
20
840
eV
720
600
480
360
240
120
41
43
45
47
74
76
78
91
93
95
ATOMIC NO.→

FIGURE 3

Akalayev et al. (1964) have already examined this point with a measurement of the mean L shell yields of Neptunium (Z = 93) and Plutonium (Z = 94). A mixed source of Eu 154, ~~and~~ Cm 244 and Cm 242 was used. The intensities of the L conversion lines from the approximately 42 keV transitions in Plutonium, and the K conversion line from the 122 keV transition in Gadolinium were compared using a β-spectrometer with $\pi\sqrt{2}$ geometry. The gamma spectrum from the same source was then examined with a scintillation counter, and the relative intensities of the Plutonium L X rays and of the 122 keV gamma ray in Gadolinium were measured. From a knowledge of the K conversion coefficient of the 122 keV gamma ray and of the efficiencies of detection of the scintillation counter for the various radiations, a value of $\bar{\omega}_L = 0.73 \pm 0.10$ was obtained for Plutonium. This value is very high indeed and is in gross disagreement with the values reported by Woods Halley and Engelkeiner (1964), and by the present author for Cm 244 decay, and by Salguiero et al. (1961) for Cm 242 decay. For Neptunium (Z = 93) the electron spectrum following Am 241 alpha decay was examined with the β-spectrometer. From this examination of the β-spectrum a measure of the relative numbers of primary vacancies in the L subshells and of the relative number of Auger electrons ejected from the three subshells was obtained. These results were then combined with Day's (1955) measurements of the relative intensities of the Np L X-rays to obtain the separate L subshell yields. These measurements are also shown in Figure 2. For

Neptunium they found $\bar{\omega}_L = 0.66 \pm 0.08$. They concluded that the increasing value of $\bar{\omega}_L$ going from Z = 93 to Z = 94 disproved Listengarten's prediction that ω_2 decreases with increasing Z in this region. Their results are unreliable, and seem undoubtedly to be too high. Their measurements are too inaccurate to reveal the correct variation of ω_2 with Z, and their conclusion, that Listengarten's prediction is wrong, is very much open to doubt.

M Shell Yields

Only three measurements of the fluorescence yield of the M shell are known to the author. The complexity of the M X-ray and M Auger electron spectra has restricted the measurements to the mean M shell fluorescence yield $\bar{\omega}_M$, which is an even more complex quantity than $\bar{\omega}_L$, since there are five M subshells and ten possible Coster-Krönig transfers.

Lay (1934) measured $\bar{\omega}_M$ for Uranium in the same manner as for his measurements of $\bar{\omega}_L$. Jaffe (1954) measured $\bar{\omega}_M$ for Bismuth (Z = 83) by measuring the intensity of M X-rays emitted by a Ra D source and comparing this with the known decay rate of the source. Finally Jopson et al. (1965) measured $\bar{\omega}_M$ for Bismuth, Lead, Osmium, and Gold using an extension of their method for determining $\bar{\omega}_L$. The results obtained in these investigations are shown in Table 2.

TABLE 2.

Author	Element	$\bar{\omega}_M$
Lay (1935)	Uranium (Z = 92)	0.06
Jaffe (1954)	Bismuth (Z = 83)	0.037 ± 0.007
Jopson et al. (1965)	Bismuth (Z = 83)	0.037 ± 0.007
"	Lead (Z = 82)	0.032 ± 0.006
"	Gold (Z = 79)	0.030 ± 0.006
"	Osmium (Z = 76)	0.016 ± 0.003

The Object of the Present Measurements of Fluorescence Yields

The present research arose initially from the study of the decay of RaD in the Department of Natural Philosophy of the University of Edinburgh. One of the many stumbling blocks which arose in attempts to establish whether or not the ground state to ground state β^- transitions in RaD exists was the inaccuracy of such auxiliary measurements as the values of the L shell fluorescence yields and internal conversion coefficients. This led to a programme of measurements of the L shell fluorescence yields in heavy elements, with the object of determining the L shell yields as precisely as possible.

The present work is a direct extension of the work of Salguiero et al. (1961). They measured the LII shell yields of Plutonium following Curium 242 alpha decay.

The present author has measured the LII shell yields of Uranium following the alpha-decay of Plutonium 238 and of Plutonium 240, and of Plutonium following Curium 244 alpha decay. The latter measurement allows a comparison with the values of Salguiero et al. A comparison of the results for the two elements, Uranium and Plutonium, then allows us to determine the trend of the LII fluorescence yield with Atomic number in the region above $Z = 91$. These measurements should shed some light on the validity of the predictions made by Listengarten about the form of the variation of the LII shell yield with Atomic number.

References - Chapter 2

(1) Akalayev, G.G., Vartanov, N.A., and Samoilov, P.S. (1964), Isvest. Akad. Nauk SSSR, Ser. Fiz. 28, 1259.

(2) Auger, P. (1926), Ann. de Phys., Paris, 6, 183.

(3) Asaad, W.N. (1959), Proc. Roy. Soc. 294, 555.

(4) Bower, M. (1936), Proc. Roy. Soc. A, 157, 662.

(5) Burde, J. and Cohen, S.G. (1956), Phys. Rev. 104, 1085.

(6) Burhop, E.S. (1935), Proc. Roy. Soc. A, 148, 272.

(7) Burhop, E.S. (1952), The Auger Effect and Other Radiationless Transitions (Cambridge University Press, Cambridge.)

(8) Burhop, E.S. (1955), J. Phys. Rad. 16, 625.

(9) Cooper, J.N. (1942), Phys. Rev. 61, 234.

(10) Coster, D. and Krönig, R. (1935), Physica 2, 13.

(11) Day, P.P. (1955), Phys. Rev. 97, 689.

(12) Jaffe, A.A. (1954), Bull. Res. Coun. Israel 3, 316.

(13) Jopson, R.C., Mark, H., Swift, C.D. and Zenger, J.H. (1961) Phys. Rev. 124, 157.

(14) Jopson, R.C., Mark, H., Swift, C.D. (1962), Phys. Rev. 128, 2671.

(15) Jopson, R.C., Mark, H., Swift, C.D. and Williamson, M.A., (1963), Phys. Rev. 131, 1165.

(16) Jopson, R.C., Khan, J.N., Mark, H., Swift, C.D. and Williamson, M.A. (1964a), Phys. Rev. 133A, 381.

(17) Jopson, R.C., Mark, H., Swift, C.D. and Williamson, M.A. (1964b), Phys. Rev. 136A, 69.

(18) Jopson, R.C., Mark, H., Swift, C.D., and Williamson, M.A. (1965), Phys. Rev. 137A, 1353.

(19) Kinsey, B.B. (1948a), Can. J. Res. 26, 404.

(20) Kinsey, B.B. (1948b), Can. J. Res. 26, 421.

(21) Kustner, H. and Arends, E. (1937), Ann. Phys. 22, 443.

References - Chapter 2 (Contd.)

(22) Laberrigue-Frolov, J. and Radvanyi, P. (1956), J. Phys. Rad. 17, 944.

(23) Lay, H. (1934), Z. Phys. 91, 533.

(24) Listengarten, M.A. (1961), Isvest. Akad. Nauk. SSSR, Ser. Fiz. 24, 1041.

(25) Massey, N.S. and Burhop, E.S. (1936), Proc. Camb. Phil. Soc. 32, 461.

(26) Pincherle, L. (1935), Nuovo Cimento 12, 81.

(27) Risch, K. (1958), Z. Phys. 150, 87.

(28) Roos, C.E. (1960), Quoted by Robinson, B.L. and Fink, R.W. (1960), Rev. Mod. Phys. 32, 1171.

(29) Ross, M.A.S., Cochran, A.J., Hughes, J., and Feather, N. (1955), Proc. Phys. Soc. A, 68, 612.

(30) Sachenko, L. (1957), Scientific Notes, Rostov on the Don University 68, 91. Quoted in Reference (24).

(31) Salguiero, L., Ferreira, J.G., Park, J.J.H. and Ross, M.A.S. (1961), Proc. Phys. Soc. 77, 657.

(32) Sliv, L.A. and Listengarten, M.A. (1952), Zhur. Eksp. i. Teor. Fiz. 22, 29.

(33) Stephenson, R.J. (1937), Phys. Rev. 51, 637.

(34) Tousset, J. and Moussa, A. (1958), J. Phys. Rad. 19, 39.

(35) Wapstra, A., Njigh, G. and Van Lieshont, R. (1959), Nuclear Spectroscopy Tables (North Holland Publishing Co., Amsterdam).

(36) Wentzel, G. (1927), Z. Phys. 43, 524.

(37) Woods Halley, J. and Engelkeimer, D. (1964), Phys. Rev. 134A, 24

CHAPTER 3

THE PRESENT METHOD OF MEASURING L SHELL FLUORESCENCE YIELDS

The problem of determining the nine fluorescence, Auger and Coster-Krönig yields of the L subshells has been discussed by Kinsey (1948a). Kinsey's early work was later supplemented and extended by Ross, Cochran, Hughes and Feather (1955) in a thorough and exhaustive analysis of the possible experimental measurements which can be used to determine the L shell yields. Listengarten (1961) has repeated the discussion and argument of the above two papers.

The equations governing the L shell yields in the most general case, where ionisation occurs in all three subshells, were formulated by Ross et al. The notation introduced in their paper has been adopted by the present author, and will be used throughout this work. The symbols employed are as follows:

ω_1, ω_2, ω_3 - The fluorescence yields of the LI, LII and LIII subshells respectively.

a_1, a_2, a_3 - The Auger yields of the LI, LII and LIII subshells respectively.

f_{ij} - The Coster-Krönig transfer yield from the i-th to the j-th subshell.

n_1: n_2: n_3 - The number of primary ionising events per disintegration in the LI, LII and LIII subshells respectively.

I, F - The total number per disintegration of L-ionisations and L fluorescent quanta respectively.

C_3' - The ratio of the number of primary ionisation vacancies in the LIII subshell to the number in the LII subshell.

F_3' - The ratio of the number of photons from the LIII subshell to the number from the LII subshell.

From the definitions of the L subshell yields three identities obviously follow. They are

$$\begin{aligned} \omega_1 + a_1 + f_{12} + f_{13} &= 1 \\ \omega_2 + a_2 + f_{23} &= 1 \\ \omega_3 + a_3 &= 1 \end{aligned} \qquad (3.1)$$

This reduces the number of independent subshell yields to six; three related to the LI shell, two to the LII shell, and one to the LIII shell. A complete determination of all six requires the measurement of six independent quantities.

The complexity of this situation is considerably reduced if the primary ionisation is effectively confined to the LII and LIII subshells. The number of independent yields and hence the number of independent quantities to be measured is then reduced to three. A marked reduction in the effect of the cumulative error is also achieved.

The equations governing the L shell fluorescence yields in this more restricted case can be derived from the general equations formulated by Ross et al. (1955).

The equations for the restricted case have been derived on the basis of two assumptions. The first assumption is that the primary ionisation is confined to the LII and LIII subshells. The second assumption is that the fluorescence yield of an atom singly ionized in a given L level is to a good approximation the same as the L fluorescence yield for an atom ionised in both the given L level and in an M or higher shell. Kinsey (1948a) has shown that the latter is a reasonable assumption. The equations relating the required LII and LIII shell yields to the quantities determined by experiment are:

$$C_3' = n_3/n_2$$

$$\begin{aligned} \omega_2 n_2 + \omega_3(n_3 + f_{23} n_2) &= F \\ n_2 + n_3 &= I \\ \omega_2 n_2 F_3' &= \omega_3(n_3 + f_{23} n_2) \end{aligned} \qquad (3.2)$$

Hence $$\omega_2 = F(1 + C_3')/I(1 + F_3') \qquad (3.3)$$

and $$f_{23} = \omega_2 F_3'/\omega_3 - C_3' \qquad (3.4)$$

Thus when the primary ionisation is confined to the LII and LIII subshells, the LII shell yields can be obtained by measuring the five quantities F, F_3', C_3', I, and ω_3.

At least three modes of primary ionisation exist which effectively restrict the production of vacancies to the LII and LIII subshells. All three have been employed in experiment. Kuster and Arends (1937) used a homogeneous X-ray beam, of wavelength intermediate between

the wavelengths of the LI and LII absorption edges of the target material, to excite fluorescence in the element studied. Their measurements were described in more detail in Chapter 2. This method is readily extended to the production of ionisation in the LIII shell alone, by which means Kustner and Arends were able to measure ω_3 alone.

The method of Jopson and his collaborators (1961, 1962, 1963, 1964a and 1964b) depends on the fact that radiative transitions of the type K — LI are forbidden. Hence the filling of a K shell vacancy by an L electron with the emission of K_α X-radiation results in the production of vacancies in the LII and LIII subshells alone. The extensive series of measurements exploiting this method carried out by Jopson et al. were described in Chapter 2. As with the first method, this can be extended to produce vacancies in the LIII subshell alone. In principle both of these methods apply to each and every element.

The third method is of more limited application, and its possible use is confined mainly to the heaviest elements, of even Atomic number. This method uses the internal conversion of low energy Electric Quadrupole (E2) gamma radiation, which produces vacancies mainly in the LII and LIII subshells and only slightly in the LI subshell. This approach was adopted by Salguiero et al. (1961) and by Woods Halley and Engelkeiner (1964).

Vacancies were produced in the LII and LIII subshells of the daughter element by the internal conversion of a low energy E2 transitions from the first excited state to the ground state of the daughter, following the alpha disintegration of a heavy, even-even nucleus. This method is particularly suited to the study of those elements with an isotope having the very simple decay scheme associated with heavy, even-even, alpha emitting nuclei, the type examined by the two groups mentioned above.

The Present Experiment - The Alpha Disintegrations Studied

The third method described above was adopted in the present series of experiments. The three experiments which are described in the following pages make use of the internal conversion of the E2 gamma rays which are emitted following the alpha decay of Curium 244, Plutonium 238 and Plutonium 240, as a mechanism for producing vacancies in the LII and LIII subshells of the daughter elements. The decay schemes of the three isotopes provide the background to the experiments and our present knowledge of them is reviewed below. The current pictures of the three decay schemes are shown in Figures 4, 5 and 6.

For even-even nuclei in a region far removed from closed nucleon shells Bohr and Mottelson (1954) predicted a series of low lying energy levels constituting a rotational band in which only even states (0+, 2+, 4+,...)

FIGURE 4

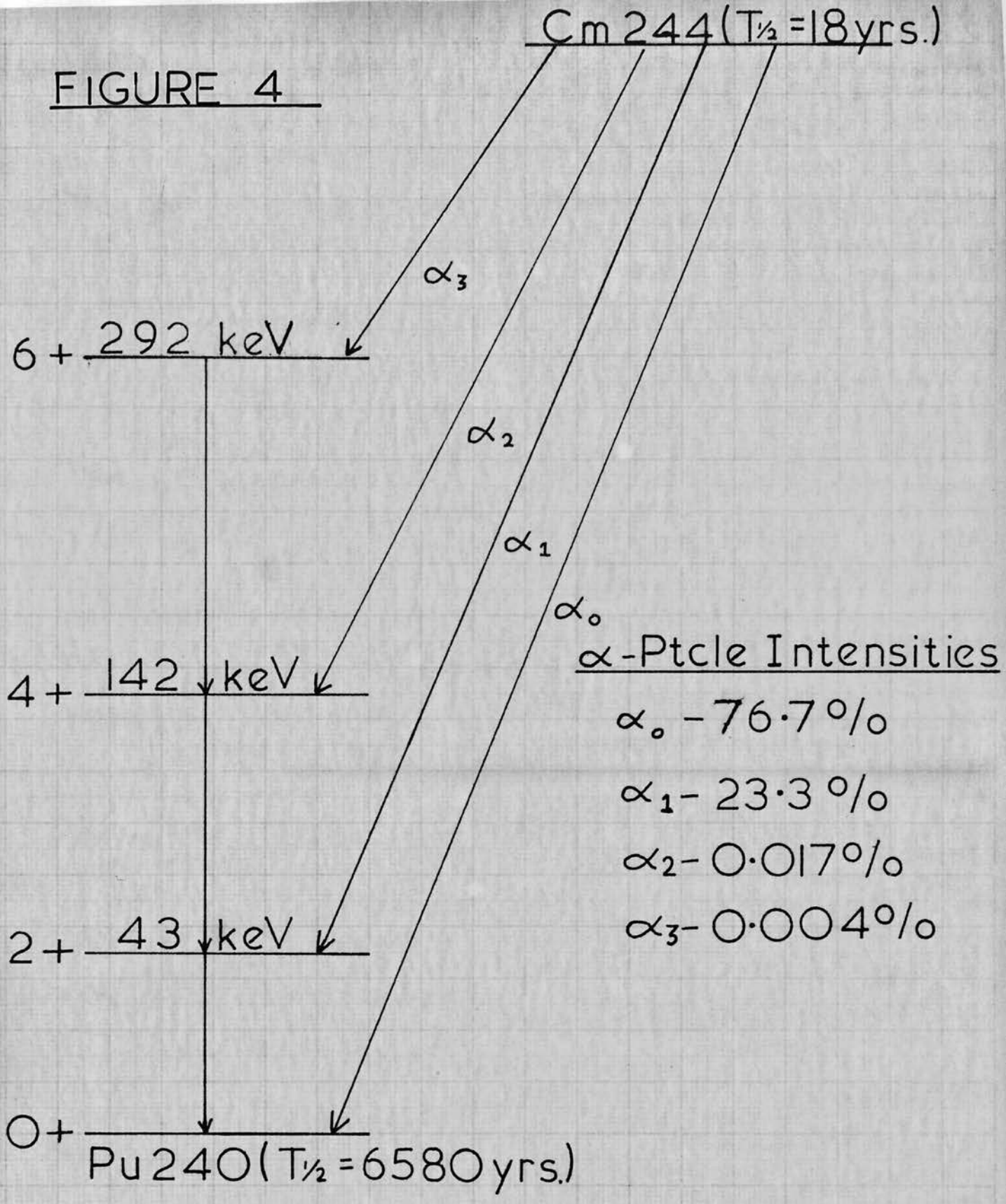

α-Ptcle Intensities

α_0 - 76·7 %

α_1 - 23·3 %

α_2 - 0·017 %

α_3 - 0·004 %

PARTIAL LEVEL SCHEME OF Pu 240, ACCORDING TO HUMMEL (1956).

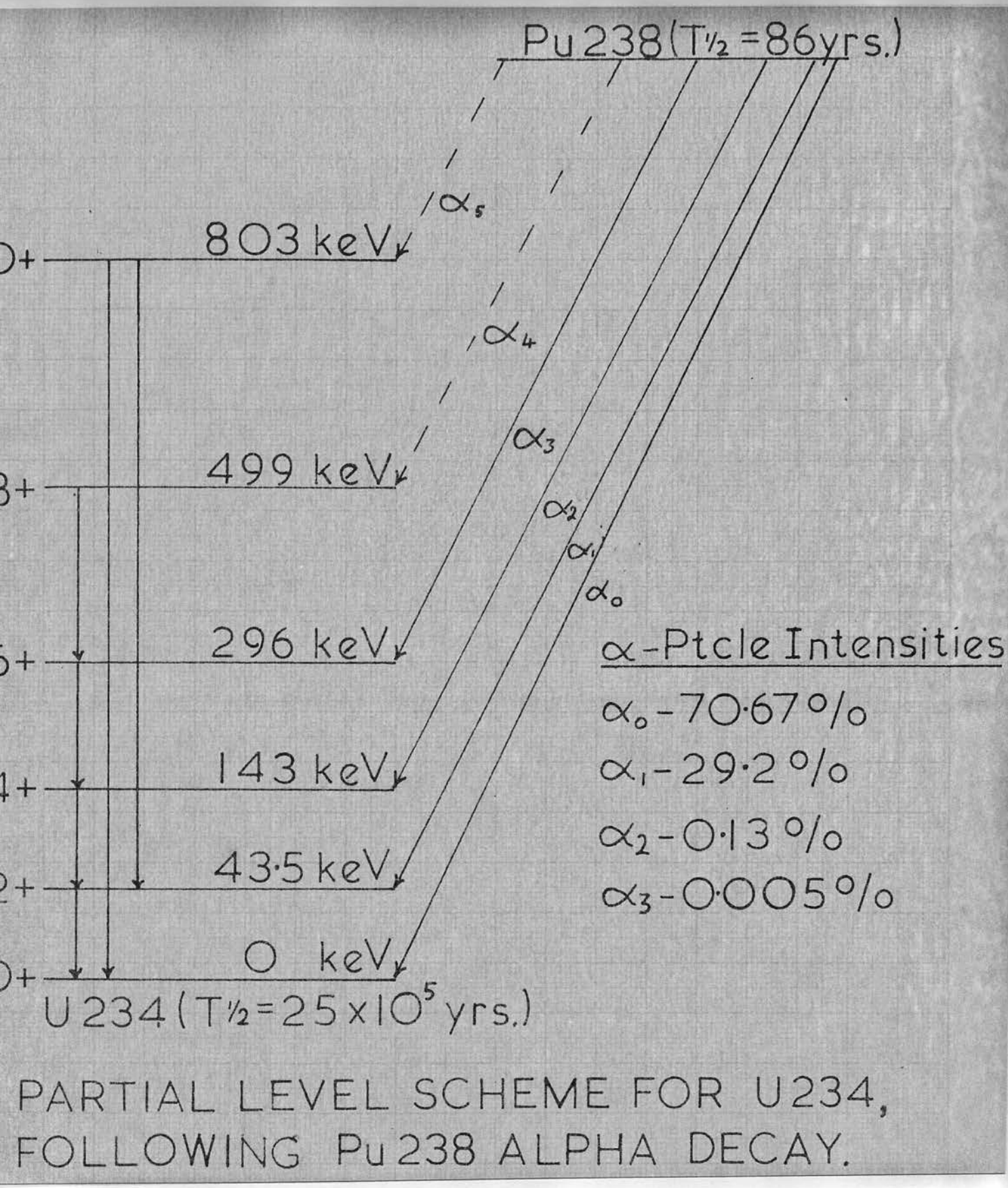
Pu 238 (T½ = 86 yrs.)
α5
α4
α3
α2
α1
α0
803 keV
499 keV
296 keV
143 keV
43·5 keV
0 keV
U 234 (T½ = 25 x 10^5 yrs.)
α-Ptcle Intensities
α0 - 70·67 %
α1 - 29·2 %
α2 - 0·13 %
α3 - 0·005 %
PARTIAL LEVEL SCHEME FOR U234,
FOLLOWING Pu 238 ALPHA DECAY.

Figure 5

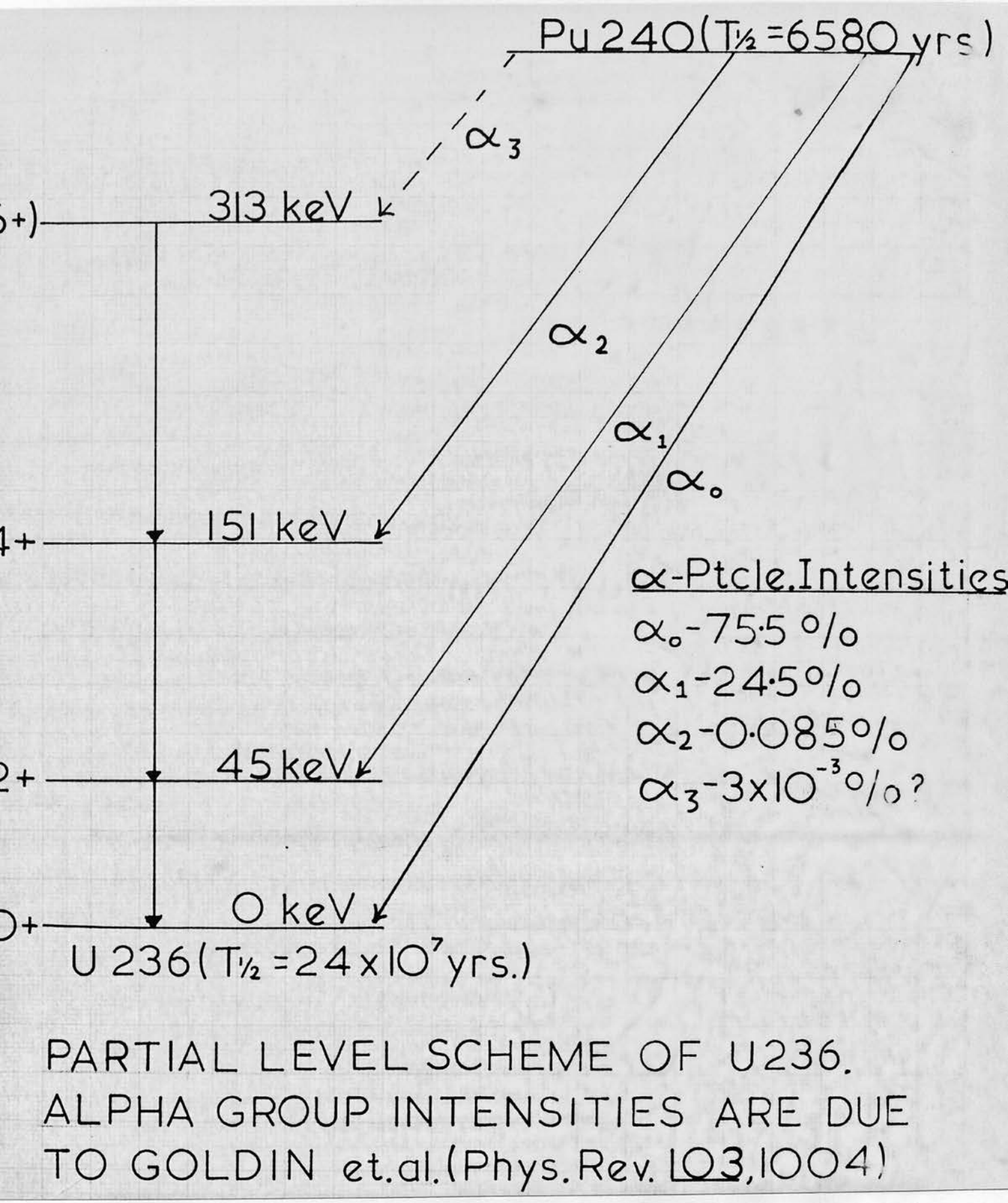

PARTIAL LEVEL SCHEME OF U236.
ALPHA GROUP INTENSITIES ARE DUE
TO GOLDIN et.al. (Phys. Rev. 103, 1004)

Figure 6

would appear. This prediction, based on the Unified Nuclear model, was strikingly borne out by experiment. Two groups of even-even nuclei, in the rare earth region, and in the heavy element region, have been shown to possess this characteristic feature. A recent review of the properties of such nuclei by Nathan and Nilsson (1965) shows that in general they are in very good agreement with the predictions of the Unified Model. The three disintegrations studied here, the alpha emitters Cm 244, Pu 238 and Pu 240 are excellent examples of this general type, and their properties conform to the theoretical picture extremely well.

As can be seen in Figures 4, 5 and 6 the most abundant alpha transition is to the ground state of the daughter nucleus. A second prominent alpha group, some forty or fifty keV lower in energy, feeds the first excited state of the daughter element with an abundance of between twenty and thirty per cent of the total number of decays. Several additional groups of alpha particles of lower energy, and in low intensity have been observed in each case. These groups populate the higher states of the ground state rotational band and other excited states. The gamma rays de-exciting the low lying excited states of the rotational band have been assigned pure E2 polarity on the basis of measurements of their absolute conversion coefficients, and their relative L subshell conversion coefficients. This assignment is confirmed by the failure to observe cross-over transitions from the

higher excited levels to the ground state. This confirms the predictions of spins and parities 2+, 4+,...., for the first, second and higher excited states respectively. In the decay schemes shown in Figures 4, 5, and 6 the spins and parities which have been assigned on theoretical grounds alone are shown in brackets.

As already mentioned these decays are employed solely as a mechanism which causes vacancies in the LII and LIII subshells and not in the LI subshell. Since only a small fraction of the alpha decays proceeds via the higher energy states, and the energy of the transition de-exciting the first excited state is too low to ionise the K shell, the internal conversion of this transition is the main process producing vacancies in the LII and LIII subshells following the alpha decay of the three isotopes studied here. Small corrections must be made for the production of vacancies by other means, such as the internal conversion of the higher energy gamma rays, before the experimental measurements can be applied to the determination of the L shell yields. These corrections will be discussed fully after the presentation of the experimental data.

The Measurements Required to Determine the Fluorescence Yields.

The required LII shell fluorescence yields are obtained by measuring the five quantities ω_3, I, C_3', F, and F_3' for each of the three decays studied. Only the

last two quantities were measured by the author, and values of the other three quantities were obtained from the literature.

As we have already seen in Chapter 2, only a few measurements of the LIII subshell fluorescence yield, ω_3, have been made. But these measurements are reasonably consistent and we can readily obtain reliable values of ω_3 for the elements concerned.

Very few reliable measurements of the internal conversion coefficients involved are available in the literature. However, the theoretical values of Sliv and Band (1957) and of Rose (1958) should be reliable for low energy E2 transitions. The "dynamic penetration" effects in internal conversion due to the finite size of the nucleus, which have been postulated by Church and Weneser (1955, 1956a, 1956b, 1960) and observed by several workers, e.g. Herrlander and Graham (1964), are not expected to affect E2 transitions to any significant extent. They are expected to affect M1 and E1 transitions mainly, especially where the gamma ray transition is strongly retarded compared with single particle Weisskopf estimates, and especially in heavily deformed nuclei. Some evidence that E2 transitions are affected, and that the observed internal conversion coefficients for E2 transitions deviate from the computed values was obtained by a few workers, notably McGowan and Stelson (1957). However this evidence is open to

doubt and later careful measurements by Rester et al. (1961), and by Hultberg et al. (1965) failed to confirm the discrepancy and gave results in good agreement with the theoretical values. Since the computed values of Sliv and Band were by far the most reliable which were available, the values of C_3' and I were derived mainly from their calculations.

The remaining two quantities, F and F_3', were measured for each of the three isotopes by the present author. The method and apparatus used to measure F are described in Chapter 4, and the results obtained are presented and discussed in Chapter 5. In Chapter 6 the measurement of F_3' following Pu 238 decay, using a twenty centimetre radius, curved crystal spectrograph is described, and values of F_3' for the other two decays are derived from this measurement, and from a similar measurement by Salguiero et al. (1961) for Cm 242 decay. F_3' was also measured for the three disintegrations using a proportional counter, and these measurements are described fully in Chapter 7. In the same chapter some measurements on the X-rays and low energy gamma rays emitted, following Am 241 alpha decay are also presented. Finally in Chapter 8, the required fluorescence and other yields are derived from the five quantities, ω_3, I, C_3', F and F_3', and their significance is discussed.

REFERENCES - CHAPTER 3

(1) Bohr, A. and Mottelson, B.R. (1953), Dan. Mat. Fys. Medd. 27, No. 16.

(2) Church, E.L. and Weneser, J. (1955), Phys. Rev. 100, 943.

(3) Church, E.L. and Weneser, J. (1956a), Phys. Rev. 103, 1035.

(4) Church, E.L. and Weneser, J. (1956b), Phys. Rev. 104, 1382.

(5) Church, E.L. and Weneser, J. (1960), Ann. Rev. Nuc. Sci. 10, 193.

(6) Herrlander, C.J. and Graham, R.L. (1964), Nuc. Phys. 58, 544.

(7) Hultberg, S., Horen, D.J. and Hollander, J.M. (1965), University of California Report 9608.

(8) Jopson, R.C., Mark, H., Swift, C.D. and Zenger, J.H. (1961), Phys. Rev. 124, 157.

(9) Jopson, R.C., Mark, H., Swift, C.D. (1962), Phys. Rev. 128, 2671.

(10) Jopson, R.C., Mark, H., Swift, C.D. and Williamson, M.A. (1963), Phys. Rev. 131, 1165.

(11) Jopson, R.C., Khan, J.N., Mark, H., Swift, C.D. and Williamson, M.A. (1964a), Phys. Rev. 133A, 381.

(12) Jopson, R.C., Mark, H., Swift, C.D. and Williamson, M.A. (1964b), Phys. Rev. 136A, 69.

(13) Kinsey, B.B. (1948), Can. J. Res. 26, 404.

(14) Kustner, H. and Arends, E. (1937), Ann. Phys. 22, 443.

(15) Listengarten, M.A. (1961), Isvest. Akad. Nauk, SSSR, Ser. Fiz. 24, 1041.

(16) McGowan, F.K. and Steloen, P.H. (1957), Phys. Rev. 107, 1674.

(17) Nathan, O., and Nilsson, S.G. (1965), In α-, β-, and γ-Ray Spectroscopy, Edited by K. Siegbahn, (North Holland Publishing Co., Amsterdam).

(18) Rester, D.H., Moore, M.S. Durham, F.E. and Class, C.M., (1961), Nuc. Phys. 22, 104 (1961).

REFERENCES - CHAPTER 3 (Contd.)

(19) Rose, M.E. (1958), Internal Conversion Coefficients (North Holland Publishing Co., Amsterdam).

(20) Ross, M.A.S., Cochran, A.J., Hughes, J. and Feather, N. (1955), Proc. Phys. Soc. A68, 612.

(21) Salguiero, L., Ferreira, J.G., Park, J.J.H. and Ross, M.A.S. (1961), Proc. Phys. Soc. 77, 657.

(22) Sliv., L.A. and Band, I.M. (1957), Leningrad Physico-Technical Institute Report (Translation: 1958, Reports 57, ICCKI, 58ICCLI, Physics Department, University of Illinois.)

(23) Woods Halley, J. and Engelkeiner, D. (1964), Phys. Rev. 134A, 24.

CHAPTER 4

THE EXPERIMENTAL ARRANGEMENT FOR THE MEASUREMENT OF F.

Falk-Vairant et al. (1954) have studied the angular correlation between the alpha particles of Th 230 and the L X-rays emitted following the internal conversion of the Electric quadrupole transition de-exciting the first excited level of Ra 226. Within the experimental error ($\pm$ 4 per cent) they showed that the L X-ray photons are emitted isotropically with respect to the alpha particle direction. Th 230 is typical of many heavy, even-even, alpha emitting isotopes and it is a reasonable assumption that the L X-rays are radiated isotropically with respect to the alpha particle direction in other similar decays. On this assumption F, the number of L X-ray photons emitted per alpha disintegration, can be measured for decay schemes of this type by counting the number of L X-ray photons radiated into a known geometrical solid angle in coincidence with alpha particles. Since all three of the decays studied here are of this type, F was measured using this method.

The apparatus used in the determination of F is shown schematically in Figure 7. The alpha particle sources were deposited on thin aluminium foils, of known superficial density, attached to a brass cap, which was held in position by a screw thread. The alpha particles were detected in a silicon semiconductor counter, placed a few millimetres from the open side of the source. The

THE APPARATUS USED FOR THE MEASUREMENT OF F

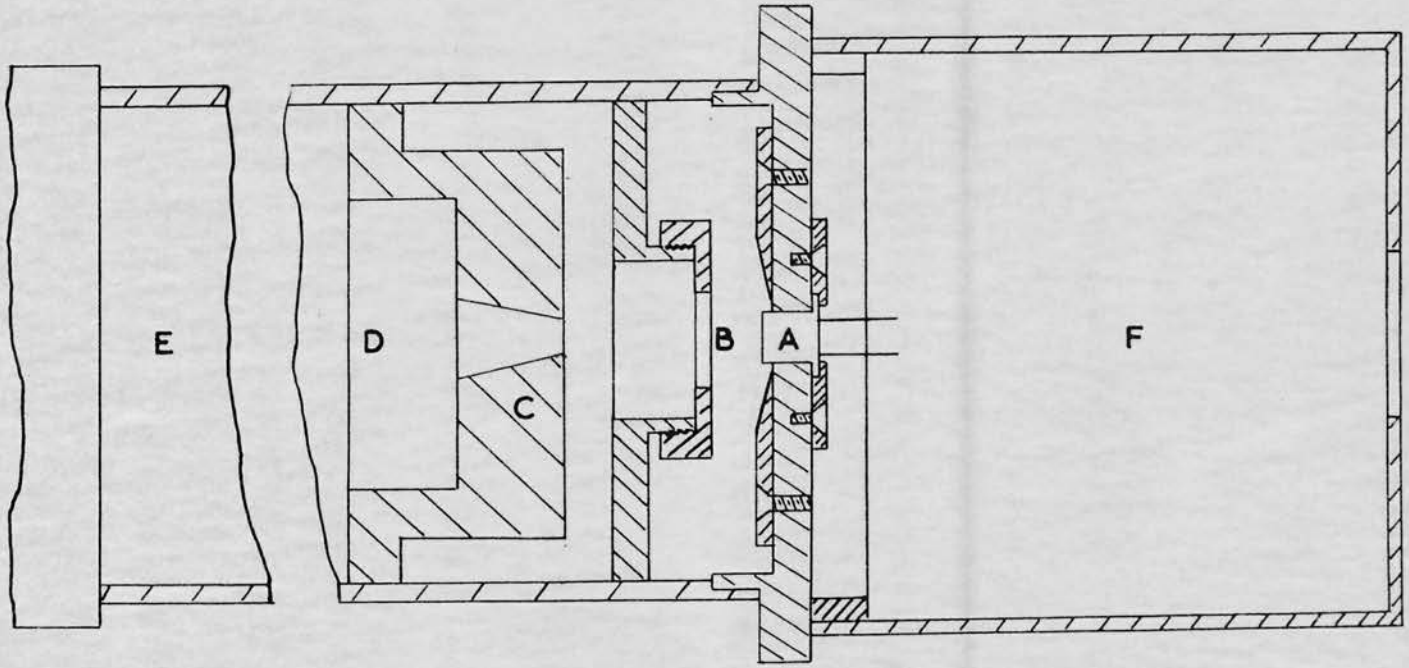

Figure 7

A SEMICONDUCTOR α - DETECTOR
B SOURCE FOIL
C LEAD COLLIMATOR
D NaI [Tℓ] CRYSTAL
E PHOTOMULTIPLIER HOUSING
F COLLECTOR CIRCUIT FOR α - DETECTOR

L X-ray photons were detected by a NaI (Tℓ) crystal scintillation counter on the other side of the source foil. A lead collimator, of accurately measured dimensions, was placed in front of the scintillation counter. This collimator defined the geometrical solid angle for the collection of L X-rays by the scintillation counter.

This solid angle depends on the diameter of the collimator aperture and on the distance from the source to the aperture. The solid angle was varied by altering the source to aperture distance, using a series of accurately measured spacers of brass tubing interposed between the photomultiplier housing and the source holder. Several collimators of different aperture diameters were also used. To prevent the detection of secondary lead L X-rays from the collimator in the scintillation counter, the collimator was lined with 0.005 inch thick cadmium sheet with a layer of 0.001 inch thick aluminium on top. Coincidence measurements were made with and without this lining in position and no difference was observed in the coincidence counting rate.

Coincident events occurring in the two detectors were registered using a conventional 'slow' coincidence circuit with measured resolving time $2\tau = 6.678 \pm 0.005$ microseconds. A brief description of the details of the experimental arrangement follows.

1. The Alpha Detector

The alpha detector used in the experiment to measure F was a silicon semiconductor counter. Before discussing the reasons for the choice of this instrument and describing its performance, a short account of the theory and operation of the junction counter will be given. Although such an account is not entirely necessary for the understanding of the experiment described here, it is given for the sake of completeness. For a more detailed description of the properties of these counters the reader is referred to the books by Dearnaley and Northrop (1963) and by Sharpe (1964), and the review articles by Northrop and Simpson (1962) and by Gibson et al. (1965).

Since the production of the first useful semiconductor junction detectors by Mayer and Gossick (1956), this form of detector has undergone a very rapid development. In essence the silicon junction counter consists of a reverse biased p - n junction. The two principal methods of production of such a junction are by diffusion and by the 'surface barrier' technique. In the former method an n-type doping agent of which phosphorus is most common, is diffused into p-type silicon at a temperature of 700 to 900°C to form a thin surface layer. In the alternative process a very thin p-type surface layer is allowed to form spontaneously by the oxidation of a chemically etched wafer of n-type silicon or germanium. A contact is then made to the requisite sensitive area by evaporation of

gold in vacuum. Gold is usually employed because of its good electrical conductivity and chemical stability.

However the junction is formed, some electrons from the n-type region will tend to cross it into the p-type region and there recombine with holes. Conversely, holes will effectively cross into the n-type region and be filled by electrons. The process ceases when a small potential difference is established across the junction, which prevents the further movement of charge. A shallow region is formed between the two types of material which is free of charge carriers, but contains ionised impurity atoms. These are positive in the n-region, and negative in the p-region. This is the state of affairs in the 'forward-biased' junction. A simple picture of this situation is shown in Figure 8, which also shows the distribution of charge and of electrons, holes, and ionised impurity atoms across the counter.

If now a potential difference is applied of the same sign as that established across the junction it tends to increase the width of the barrier. A region extending up to one millimetre is formed, which has very low conductivity. This is the so-called depletion layer, which forms the sensitive volume of the detector.

When a charged particle of a few MeV energy enters this region of the crystal, it is brought to rest in a time of the order of 10^{-11} seconds. Its energy is dissipated in producing electrons up to a few keV in energy

FIGURE 8

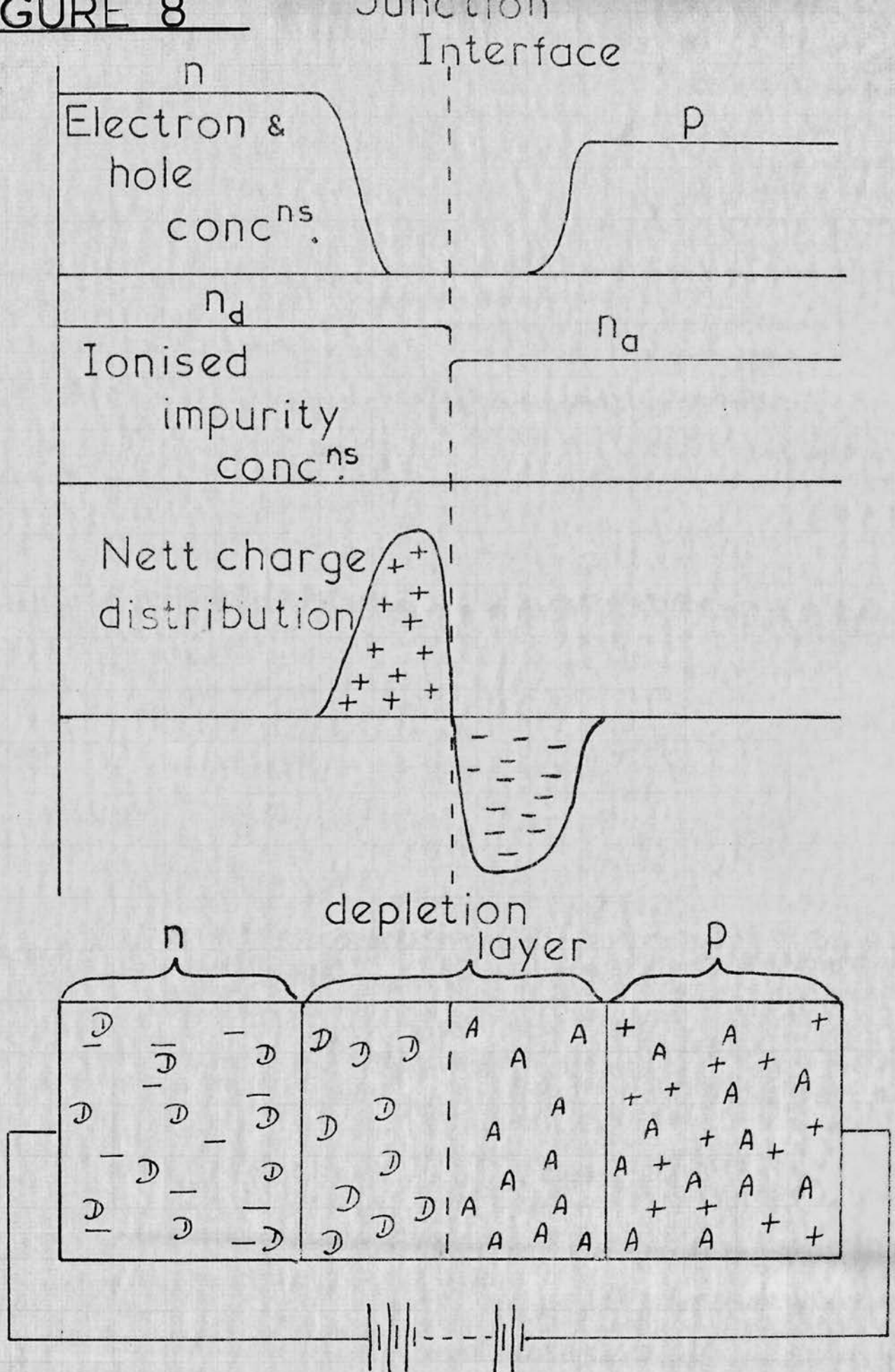

The charge distribution in a p-n junction

in a cylinder about the track, of radius approximately 200 Å. In their turn these electrons lose their energy in creating electron-hole pairs, and when their energy is low enough, in producing phonons and other lattice vibrations. All of the energy of the charged particle is dissipated in this way, in a time of the order of 10^{-12} seconds.

Once the electron-hole pairs have been created they begin to separate under the applied field. When the column of ionisation becomes polarised, a space charge field is set up which opposes, and may completely overcome the applied field. Charge separation then continues by normal ambipolar diffusion, and finally the applied field takes control again as the charge separation becomes large, and charges are induced at the electrodes. The resulting pulse may have a rise time which is as short as 10^{-9} seconds.

In addition to this lower limit on the rise time of pulses from the junction counter, other effects may increase it in practice. The presence of trapping centres, imperfections in the lattice, is one such effect. Charge carriers may spend some time in these traps before being released. This introduces a slow component into the pulse. If the trapping time becomes very long the number of electron-hole pairs recombining becomes important, this charge is lost from the signal and there will no longer be a linear relationship between the energy of the particle and the pulse height observed.

The fundamental limit on the energy resolution of an ionisation chamber is set by statistical fluctuations in the number of ion pairs produced by monoenergetic particles. Since the events resulting in the generation of N ion pairs are all independent, these fluctuations are given by $(\overline{\Delta N})^2 = \overline{N}$, where $\overline{N}$ equals the average number of ion pairs per event. Hence the lower limit of resolution is $\frac{1}{\sqrt{N}} \times 100$. Since in Air, 30 eV energy is required to create an ion pair, compared with 3.6 eV in silicon, eight times the number of ion pairs are created in the solid. Consequently the basic limit on energy resolution is lower by a factor of three in the solid state ionisation chamber compared with the gas counter.

In practice, to obtain the optimum resolution in the detection of charged particles with a semiconductor counter, the detector must be collimated and operated in vacuum. The collimation masks the edge of the detector, where an irregular collecting field leads to output pulses of reduced amplitude. Operation in vacuum reduces the range straggling of heavy charged particles. Operation at low temperatures also improves the resolution since it lowers the detector noise. The resolution of a typical detector varies with the applied reverse bias, showing a considerable increase at low bias voltages. The poor resolution at low bias is probably due to a combination of a poorer signal to noise ratio and a non-

uniformity in collection efficiency over the sensitive area. A resolution of 15 keV, measured as full width at half maximum for the 5.48 MeV alpha particles of Am^{241}, has been achieved by Blankenship and Borkowski (1960) with a silicon surface barrier detector of 1 cm^2 area. On cooling to 78°K to reduce detector noise the resolution improved to 13 keV. This compares favourably with the resolution of the fast, gridded, parallel plate gas ionisation chamber, which has rarely been better than 30 keV. It is inferior to the resolution obtained with a magnetic spectrometer, but the junction counter has a much superior collecting power compared with that instrument.

The choice of a silicon surface barrier counter in the experiment described here was dictated by the requirements of the experiment. The coincidence technique required an instrument capable of moderate energy resolution, high counting rate, low background, fast rise time, and as large a collecting power as possible. In addition simplicity of operation, low cost, and stability of operation over the long periods of counting involved were also demanded. Of the three instruments readily available, the scintillation counter, the gas ionisation chamber, and the solid state detector, the latter is as good as or superior to the others on all counts except that of collecting power. Simple calculation showed that with the sources available the coincidence counting rate obtained would be practicable. Consequently the other advantages of the junction counter rendered it first choice.

The counter employed in the determination of F was a silicon surface barrier detector, of 2 sq. mm. surface area, manufactured by the Hughes Aircraft Company (Los Angeles). Since the solid angle presented by the instrument for the collection of alpha particles did not require to be measured, the counter was placed close to the source foil, to ensure as large a counting rate as possible. In this experiment only moderate resolution was required to distinguish the alpha particles under examination from those of possible impurity atoms, hence no attempt was made to achieve the maximum resolution possible. The counter was operated in air, sometimes with a collimator to mask the edges of the detector. The pulse collector circuit is shown in Figure 9a. The Counter bias was normally set at 72V. Typical pulse height spectra of the alpha particles of Th(B-C-C'-C''), and of Cm^{244} are shown in Figures 10, and 11 respectively. This counter operated satisfactorily over a period of more than three years, without showing any signs of deterioration.

A fast, gridded, parallel plate gas ionisation chamber (Park (1961)) was also available and although no coincidence experiments were carried out with it, the Curium and Plutonium sources were examined using it. This served only to confirm the observations made with the semiconductor detector.

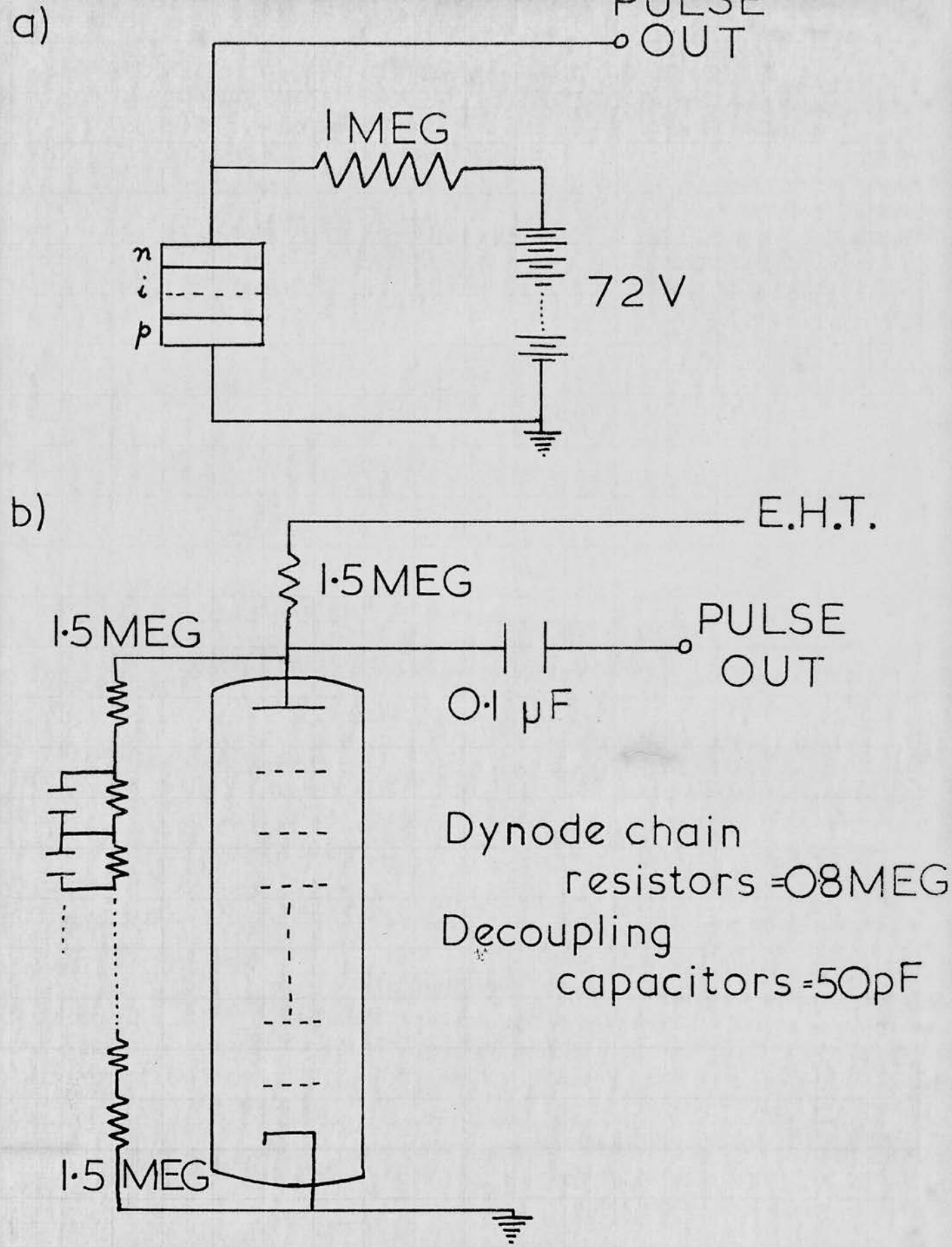

FIGURE 9

a) Pulse collection circuit for α-particles.

b) Photomultiplier dynode chain

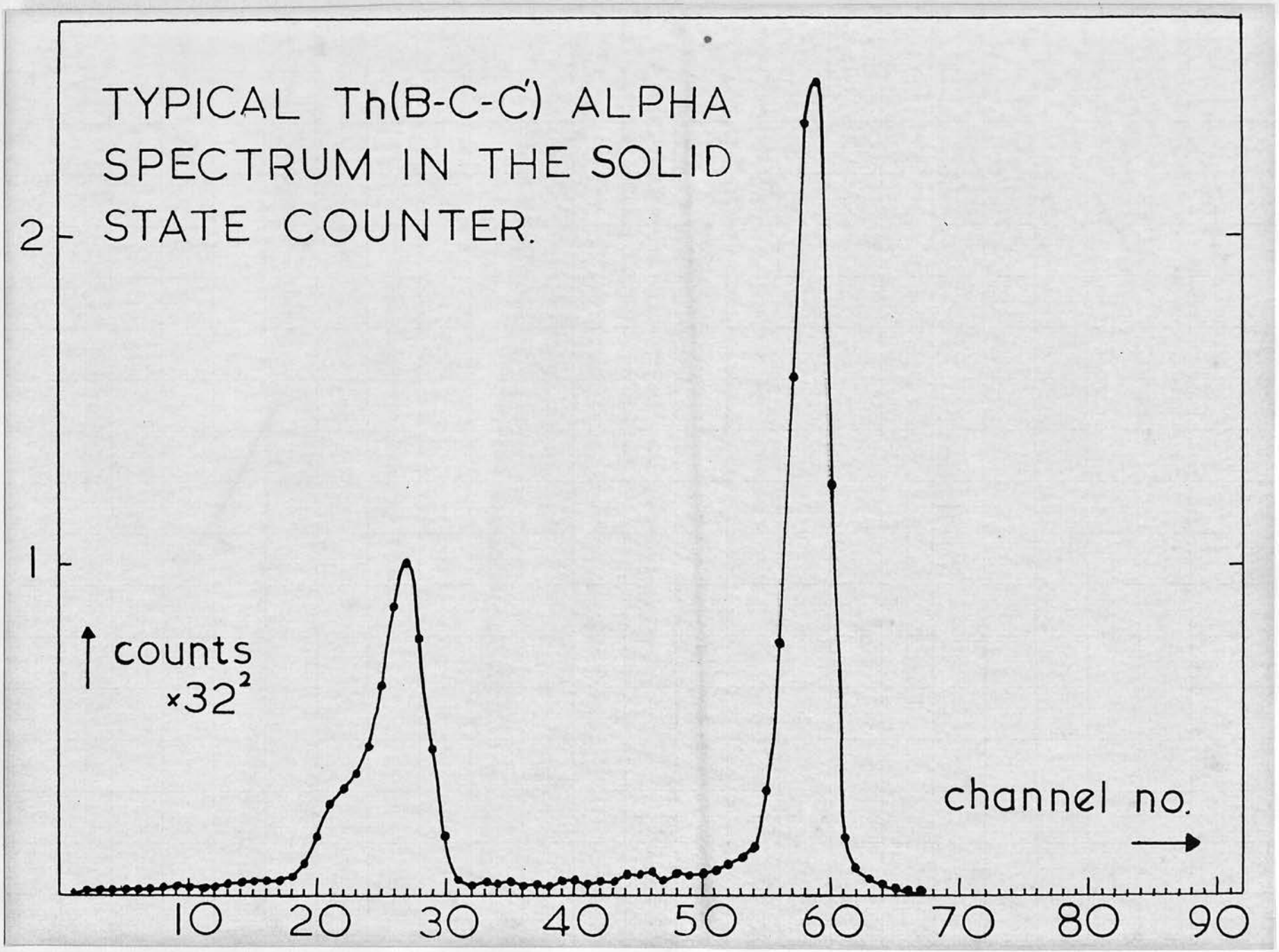
TYPICAL Th(B-C-C') ALPHA SPECTRUM IN THE SOLID STATE COUNTER.
2
1
counts ×32²
channel no.
10
20
30
40
50
60
70
80
90

Figure 10

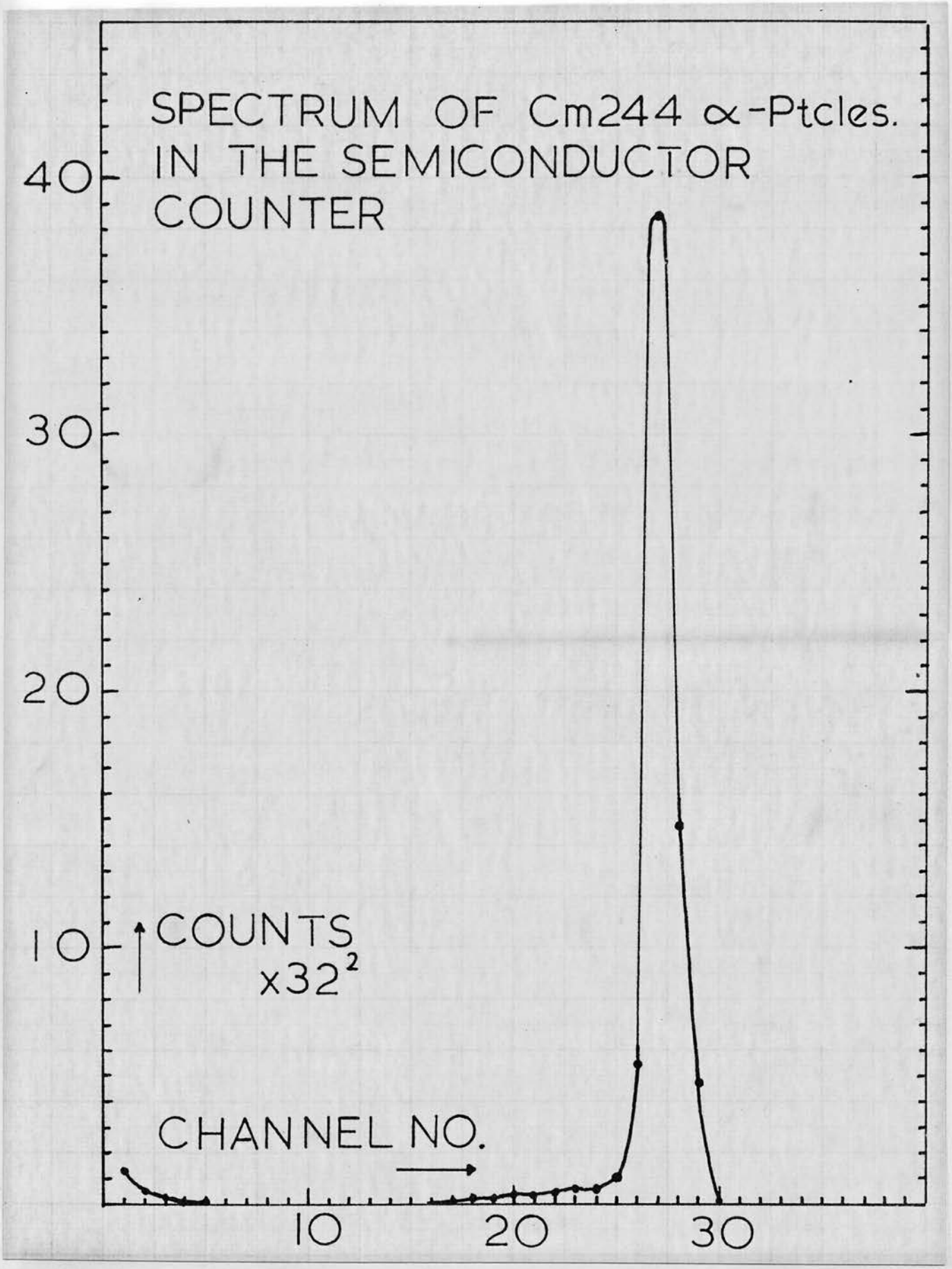
SPECTRUM OF Cm244 α-Ptcles.
IN THE SEMICONDUCTOR
COUNTER
40
30
20
10
COUNTS
x32²
CHANNEL NO.
10
20
30

Figure 11

2. The Scintillation Counter

The photons emitted by the Curium and Plutonium sources were detected in a NaI (Tℓ) crystal Scintillation counter, of dimensions 2 cm x 2 cm. Since the L X-rays of Plutonium and Uranium are of low energy, 13-22 keV, the scintillation counter window was made especially thin. The window had a total thickness of 18 mgm/cm^2, composed of 7 mgm/cm^2 araldite, 6 mgm/cm^2 magnesium oxide and 5 mgm/cm^2 aluminium. The scintillation counter was optically coupled to an E.M.I. 6097B photomultiplier tube using a special silicone grease manufactured by Nuclear Enterprises (G.B.) Ltd.

The voltage divider network employed with this photomultiplier tube is shown in Figure 9b. A high gain was provided on the first stage to cut noise due to the random fluctuations in the multiplication process. The high gain on the last stage provided the least fluctuation consistent with maximum gain. The high voltage supply was derived from a Type 1033A power unit which supplies 0.25 ma at 0-3000 volts and was manufactured by E.K. Cole Ltd. The E.H.T. was usually set at 1000 volts.

3. The Electronic Equipment

A block diagram of the circuit employed in the coincidence experiment is shown in Figure 12. The ideal shapes of pulses are shown at each stage in the circuit. The arrangement of units shown is that appropriate to the

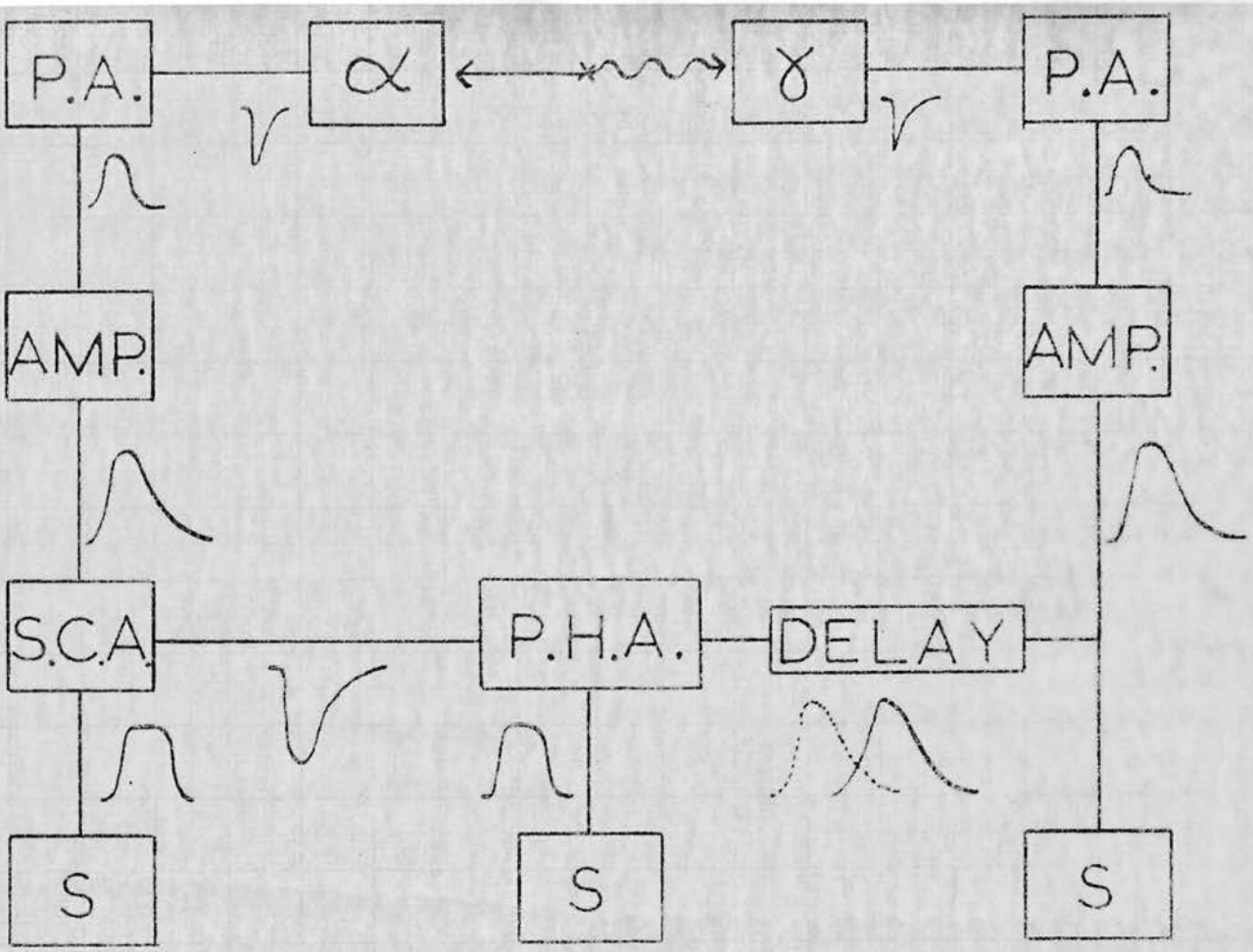

LEGEND:

α-Semiconductor alpha detector

γ-NaI(Tl) scintillation counter

P.A.-N568B preamplifier

AMP.-N568B amplifier

S.C.A.-Single channel analyser

P.H.A.-Multi-channel pulse height analyser

S.-Scaler

BLOCK DIAGRAM OF THE 'SLOW' COINCIDENCE ASSEMBLY.

Figure 12

recording of coincident events in the two counters, or for the recording of the spectrum of photons detected in the scintillation counter. The alpha counter could easily be connected into the other side of the circuit however in order to record alpha spectra alone. The power for all of the electronic equipment was supplied from stabilised mains.

(i) Amplifiers

The outputs of the two counters were fed into N568B preamplifiers set for a gain of 50, and then into N568B pulse amplifiers. The voltage gain of these amplifiers could be reduced in forty equal steps with a maximum attenuation of forty dbs. The low and high frequency characteristics of the pulses could be adjusted separately. Normally both differentiation and integration times were set at 1.6 μsecs. The output from the amplifier following the scintillation counter was connected to a commercial delay line, made by A.R.W. Ltd., which provided a total delay of 4 μsecs in steps of 0.1 μsecs. The optimum delay required was determined to be 2.0 μsecs by altering the delay time when recording coincident events in the two channels. The delay required is that delay for which the maximum number of coincident events is recorded. This delay was also measured on an oscilloscope, and was again found to be 2.0 μsecs.

(ii) Single Channel Analyser.

This instrument was required to select pulses induced by alpha particles within a given energy range, and to provide a gating pulse for the coincidence circuit for each selected alpha particle pulse. The instrument used was built by Dr. J.J.H. Park, formerly of this department, and is based on a germanium diode discriminator developed by Park (1956). The lower level of the discriminator could be varied from 0-60 volts, and the channel width from 0-20 volts. The time lag between an input pulse and the corresponding output pulse was independent of the pulse height, which was ideal for this experiment, since it allowed the use of a fixed delay in the other channel to equalise the delay in the two sides of the circuit. The multichannel analyser described below required a negative gating pulse greater than twenty five volts for at least one μsec, and the single channel analyser was adjusted to give output pulses with these characteristics. A second, positive output pulse could be used to operate a scalar. Park (1961) gives a detailed description of the instrument.

(iii) Scalars

All Scalars were of type 1009B, made by Dynatron Radio Ltd. Fitted with 'fast counting' mechanical registers these instruments were capable of recording pulses at counting rates of up to two thousand five

hundred counts per second.

(iv) Pulse Height Analyser

The recording and pulse height analysis of the spectra of alpha particles, and L X-rays was performed with a Hutchinson-Scarrot multichannel pulse spectrograph (1951). This instrument, manufactured by Sunvic Ltd., could be used to sort pulses into 60-, 80- or 120-channels, the total storage capacity remaining constant. Normally it was operated with 80 channels. It is proposed to describe here only those features of the instrument which affected its performance in this experiment.

In general the performance of the multichannel analyser was entirely satisfactory. Because of its mode of pulse height analysis, however, the 'kicksorter' has a long 'dead' time of 740 μsecs. At large counting rates this large 'dead' time necessitates a serious correction to the observed counting rate, which arises in the following way.

After passing through a series of pulse shaping and amplifying circuits the input pulses are passed to a comparison circuit which compares the voltage amplitude of the input pulse with the voltage of a linear sweep. The latter is changing linearly with time so that a certain time after it has started, its sweep will be equal to the voltage of the input pulse. The comparison circuit generates an output voltage when the voltages of the two waveforms are equal but with the linear sweep becoming

more negative. Hence the period which elapses between the start of the linear sweep and the instant of comparison is proportional to the amplitude of the input pulse. The pulse from the comparison circuit primes a coincidence circuit so that the latter generates a pulse coincident with the next pulse in a series of acoustic pulses continuously circulating in a magnetostrictive acoustic delay line. A binary number associated with this circulating pulse is increased by unity. Hence each number stored in the delay line corresponds to a certain pulse amplitude. The later the number is to pass through the adding gate relative to the start of the linear sweep, the greater the pulse amplitude it represents.

Circuits are incorporated to prevent further input pulses being accepted while one is stored awaiting sorting. On average this waiting period is equal to half the period of the linear sweep, i.e. equal to 740 μsecs. Normally the observed counting rate (N_o) in a scaling circuit is corrected for the dead time (T) using the formula $N = N_o/(1 - N_oT)$. In this case, where there is a variable dead time, we must use the formula

$$N = -\frac{1}{T}\log_e(1 - N_oT) \qquad (4.1)$$

Even this formula is not exact. In the absence of trigger pulses, there is a fixed quiescent period of between twenty five and ninety μsecs. before each linear sweep. Formula (1) does not properly take account of the dead time due to this waiting period.

In practice it was more accurate to correct for the dead time by calibrating the counting rate on the pulse height analyser by comparing its counting rate with that measured in a scalar set at zero paralysis. This procedure was carried out and the resulting graph of observed counting rate (on the scalar) versus the true counting rate is shown in Figure 13.

The 'kicksorter' also incorporated facilities for recording coincidence and anti-coincidence spectra. In the former case it accepts only those pulses which are coincident with negative gating pulses. In the latter it rejects pulses which are coincident with positive gating pulses. In the measurement of F the pulse height analyser was operated in the former mode. The negative gating pulses, of amplitude greater than twenty five volts, and of length greater than one microsecond, were obtained from the single channel analyser built by Park (1961).

The measured resolving time of this 'slow' coincidence circuit was 6.675 ± 0.005 μsecs. This value was obtained by counting coincidences between pulses from two unrelated sources, and using the formula for accidental coincidences between the two, $N_{ACC} = 2\tau N_1 N_2$. The value obtained by this method was checked by introducing a long delay into one channel of the coincidence circuit, and counting the number of accidental coincidences. The two methods always gave the same result.

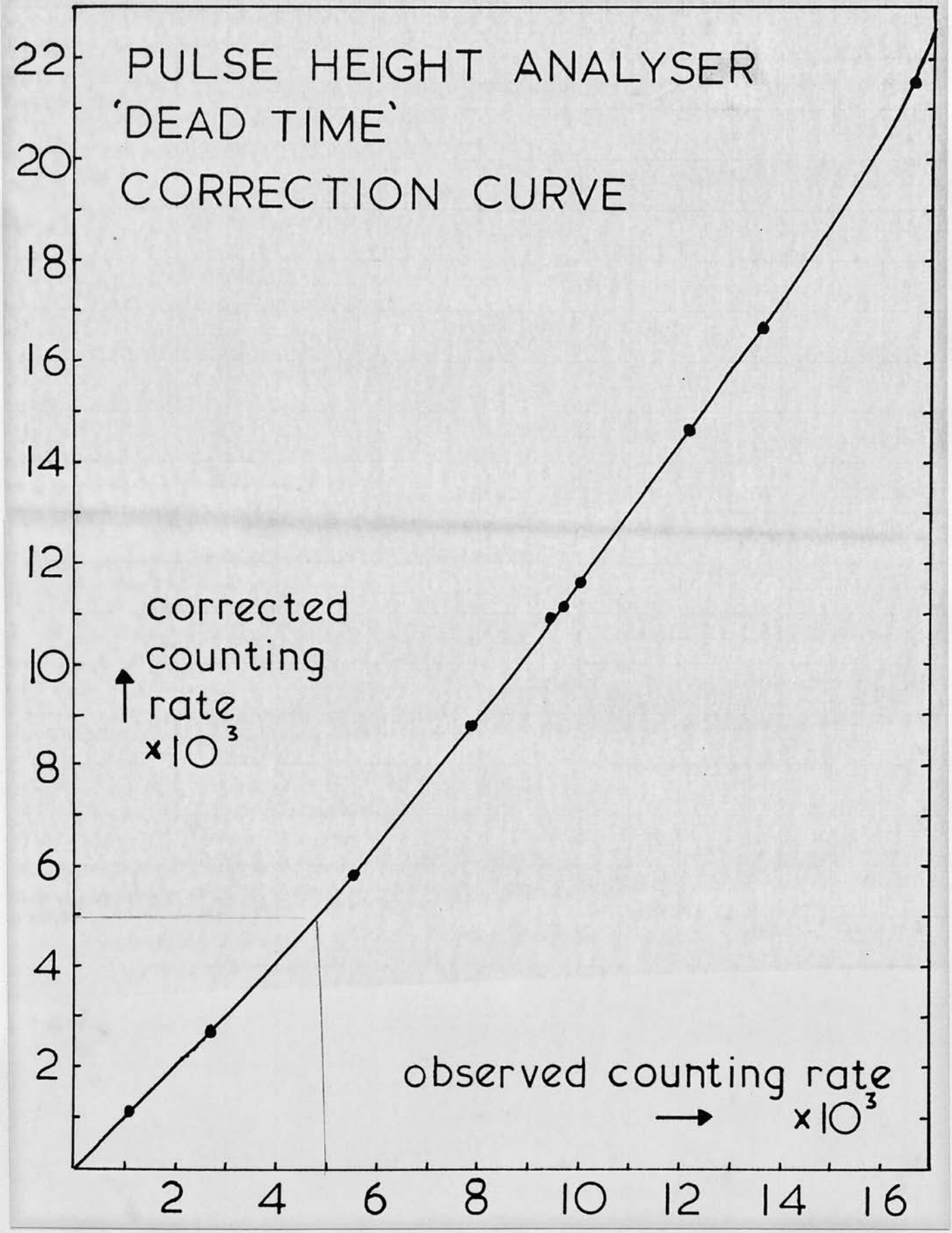
PULSE HEIGHT ANALYSER
'DEAD TIME'
CORRECTION CURVE
corrected
counting
rate
x10³
observed counting rate
x10³
22
20
18
16
14
12
10
8
6
4
2
2
4
6
8
10
12
14
16

Figure 13

REFERENCES - CHAPTER 4

(1) Blankenship, J.L. & Borkowski, C.J. (1960), I.R.E. Trans. Nucl. Sci. NS7, 190.

(2) Dearnaley, G. & Northrop, D.C. (1963), 'Semiconductor Counters for Nuclear Radiations,' (E. & F.N. Spon Ltd., London.)

(3) Falk-Vairant, P., Teillac, J., Valladas, G. and Benoist, P., (1954), C.R. Acad. Sci. Paris 238, 1409.

(4) Gibson, W.M., Miller, G.I. and Donovan, P.F. (1965), 'Semiconductor Particle Spectrometers' in α-, β- and γ-Ray Spectroscopy. Edited by K. Siegbahn, (North Holland Publishing Co., Amsterdam).

(5) Hutchinson, G.W. & Scarrot, G.C. (1951), Phil. Mag. 42, 792.

(6) Mayer, R.D, and Gossick, B.R. (1956), Rev. Sci. Inst. 27, 407.

(7) Northrop, D.C. and Simpson, R. (1962), Proc. Phys. Soc. 80, 262.

(8) Park, E.C. (1956), J. Sci. Instr. 33, 257.

(9) Park, J.J.H. (1961), Thesis, University of Edinburgh.

(10) Sharpe, J. (1964), Nuclear Radiation Detectors, (Methuen & Co., London).

CHAPTER 5

THE RESULTS OF THE MEASUREMENTS OF F

Measurements were made of the number of L X-ray photons per alpha disintegration for Curium 244, Plutonium 238, and Plutonium 240 decay. These three decays are of the type discussed in Chapter 4, such that the L X-rays, mainly produced following the internal conversion of a low energy electric quadrupole transition, are emitted isotropically with respect to the alpha particle direction. Accordingly, the value of F was measured for the three disintegrations using the method and apparatus described in the previous chapter.

In this chapter, the procedure followed in these experiments is first outlined. The results are then presented in tabular form, and are compared directly with the few measurements of F, for these alpha disintegrations, which have been made by other authors. Finally, the contribution of several other processes to the intensity of the L X-rays emitted by these isotopes is discussed. The significance of the measured values of F for the evaluation of the fluorescence yields of Plutonium and Uranium is not discussed until Chapter 8.

The Alpha Active Sources

The sources used in the experiments to measure F were obtained from the Radiochemical Centre, Amersham. Some of the characteristics of these alpha active,

TABLE 3

Characteristics of the Sources Used in Measurements of F.

Parent Isotope	Daughter Isotope	Nominal Activity	Mounting	Superficial Density of Source foil	Source Area
Pu 238 ($T_{1/2}$ = 86 yrs)	U 234 ($T_{1/2}$ = 2.5×10^5 yrs)	$1.19 \pm .06\mu C$	Sublimed on Al. foil, which was attached to a Brass screw cap by Zapon	0.58 mgm/cm^2	2mm diameter
Cm 244 ($T_{1/2}$ = 18 yrs)	Pu 240 ($T_{1/2}$ = 6580 yrs)	$1.55 \pm .08\mu C$	"	0.68 mgm/cm^2	2mm diameter
Pu 240 ($T_{1/2}$ = 6580 yrs)	U 236 ($T_{1/2}$ = 2.4×10^7 yrs)	$0.66 \pm .04\mu C$	"	1.22 mgm/cm^2	2mm diameter

carrier free sources are listed in Table 3.

Before commencing the coincidence experiments to determine F, each source was examined carefully for any indication of the presence of radioactive impurities, which might affect the measurements. To this end, the alpha and gamma spectra from the sources were examined using the semiconductor detector, and NaI(Tℓ) crystal scintillation counter described in Chapter 4. No impurities were detected in any of the sources. Repeated examination of the spectra over the following three years, with the same detectors, confirmed these observations. The alpha particle spectra were also examined with the fast, gridded, parallel plate ionisation chamber of Park (1961), and again no impurities were detected. In addition, Mr. F. Shaikh of this department and the present author, in the course of the measurements of the relative intensities of the L_α, L_β, and L_γ X-ray groups, which are described in Chapter 7, examined the electromagnetic radiation from the sources in the energy range 3-80 keV, without finding any radiation which could be attributed to an impurity. On the strength of this evidence, the author proceeded on the assumption that any impurities in the sources were present in negligible amounts.

The strong similarity in the decay schemes of the three isotopes studied meant that the observed alpha and gamma spectra from the three sources looked very much alike. Hence the spectra from Plutonium 238, which are

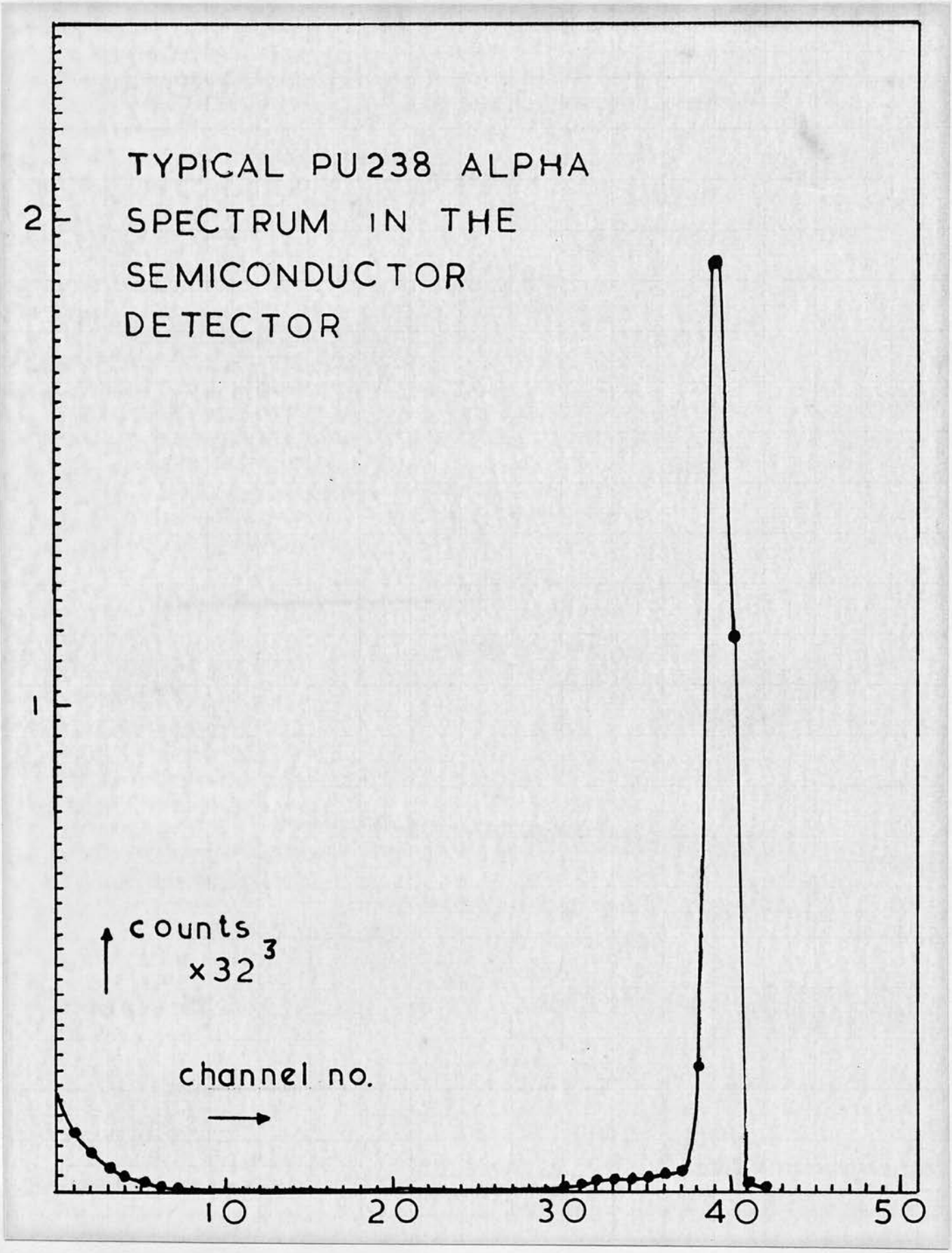
TYPICAL PU238 ALPHA
SPECTRUM IN THE
SEMICONDUCTOR
DETECTOR
2
1
counts
x32 3
channel no.
10
20
30
40
50

Figure 14

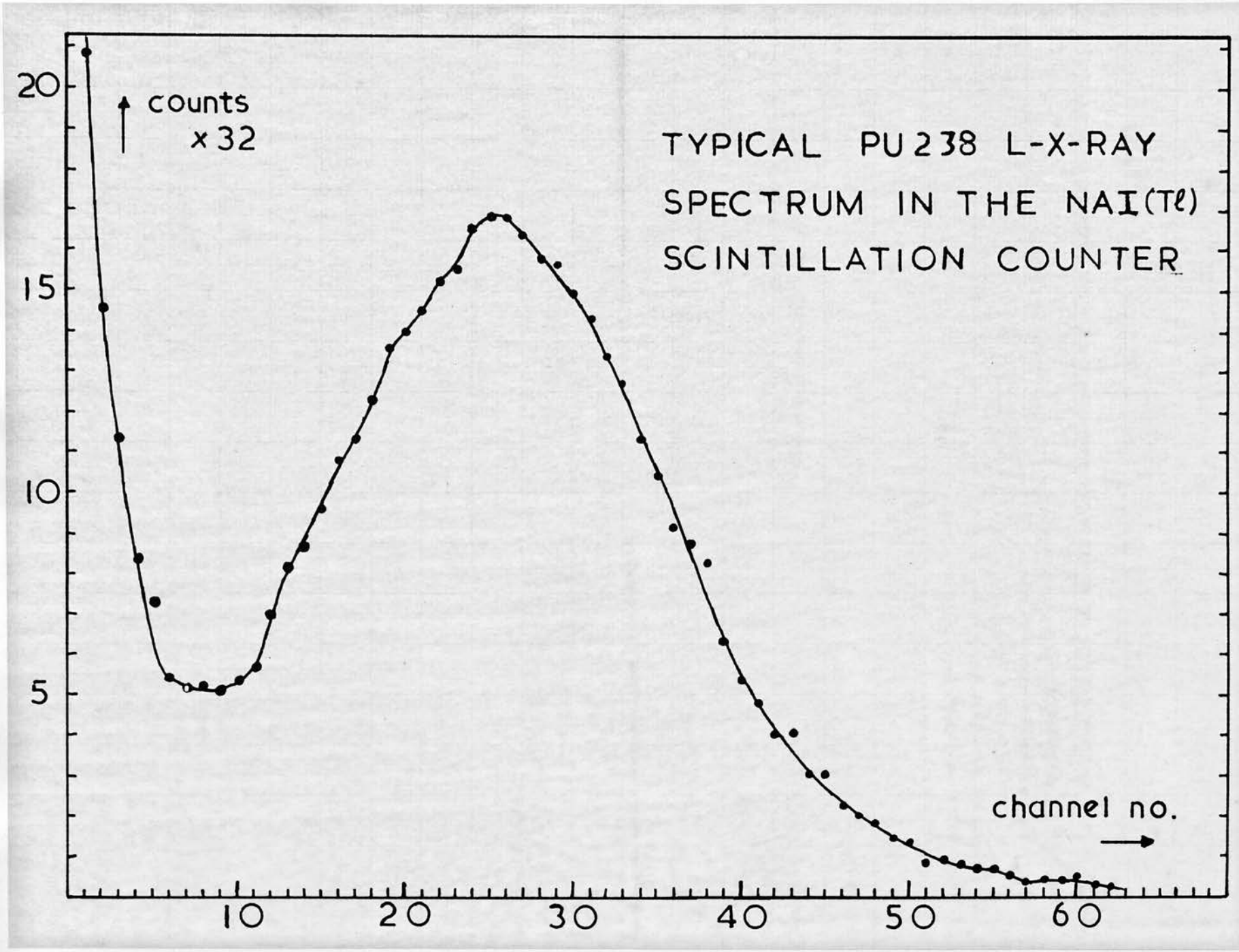
TYPICAL PU 238 L-X-RAY
SPECTRUM IN THE NAI(Tℓ)
SCINTILLATION COUNTER
counts
x 32
channel no.
20
15
10
5
10
20
30
40
50
60

Figure 15

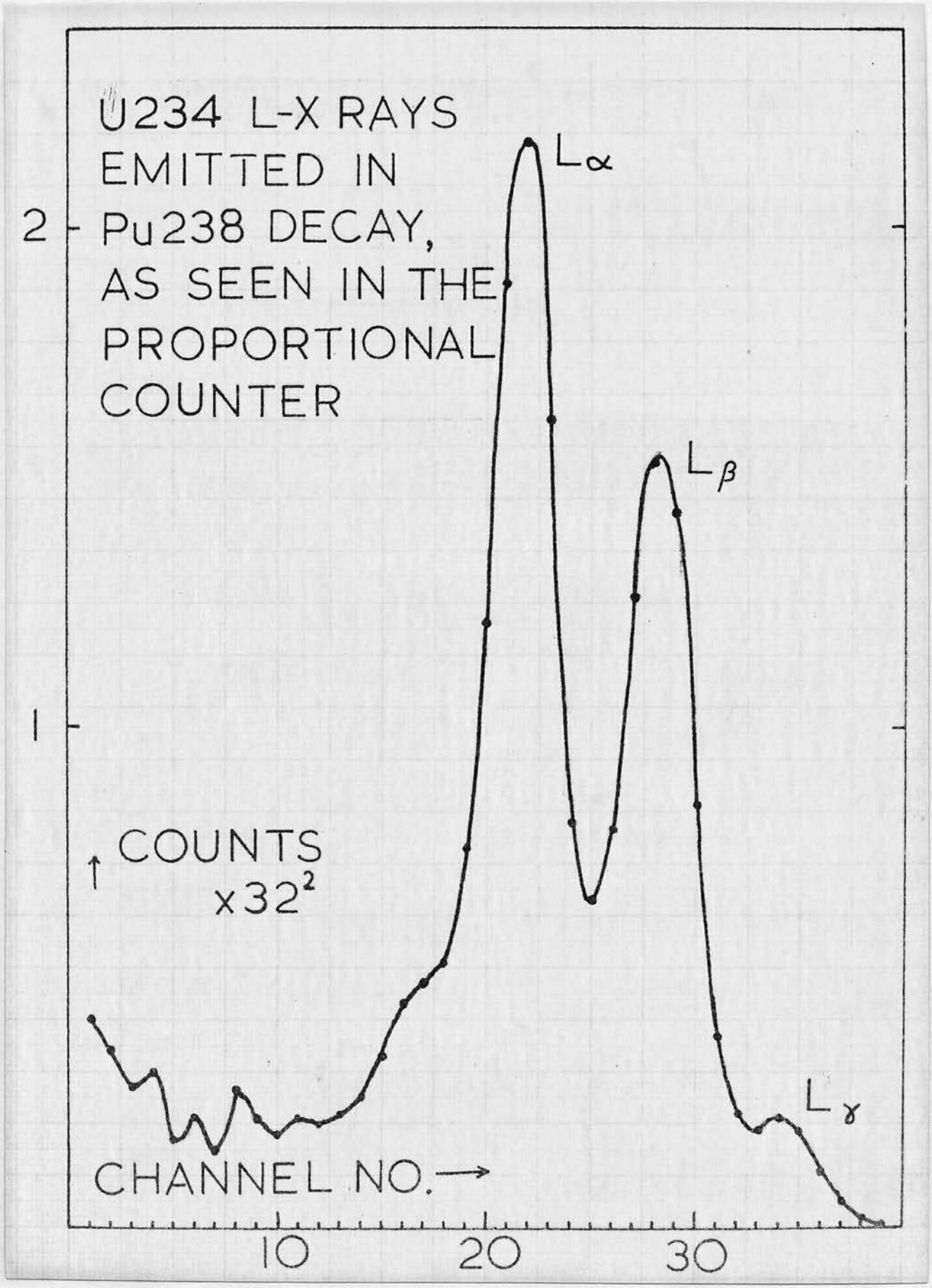
U234 L-X RAYS
EMITTED IN
Pu238 DECAY,
AS SEEN IN THE
PROPORTIONAL
COUNTER
Lα
Lβ
Lγ
2
1
COUNTS
x32²
CHANNEL NO.→
10
20
30

Figure 16

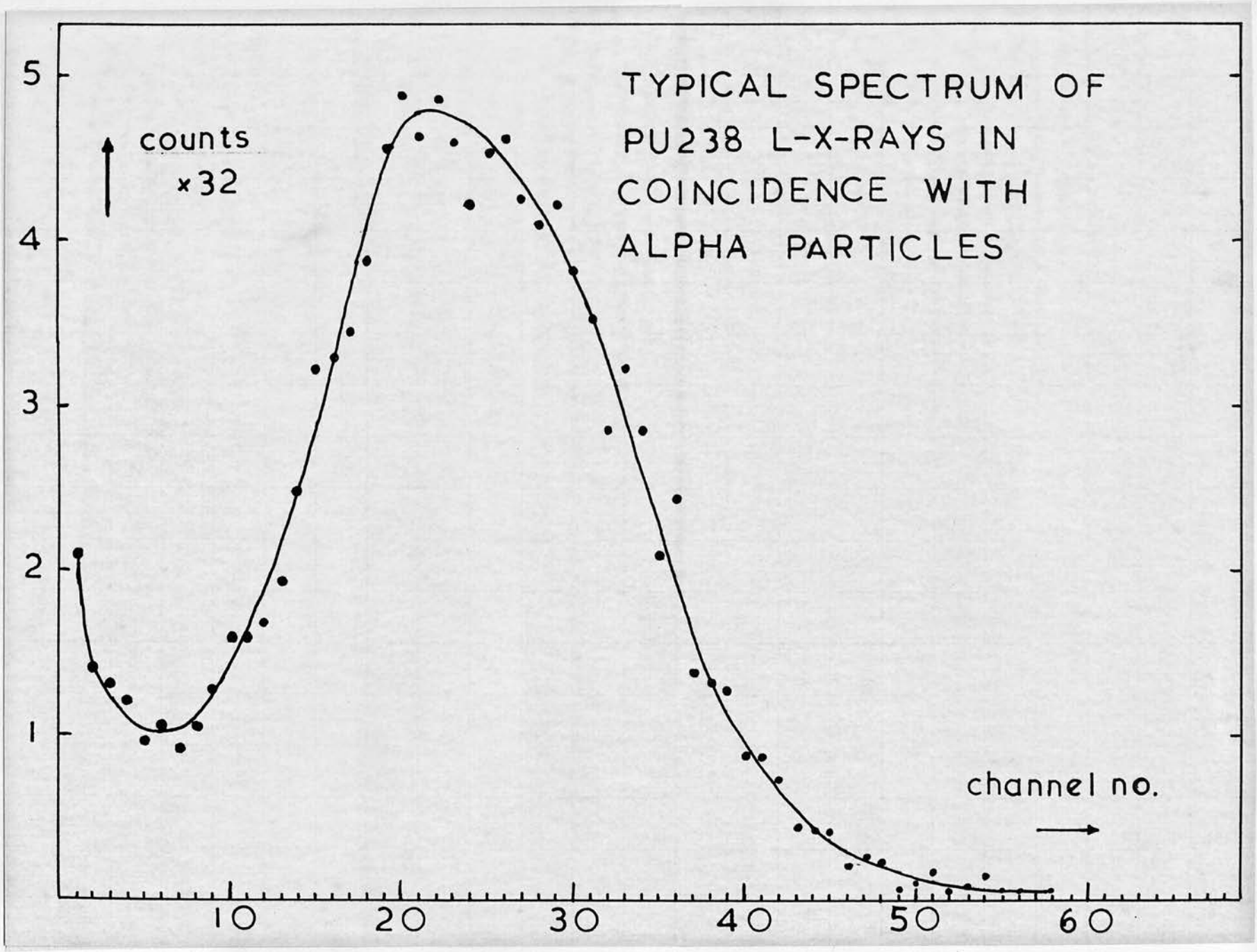
TYPICAL SPECTRUM OF
PU238 L-X-RAYS IN
COINCIDENCE WITH
ALPHA PARTICLES
counts
×32
channel no.
1
2
3
4
5
10
20
30
40
50
60

Figure 17

shown in Figs. 14, 15 and 16, are typical of the alpha and gamma spectra from the three sources. A typical Uranium L X-ray spectrum in coincidence with the alpha particles of Plutonium 238 is also shown, in Figure 17.

Observational Procedure.

Before beginning a series of measurements of F, the resolving time (2τ) of the coincidence circuit was measured, using the method of counting accidental coincidences between pulses from two unrelated sources (see Wapstra (1965)). The apparatus was then set up to measure F as described in Chapter 4, with a lead collimator of known dimensions set in front of the scintillation counter, at a known distance from the source foil. From the dimensions of the collimator, and its distance from the source foil, the geometrical solid angle for the detection of L X-rays could be calculated. The measurement of the resolving time of the coincidence circuit was then confirmed, by introducing a long delay into one arm of the circuit. This effectively made the pulses from the two counters independent, and the resolving time was remeasured, using the same method as before. At regular intervals throughout the whole series of measurements of F, the resolving time was checked in this way.

On commencing a coincidence experiment, the spectrum of L X-ray photons coincident with the alpha particles, selected by the single channel analyser, was recorded on the multichannel pulse height analyser. Simultaneously,

the number of alpha particle gating pulses, and the number of L X-ray photons entering the 'kicksorter' were recorded on scalars. It was necessary to record these 'singles' counting rates, in order to correct the coincidence counting rate for the occurrence of chance coincidences between the pulses from the two counters. This correction was made using the formula,

$$N_C = N_{CO} - 2\tau(N_\alpha - (N_{CO} - N_C)(N_L - (N_{CO} - N_C)) \quad (5.1)$$

where N_C and N_{CO} are the corrected and observed coincidence counting rates respectively, and N_α and N_L are the alpha particle, and L X-ray 'singles' counting rates.

The recorded coincidence counting rates varied from 0.8 to 10.5 counts per minute, depending on the source and the solid angle used. As a result, the total counting times required were very long. This introduced problems concerning the stability of the apparatus, which were countered by counting coincidences for only a few hours at a time. Between periods of counting the settings of the various instruments were checked. This procedure was followed throughout the experiments described here.

The Results.

For each source, the measurement of F was repeated with four different solid angles for the collection of L X-rays. For each setting of the solid angle, the measurements were continued until at least six thousand coincidence events were recorded. In most cases, they were

continued for a considerably longer period. For each source the measurements were spaced out over a period of at least a year. The values obtained, remained consistently the same for each solid angle used, and the results for different solid angles agreed within the experimental error. For Curium 244, the measurements made with one particular collimator were repeated some eighteen months later to check their consistency. The same result was obtained as before. Both sets of results are presented here.

The results of the measurements of F_o, the observed number of L X-ray photons per alpha particle, for Plutonium 240, Plutonium 238, and Curium 244 decay are shown in Tables 4, 5, and 6 respectively. The counting rates shown in these tables have been corrected for 'dead time' effects in the scaling circuits. The coincidence counting rates, used to compute F_o, have been corrected for the occurrence of random coincidences. The values of F_o shown in these tables are uncorrected for the absorption of the L X-rays in the path between the source and the Sodium Iodide crystal.

The final, mean values of F for the three sources, corrected for absorption effects, are shown in Table 7. The correction for the absorption of the L X-rays was made using the known absorption coefficients and superficial densities of the materials between the source and the crystal. The lead collimator in front of the Sodium

TABLE 4

Measured Values of F_o for Plutonium 240 Uranium 236 Decay

	Solid Angle /4π	Coincidence Count N_{CO}	Alpha Count N_α	Gamma Count N_γ	F_o - The observed No. of L X-rays per α-particle
1.	2.2421×10^{-3}	10503 (9215)	38650179 (9215)	4425198 (9215)	0.09725
		1.13977 c/m	4,195.74 c/m	482.850 c/m	
2.	3.4275×10^{-3}	17614 (10122)	42671776 (10122)	7346692 (10122)	0.09771
		1.74017 c/m	4,217.23 c/m	699.033 c/m	
3.	5.87215×10^{-3}	17828 (6307)	26567998 (6307)	5752125 (6307)	0.09684
		2.82670 c/m	4,213.94 c/m	920.742 c/m	
4.	1.71537×10^{-3}	10449 (11456)	47349026 (11456)	4592863 (11456)	0.09833
		0.912098 c/m	4,274.13 c/m	402.802 c/m	

Notes.

A. The Geometrical solid angles for the collection of L X-rays are quoted as fractions of 4π.

B. In the 2nd, 3rd and 4th columns, the total count is given followed by the counting time in minutes. Beneath these two figures the counting rate, corrected for 'dead time' effects, is given.

C. The coincidence resolving time for each of these experiments was $2T = 6.678 \pm 0.005$ μsecs.

TABLE 5

Measured Values of F_o for Plutonium 238 Uranium 234 Decay

	Solid Angle /4π	Coincidence Count N_{CO}	Alpha Count N_α	Gamma Count N_γ	F_o - The observed No. of L X-rays per α-particle
1.	1.6582×10^{-3}	14518 (5422)	52760999 (5422)	3597015 (5422)	0.1210 ± .0010
		2.67761 c/m	9,741.00 c/m	668.963 c/m	
2.	1.4348×10^{-3}	6410 (2858)	35897385 (3574)	1599093 (3574)	0.1206
		2.24283 c/m	10,052.45 c/m	450.010 c/m	
3.	2.3376×10^{-3}	8770 (2438)	24622127 (2438)	1721982 (2438)	0.1183 ± .0012
		3.59721 c/m	10,107.82 c/m	712.690 c/m	
4.	5.0996×10^{-3}	16541 (2039)	20765736 (2039)	3321078 (2039)	0.1205
		8.11231 c/m	10,192.92 c/m	1663.67 c/m	

Notes

A. The Geometrical solid angles for the collection of L X-rays are quoted as fractions of 4π.

B. In the 2nd, 3rd, and 4th columns, the total count is given, followed by the counting time in minutes. Beneath these two figures the counting rate, corrected for 'dead time' effects, is given.

C. The coincidence resolving time for each of these experiments was $2T = 6.678 \pm 0.005$ μsecs.

TABLE 6

Measured Values of F_o for Curium 244 Plutonium 240 Decay

Solid Angle /4π	Coincidence Count N_{CO}	Alpha Count N_α	Gamma Count N_γ	F_o - The observed No. of L X-rays per α-particle
1. 1.4348×10^{-3}	12166 (4643)	70103847 (4647)	1821644 (4647)	0.0905
	2.62029 c/m	15,104.81 c/m	392.737 c/m	
2. 2.3063×10^{-3}	19402 (4486)	67506718 (4486)	3169277 (4486)	0.09007
	4.32501 c/m	15,067.20 c/m	713.085 c/m	
3. 5.5874×10^{-3}	38142 (3639)	54719646 (3639)	6130036 (3639)	0.0903
	10.48145 c/m	15,037.00 c/m	1684.54 c/m	
4. 5.5874×10^{-3}	40658 (4185)	57605026 (4185)	9241020 (4185)	0.0876
	9.71517 c/m	13,780.44 c/m	2271.99 c/m	
5. 2.3063×10^{-3}	41532 (8703)	120962586 (7789)	4247362 (5408)	0.0888
	4.77215 c/m	15,550.04 c/m	793.172 c/m	

Notes

A. The Geometrical solid angles for the collection of L X-rays are quoted as fractions of 4π.

B. In the 2nd, 3rd and 4th columns, the total count is given followed by the counting time in minutes. Beneath these two figures the counting rate, corrected for 'dead time' effects, is given.

C. The coincidence resolving time $2T = 6.678 \pm 0.005$ μsecs, in all of the experiments, except (4) above where the resolving time used was $2T = 5.692 \pm 0.008$ μsecs.

Iodide crystal ensured that all of the L X-rays entered the crystal near the centre, and since the mean free path in Sodium Iodide for radiation of this energy is only 0.2 mms., it was assumed in the calculation of F, that the efficiency of detection of the crystal for the L X-rays is effectively unity.

Discussion of the Measured Values of F

Very few results are available in the literature which can be compared directly with the measured values of F. Those which are available are shown in the last column of Table 7. Woods Halley and Engelkeimer (1964) have measured the mean L shell fluorescence yields of Uranium 234, and Plutonium 240 following Plutonium 238, and Curium 244 alpha decay respectively, by essentially the same method as the present author. They do not explicitly state their measured values of F, but we can readily deduce their values from the information given in this paper. In both cases their values are lower than those presented here. For Plutonium 240, they find $F = 0.0894$, compared with the present value of 0.0942 ± 0.0012, which is lower by about six per cent. For Uranium 234, their value of 0.1065 is some sixteen per cent lower than the present value of 0.1283 ± 0.0010. The reason for this disagreement is difficult to find, but it may lie in their measurement of the geometrical solid angle for the collection of photons. Since this quantity depends on the square of the distance from the

TABLE 7

Mean Values of F - The No. of L X-rays per α-Particle..

Source	L X-ray Solid Angle	F_o	F	Standard Deviation	Final Mean Value of F	Other Measurements of F
Cm 244	5.5874×10^{-3}	0.0903	0.0952	± .0015	0.0942 ± 0.0012	0.092[8]
	5.5874×10^{-3}	0.0876	0.0924	± .0014		
	2.3063×10^{-3}	0.0888	0.0937	± .0014		0.0894[11]
	2.3063×10^{-3}	0.0901	0.0950	± .0016		0.0996[4]
	1.4348×10^{-3}	0.0905	0.0955	± .0018		
Pu 240	5.8722×10^{-3}	0.0968	0.1034	± 0.0012	0.1041 ± 0.0007	0.1096[4]
	3.4275×10^{-3}	0.0977	0.1045	± 0.0013		
	2.2421×10^{-3}	0.0973	0.1042	± 0.0014		
	1.7154×10^{-3}	0.0983	0.1052	± 0.0021		
Pu 238	5.0996×10^{-3}	0.1205	0.1288	± 0.0023	0.1283 ± 0.0010	0.13[1]
	2.3376×10^{-3}	0.1183	0.1264	± 0.0027		0.1065[11]
	1.6582×10^{-3}	0.1210	0.1288	± 0.0022		
	1.4348×10^{-3}	0.1206	0.1289	± 0.0029		0.133[4]

Notes

A. Mean value of F in column 6 is a weighted mean of the values given in column 4.

B. Solid Angles are again fractions of 4π.

C. The Solid Angles are accurate to ± 0.2 per cent.

D. Accuracy is not claimed for the 4th and 5th significant figures which are quoted.

E. In column 7 the numbers in brackets refer to the reference numbers at the end of Chapter 5.

source to the collimator aperture, it is very susceptible to small variations in that distance. In their experiments they made observations for only one value of this solid angle. Any systematic error in their measurement of this quantity will thus remain hidden. The conclusion that their results are too low is reinforced by a comparison of their value of F for Th 230 decay with that of Booth, Madansky and Rasetti (1956), obtained by the same method. The latter group found F = 0.11 $\pm$ 0.015, a value some twenty six per cent higher than the value, F = 0.087, obtained by Woods Halley and Engelkeiner.

The only other experimental value available for comparison is a value of F = 0.13 for Uranium 234, following Plutonium 238 decay, given by Asaro and Perlman (1954). Although this measurement agrees well with the present one, little weight can be attached to it, since it was obtained by a rough measurement, involving a comparison with the intensity of the 60 keV gamma ray from Amerium 241.

We may also compare these results with values derived from Listengarten's (1961) semi-empirical calculations of fluorescence yields, using the theoretical conversion coefficients of Sliv and Band (1958). The values which are deduced in this manner are all slightly higher than the experimental values presented here, but are in reasonably good agreement with them. Again this agreement is not to be relied on. Listengarten's predicted L fluorescence and Auger yields of Uranium and

Plutonium differ considerably from the values derived in Chapter 8 from the present values of F. Hence the apparent agreement may be quite fortuitous.

Finally, we may compare the value of F for Plutonium 240 with a value derived from the experimental values of the plutonium yields given by Salguiero et al. (1961), using again the theoretical conversion coefficients of Sliv and Band (1958). The value obtained from their results is $F = 0.092$ which is in reasonable agreement with the present value of $F = 0.0942 \pm 0.0012$.

The author believes that the values of F presented in Table 7 are reliable, and they will be used in Chapter 8 in the calculation of the LII shell yields of Plutonium and Uranium.

Other Processes Contributing to the Value of F.

Although the internal conversion of the electric quadrupole transition de-exciting the first excited state of the daughter nucleus is the main process producing L shell vacancies in the decays studied, other mechanisms also contribute. It is important, for the subsequent calculation of fluorescence yields from the measurements described above, that the contributions from these other sources are either negligible or can be accurately accounted for. The extent of these contributions is discussed below.

L shell vacancies are produced in at least three other ways in these decays, namely:

a) The internal conversion of higher energy gamma rays in the L subshells.

b) The internal conversion of higher energy gamma rays in the K shell, followed by the emission of K_α X-rays.

c) The process known as nuclear 'shake-off'.

Processes a) and b) are readily dealt with. From the decay schemes shown in Figures 4, 5, and 6, it is readily seen that very much less than one per cent of the total number of alpha decays proceed via states higher in energy than the first. The intensities of these alpha transitions have been accurately measured, and it is a simple matter to determine the number of K- and L-shell vacancies per disintegration due to these transitions, using Sliv and Band's (1958) theoretical conversion coefficients. The correction for the production of L shell vacancies following K_α X-ray emission can then be made from a knowledge of the K fluorescence yield , and of the value of f_{KL}, the fraction of K X-rays resulting in an L shell vacancy. Values of f_{KL} can be obtained from the graph of f_{KL} versus Atomic number given by Robinson and Fink (1960). Both these corrections are small and are accurately accounted for in the calculations of the fluorescence yields of Uranium and Plutonium.

The third process is nuclear 'shake-off'. In this effect the sudden change in nuclear charge, when an alpha particle is emitted from the nucleus, produces a varying electric field in the vicinity of the atomic electron orbits. The resulting change in the electrostatic

environment of the atomic electrons may cause some of the electrons to be ejected from the atom. The resulting vacancies in the atomic electron shells are then filled by electrons from higher shells with the emission of characteristic X-rays or Auger electrons. Such a process may give rise to the simultaneous emission of an alpha particle and an L X-ray, which would be recorded as a coincidence event in the experiment to measure F.

Now the velocity (v_α) of the alpha particles emitted in alpha decay is small compared with the velocity (v_e) of the inner orbital electrons. For example in the much studied case of Po 210 alpha decay, v_α / v_e is approximately 0.087 for the K electrons. The large mass of the alpha particle means that it has a small wavelength. Classically we can view the process as one in which the alpha particle, moving slowly through the atom, causes a perturbation of the atomic electron orbit, which varies with the motion of the electron. Such a slowly varying perturbation is known to produce very small effects, so that the probability of ionisation in the K shell is expected to be small. As we progress to the outer shells of the atom, the orbital electrons have smaller velocities, and the perturbation due to the alpha particle becomes less adiabatic. The resulting ionisation probability becomes much larger.

Migdal (1941) and Levinger (1953) have treated this process as an adiabatic perturbation. They calculated the ionisation probabilities for the K- and L-shells of

Lead following Po 210 alpha decay. Levinger predicted a value of 10^{-7} electron vacancies per alpha particle for the K shell, and 1.1×10^{-4} vacancies per alpha particle for the L shell. Characteristic X-rays from the K-, L-, and M-shells of Lead, associated with Po 210 decay have been studied by several authors. Their results, quoted by Levinger, show approximately 10^{-6} K X-rays per alpha particle, and 3×10^{-4} L X-rays per alpha particle. The order of magnitude agreement between theory and experiment is considered to be satisfactory, since any refinement of the theory, such as a screening correction or the addition of higher multipole transitions (Levinger considered only dipole and quadrupole transitions) will tend to increase the number of vacancies created.

The yield of L X-rays per alpha particle from nuclear 'shake-off' in Cm 244, Pu 238 and Pu 240 alpha decays should not be very different from that observed in Po 210 decay. Hence a yield of about 0.3×10^{-3} L X-rays per alpha particle might be expected, compared with the observed total yields of approximately 0.1 L X-rays per alpha particle. Hence for our purposes this effect is negligible, and our results will not require to be corrected for it.

REFERENCES - CHAPTER 5

1. Asaro, F. and Perlman, I. (1954), Phys. Rev. 94, 381.

2. Booth, E., Madansky, L. and Rasetti, F. (1956), Phys. Rev. 102, 800.

3. Levinger, J.S. (1953), Phys. Rev. 90, 11.

4. Listengarten, M.A. (1961), Isvest. Akad. Nauk SSSR, Ser. Fiz. 24, 1041.

5. Migdal, A. (1941), J. Phys. USSR, 4, 449.

6. Park, J.J.H. (1961), Thesis, University of Edinburgh.

7. Robinson, B.L. and Fink, R.W. (1960), Rev. Mod. Phys. 32, 117.

8. Salguiero, L., Ferreira, J.G., Park, J.J.H. and Ross, M.A.S. (1961), Proc. Phys. Soc. A77, 657.

9. Sliv, L.A. and Band, I.M. (1958), Leningrad Physico-Technical Institute Report (Translation; 1958, Reports 57ICCKI, 58ICCLI, Physics Department, University of Illinois).

10. Wapstra, A.H. (1965), 'The Coincidence Method' in α-β-, and γ-Ray Spectroscopy, Edited by K. Siegbahn. (North Holland Publishing Co., Amsterdam).

11. Woods Halley, J. and Engelkeimer, D. (1964), Phys. Rev. 134A, 24.

CHAPTER 6

MEASUREMENT OF F_3' WITH A CURVED CRYSTAL SPECTROGRAPH

F_3', the ratio of the number of L X-ray photons from the LIII shell to the number from the LII shell, was determined for the L X-rays of Uranium following Plutonium 238 alpha decay. The measure of F_3' was obtained from a measurement with a curved crystal spectrograph of the relative intensities of the individual L X-ray lines. Three such instruments had been constructed and were available in this laboratory.

Originally a spectrograph, having a mica crystal bent to a cylinder of 46.40 centimetre radius, was built by Ewan (1952) to study low energy gamma rays and X-rays. Ewan used this instrument to examine the L X-ray and gamma ray spectrum of RaD. As a result of this experience he constructed two smaller instruments, having mica crystals bent to cylinders of 20.0 centimetre radii. Since the smaller radius spectrometers have a larger solid angle of collection from the same size of source, the exposure times for the recording photographic plate could be reduced by a factor of two or three, depending on the source position. Although the larger spectrometer is superior where high resolution or the accurate determination of wavelength is required, several considerations dictated the choice of one of the 20.0 centimetre radius spectrographs for the present investigation.

The primary reason was that the Plutonium 238 source available was nominally only 2.6 mC strong, which would have meant an exposure of nine months on the 46.40 centimetre radius spectrograph, compared with three months on the smaller spectrometer. The resolution of the smaller instrument was entirely adequate to resolve the L X-ray lines of Uranium. In addition, Cochran (1955) had carried out an experimental calibration of the variation of detection sensitivity with photon energy for the twenty centimetre spectrograph.

To aid the understanding of the experiment described below, it is proposed to give a brief account of the history and relevant theory of the bent crystal spectrometer, and a description of the mode of operation of the spectrograph calibrated by Cochran, before describing the present experiment, and discussing the results obtained. This account owes much to the early papers of Dumond and Cauchois, who pioneered the use of the bent crystal spectrometer, and to several excellent review articles by Knowles (1965), Bartholomew et al. (1960), and by Dumond (1955, 1961).

The Bent Crystal Spectrometer

Direct crystalline diffraction has been used to examine X-ray spectra since the experiments of von Laue and Bragg in the early years of this century. Itsuse was extended to the study of nuclear gamma rays by Rutherford and Andrade (1914), when they measured the

wavelengths of the gamma rays of Ra (B + C) after diffraction by transmission through a plane crystal lamina. Frilley (1929) and Thibaud (1924) used a similar technique to measure the wavelengths of the RadioThorium gamma rays. Two main difficulties were encountered in these experiments. The diffracted angles involved were small, and hence the diffracted image on the recording photographic film was superimposed on an intense background of directly transmitted, and diffusely scattered radiation. Also the sources available were weak, and the transmission efficiency of the crystal low, so that the exposure times required were often excessively long. The advent of the magnetic spectrometer, which allowed precise measurements of the internal conversion electrons associated with the nuclear gamma rays, and used weaker sources, caused this method to be largely superseded.

The answer to the difficulties of crystal diffraction spectroscopy was the introduction of the focussing crystal spectrograph. Dumond and Kirkpatrick (1930) and Cauchois (1932) both realised that this could be achieved by using the principle of the Rowland concave diffraction grating, which operated successfully in the optical region.

If gamma rays were to be exactly focussed by a curved crystal, two apparently incompatible conditions imposed by the Bragg equation had to be satisfied simultaneously at all points on the curved reflecting boundary of the

crystal. One condition defined the position of each point on the reflecting boundary surface, and the other defined the direction of the atomic reflecting planes at that point. It can be readily demonstrated that these two conditions cannot be simultaneously satisfied over an extended surface, if the atomic reflecting planes coincide with the reflecting boundary, and if two conjugate foci are required.

Dumond and Kirkpatrick (1930) resolved this apparent difficulty by suggesting that the crystal boundary should coincide with the reflection boundary, but that the reflecting planes need not. Further, they indicated two geometries in which their condition for exact focus held. In Figure 18(a), the reflection case, a real image is formed at I_λ of a source at S_λ. In Figure 18(b), the transmission case, a real image is formed at I_λ with a virtual source at S_λ, after transmission through the crystal from a source outside the focussing circle.

Cauchois (1932) realised that the condition fixing the position of the crystal boundaries was less stringent than that fixing the direction of the atomic reflecting planes. She constructed an approximate focussing spectrograph of the type shown schematically in Figure 19. The focal circle is then tangent to the neutral axis of the crystal. This introduces an aberration of focus for rays reflected from regions well removed from the centre of the crystal. But Cauchois was able to show that this aberration is small if the aperture width of the crystal

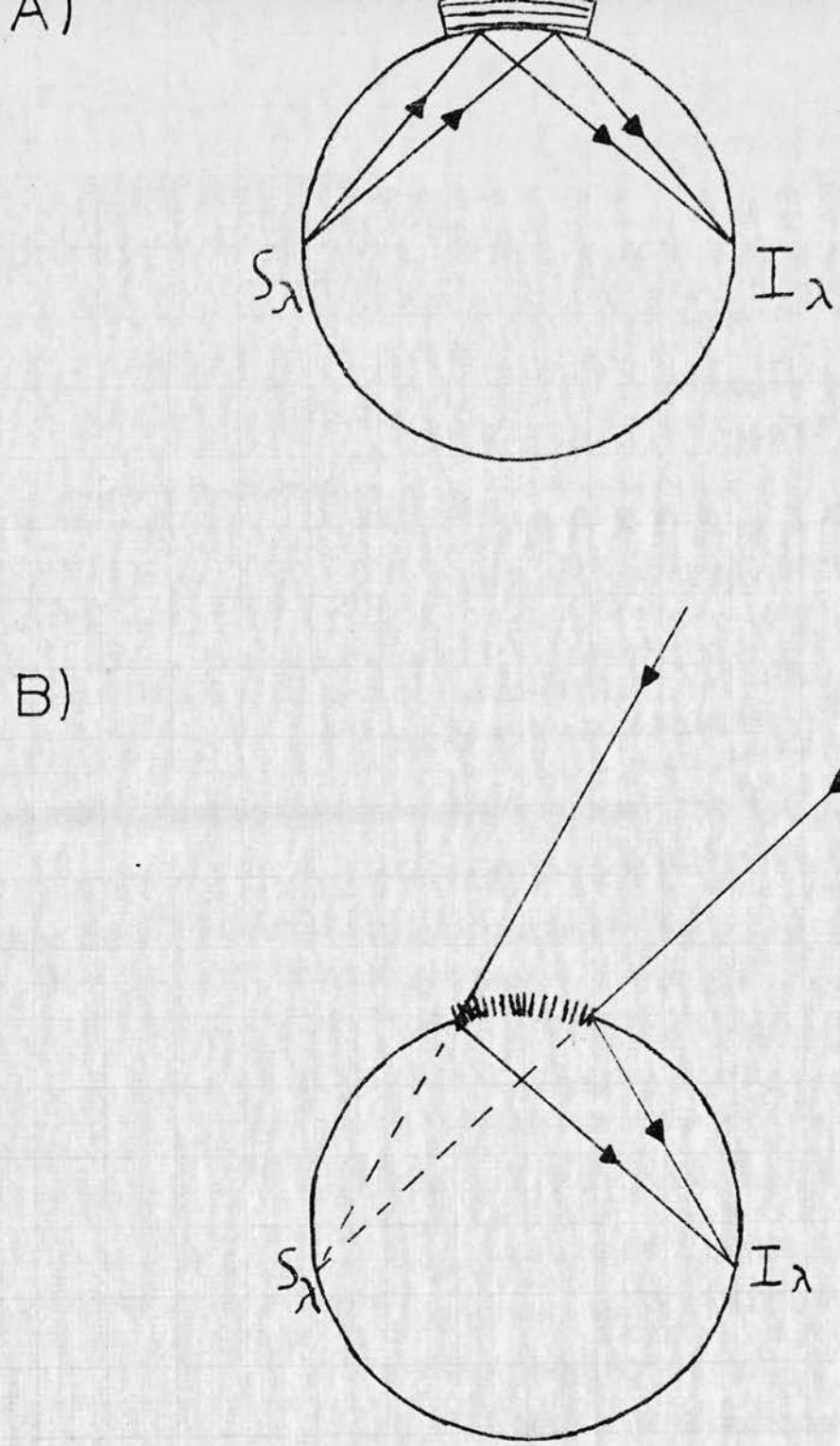

DUMOND'S TWO POSSIBLE GEOMETRIES FOR A FOCUSSING γ-RAY SPECTROMETER

A) Reflection case

B) Transmission case

Figure 18

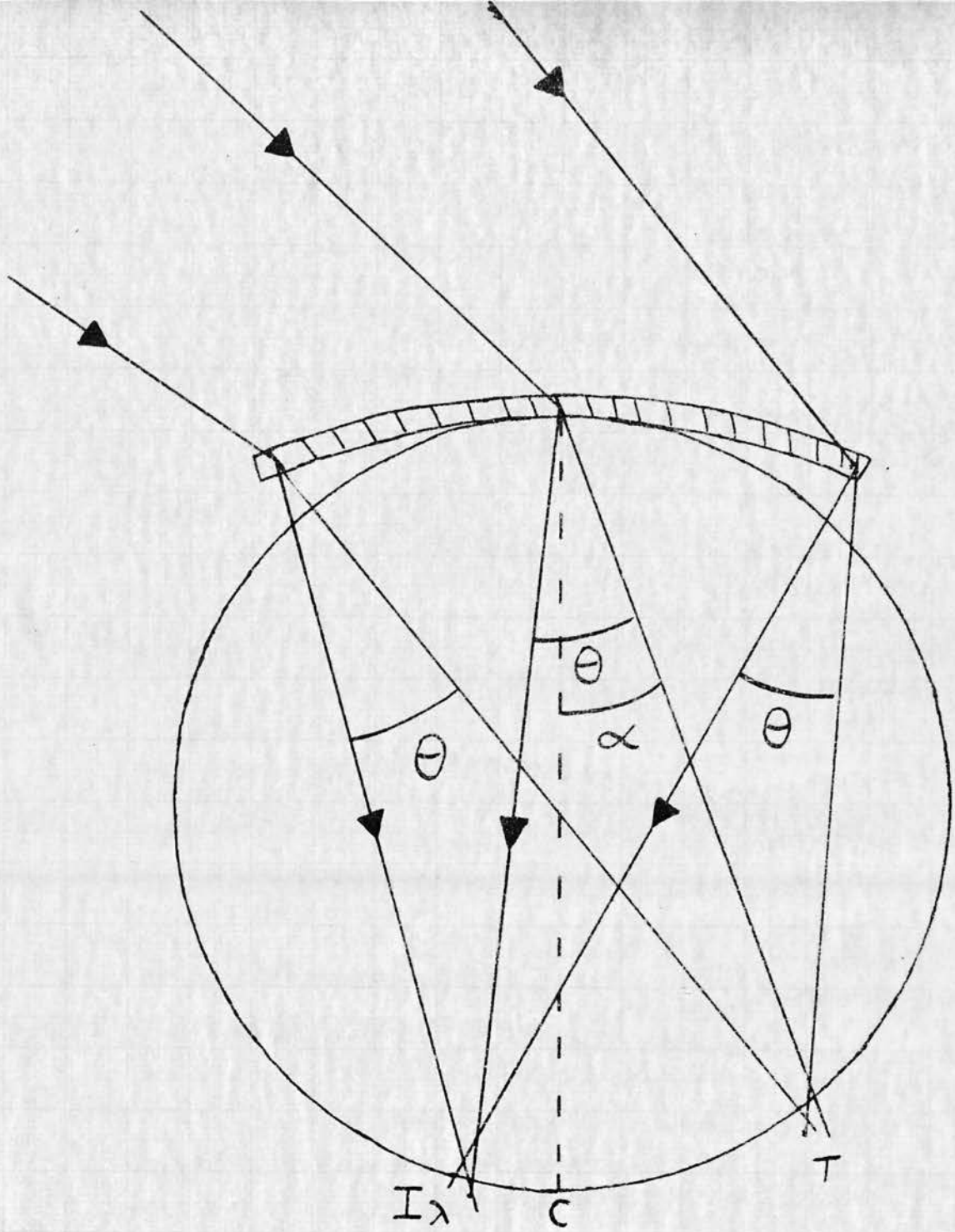

THE APPROXIMATE FOCUSSING ARRANGEMENT OF THE CAUCHOIS SPECTROGRAPH

FIGURE 19.

lamina is kept small. She also pointed out that the bending of the crystal planes introduces a 'back-to-front' focussing through the crystal, due to the dilation and contraction of the spacing of the crystal planes at the back and front of the bent crystal. This effect is such that the spectrometer appears to give perfect focus from that circle which passes through the neutral axis. Using this approximate focussing spectrograph, with an extended source and photographic recording of the transmitted, diffracted beam, Cauchois (1934) measured energies of gamma rays up to 750 keV.

The next major advance in this field was again due to Dumond (1947). He found a method of profiling the crystal surface, which enabled him to make an exact focussing spectrograph, with two metre radius of curvature. This spectrometer was operated in an arrangement which was the inverse of that of Cauchois. In the Dumond arrangement, shown schematically in Figure 20, a concentrated line source is placed on the focal circle. The source is moveable, and a spectrum is obtained by plotting the reflected intensity entering the detector as a function of the position of the source on the focal circle. With this instrument, Dumond was able to measure gamma ray energies up to 1.5 MeV with a precision of 1 in 10^3.

Each of the two modes of operation has certain advantages. The Cauchois arrangement has the advantage that all of the lines studied are recorded simultaneously. There is then no need to monitor the primary source

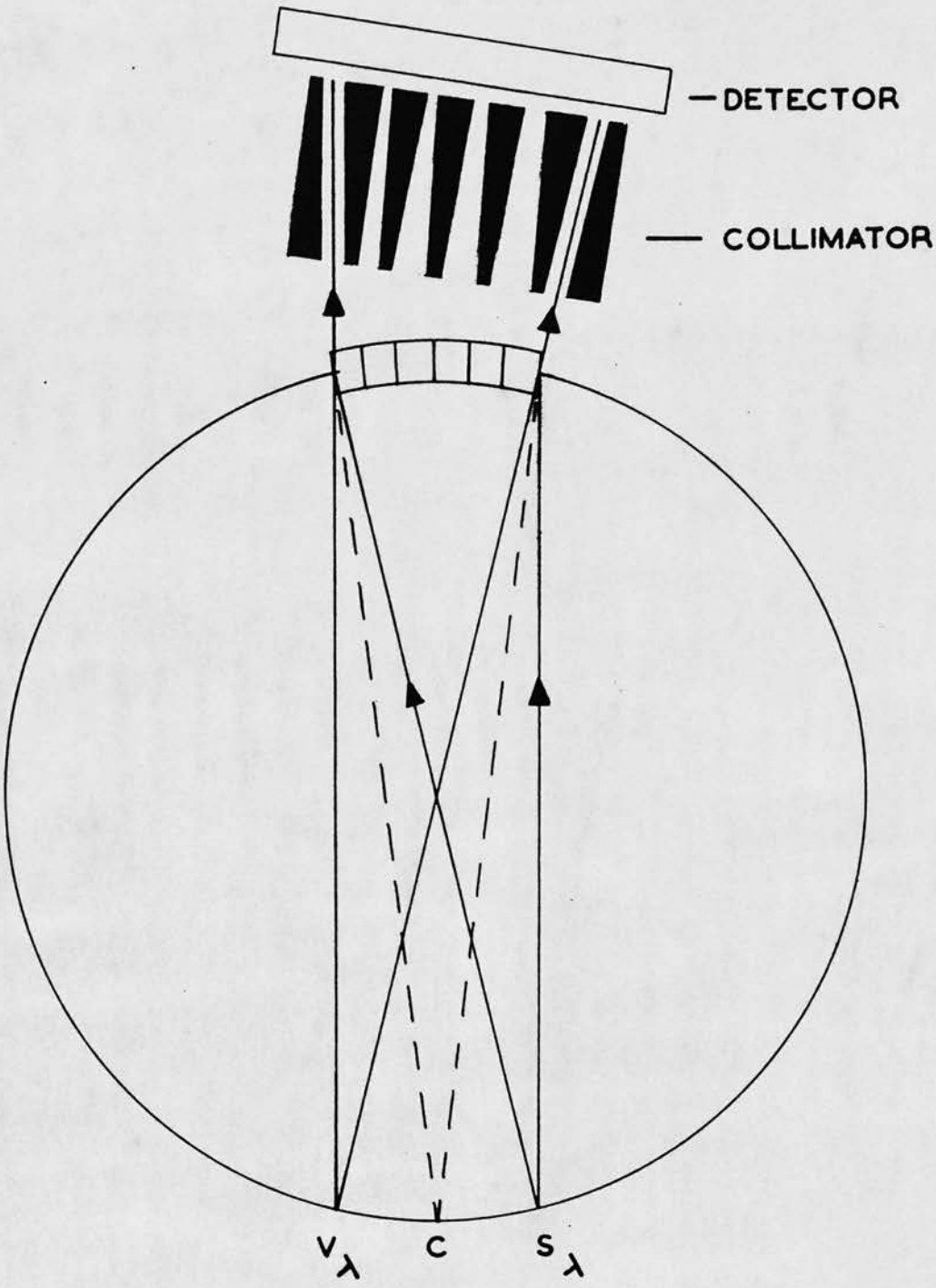

Dumond's exact focussing spectrometer

Figure 20

strength with time. At high energies this advantage is nullified by the difficulty of shielding the nuclear emulsion from the very intense direct beam. In the inverse arrangement, the Dumond arrangement, this direct beam is suppressed by a fan shaped system of baffles like that shown in Figure 20. The Dumond arrangement also has the advantage that each atom in the source can emit its characteristic radiation into the complete solid angle presented by the crystal, and after selective reflection be detected in the counter. In the Cauchois mode of operation, the condition for the reflection of radiation from a particular atom into a focussed line is only satisfied over the diffraction line width. Hence for the same source strength, the Dumond arrangement provides a considerable increase in collecting power.

In recent years curved crystal spectrometers with very large radii of curvature have been built and operated successfully in both modes of operation. Chupp et al. (1958) have used an exact focussing spectrometer of 2.0 metre radius in the Cauchois mode to measure Coulomb excited gamma rays of 2.0 MeV energy. Kazi et al. (1961) have successfully used a 7.0 metre radius Cauchois spectrograph to measure the energies of neutron capture gamma rays up to 4.0 MeV energy. Neutron capture gamma rays of several MeV energy have also been examined by Rose et al. (1957) with a 7.7 metre radius spectrometer operated in the Dumond manner.

The Present Spectrograph

The 20.0 centimetre radius spectrograph used in the present experiments uses the approximate focussing system of Cauchois (1932). A photograph of the instrument is shown in Figure 21. The crystal is of mica, a material which would be very difficult to profile to an exact radius of curvature. Hence the crystal was only bent to a radius of 20.0 cm, by clamping it between concave and convex, cylindrical, hard steel blocks.

Ewan (1952) has described the construction of the spectrograph in detail. The aberrations introduced by the approximate focussing have been calculated by ~~both Ewan (1952) and~~ Cauchois (1934).

Ilford G5 electron sensitive emulsion plates, 200 microns thick, were used to record the X-ray spectra. The film, 3" x 1", rests in a small holder on the focussing circle, as shown in the photograph. This film sits at a tangent to the focussing circle, thus introducing a further small aberration of focus. This aberration was small enough to be neglected in the present experiments, where relative intensities not energies were measured. The photographic development of the 200 micron thick nuclear emulsion requires a special technique. The method of processing used was a variant of the 'temperature cycle' development method, first conceived by Dilworth et al. (1950). This method has been used by several experimenters in this department. In

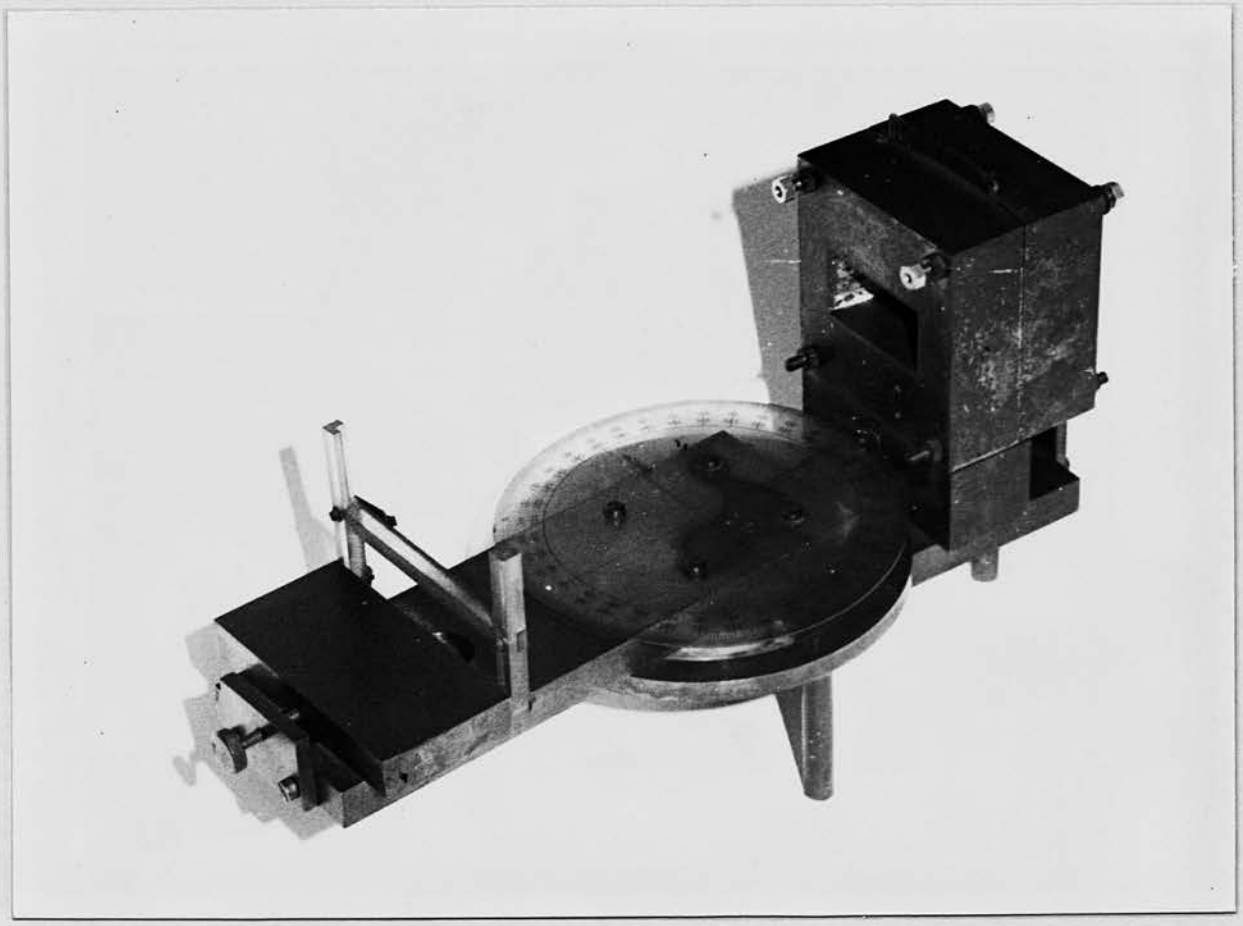

Figure 21

Photograph of the 20.0 centimetre radius Curved Crystal Spectrograph.

particular Ewan (1952), Cochran (1955), and Salguiero et al. (1961) have all used this technique to process the G5 emulsions exposed on the curved crystal spectrograph. Full details of the method adopted are given in Appendix B.

The Size and Position of the Source

When examining a large range of wavelengths with a curved crystal spectrograph it is not possible to utilise both the whole source, and the whole crystal over the complete range. Consider Figure 22. We have a source of radiation AB, which emits radiation of a number of wavelengths, the longest of which (λ_1) has a virtual source V_1, and the shortest (λ_2) has a virtual source V_2. This means that only those radiations of wavelength λ_1 which are emitted in the direction of V_1 are selectively focussed on the focussing circle at I_1.

It is immediately obvious that if the whole crystal aperture is used then different parts of the source are used for different wavelengths, namely X_1Y_1 in the case of λ_1, and X_2Y_2 in the case of λ_2. On the other hand, if we restrict the source to the limits X_1Y_2, then different parts of the crystal are used to reflect different wavelengths, e.g. PN for λ_1, and MQ for λ_2. If the first method is adopted, and a source of extent X_2Y_1 is used, then two objections are encountered. Firstly, no part of the source must be visible from I_2, since then

FIGURE 22

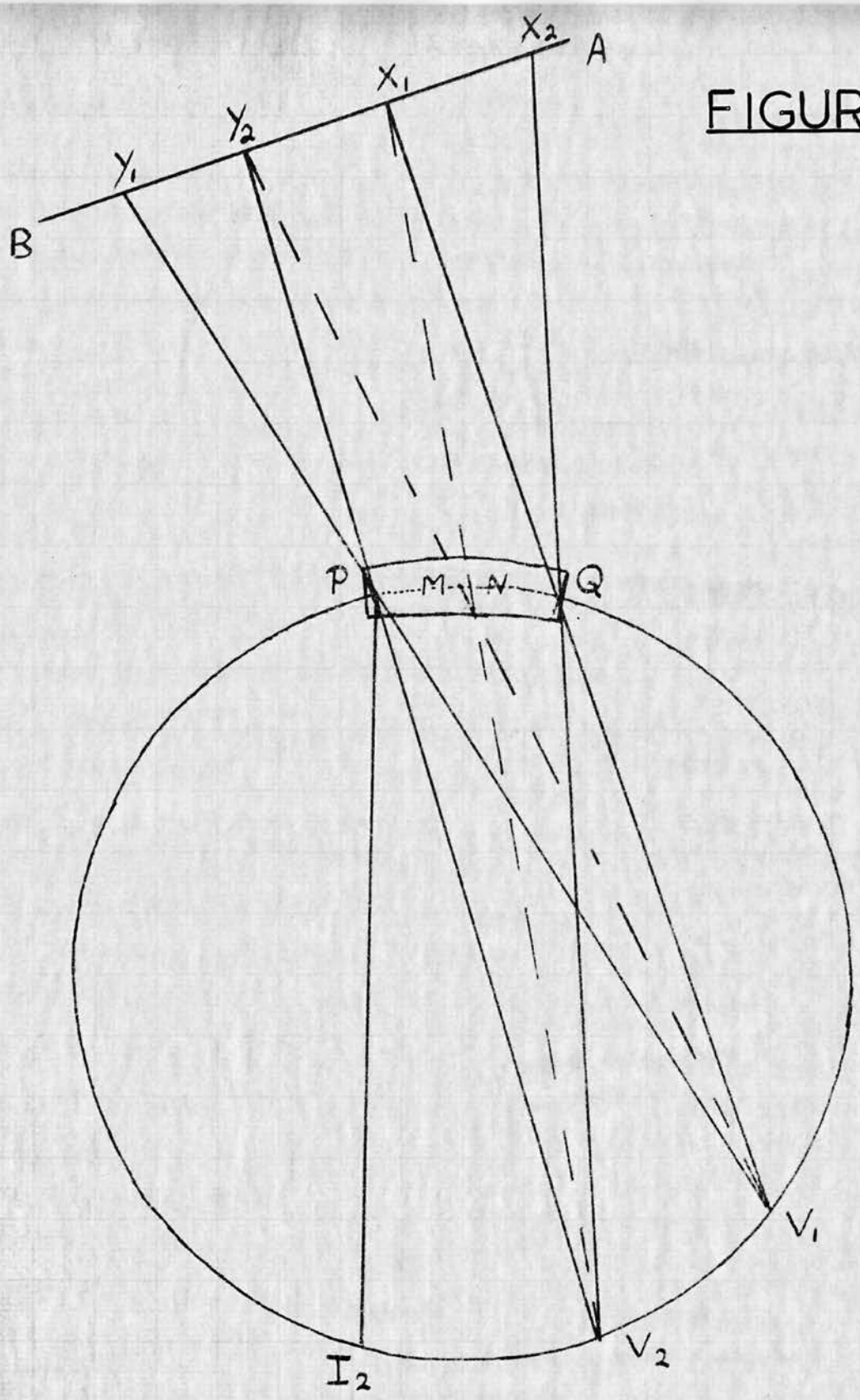

DIAGRAM SHOWING THE ALTERNATIVE SOURCE SIZES FOR INTENSITY MEASUREMENTS

the film would be fogged by the direct beam. Secondly, the source must be uniformly deposited over its entire extent. Experience has shown that this is difficult to achieve. Corresponding to the latter disadvantage in the alternative method, a source of extent less than X_1Y_2, we might expect some variation of crystal reflectivity over the crystal surface. Ewan (1952) tested this, and found no significant variation over the crystal aperture. Hence this method has generally been adopted in this laboratory.

The choice of position of the source is readily made on the following basis. It is readily seen from Figure 22 that if the lines V_2Q and V_1P diverge, then the source can be placed as far away from the crystal as desired, to prevent the direct beam from falling near I_2. If they converge, then the source must be bounded by the triangle formed by these two lines, and I_2Q produced.

Now let θ_1, θ_2 be the Bragg angles for λ_1 and λ_2 ,
and $2\omega_o$ be the angle subtended at C by the aperture PQ.
α be the inclination of the reflecting planes to the normal,
C' be the centre point of the aperture,

as shown in Figure 23. Simple geometry shows that the angles that the three lines limiting the source position make with CC' are,

The incident ray at P : $-\omega_o + \alpha + \theta_1$,
The incident ray at Q : $\omega_o + \alpha + \theta_2$,
The diffracted ray at Q : $\omega_o + \alpha - \theta_2$.

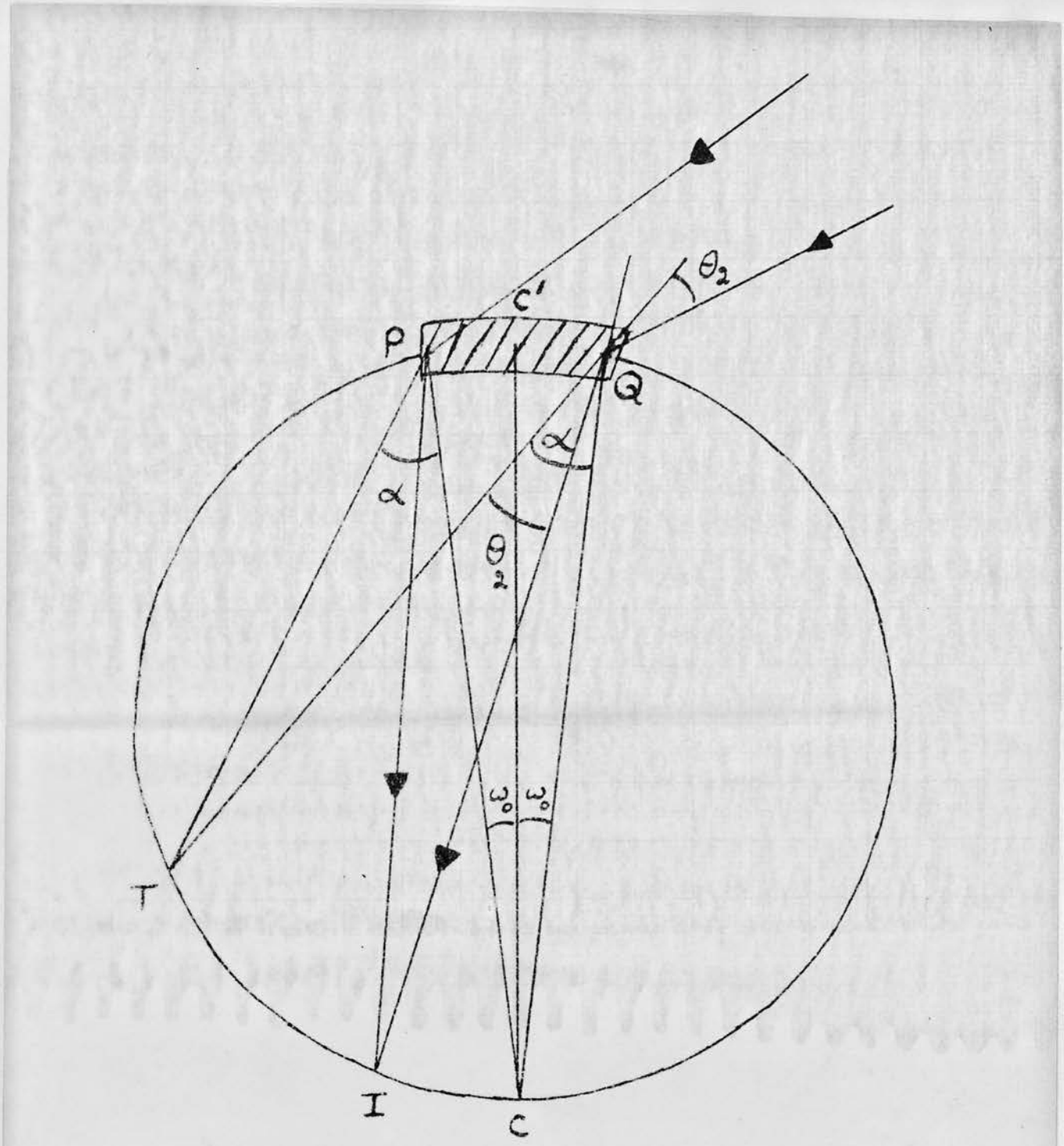

DIAGRAM SHOWING THE GEOMETRY FOR THE DETERMINATION OF THE SOURCE POSITION

Figure 23

The angles ω_o and α are properties of the spectrograph, and equal 0.04763 and 0.17742 radians respectively. θ_1 and θ_2 are defined by the wavelength range which is to be examined. Hence if we choose CC', and the tangent to the focal circle at C' as coordinate axes, we can draw the lines V_2Q, V_1P, and I_2Q on squared paper. Then we can easily choose a suitable source position.

In practice the axis CC' is achieved by a long brass tube, which slides through a hole in a brass block and can be firmly clamped. The brass block in its turn can be clamped to the steel blocks of the crystal holder, and adjusted to be accurately at right angles to the face of the steel block. The second coordinate axis is then supplied by a shorter brass tube, attached to the first at right angles, and also free to move.

An error of approximately 2-3 mm. in 100 cms. is possible in setting this coordinate system. The Plutonium 238 sourcewas 14 mms. in diameter, and this allowed an error margin of 5 mms. in setting up the source.

The Sensitivity - Energy Calibration

The greatest difficulty inherent in the determination of relative intensities of gamma ray, and X-ray lines with a curved crystal spectrograph, employed in the above mode, is the calibration of the instrument. This difficulty arises because of the rapid variation with wavelength, of both the reflectivity of the crystal

planes, and the absorption of the nuclear emulsion.

Previous work on the variation of reflectivity of the crystal with wavelength shows considerable disagreement. Jaffe et al. (1955) and Day (1955, 1956) have used curved crystal spectrometers, with Topaz crystals bent to ten inch radii, to measure the relative intensities of L X-ray lines and gamma rays, emitted following the decay of several heavy elements. In both cases they have included a correction for the variation of reflectivity (R) with wavelength (λ). The correction which was used assumed a different power of λ in the expression for R in the two cases. Jaffe et al. assumed that R was proportional to λ^2. This assumption was based on Lind et al.'s (1950) work, with a two metre radius, bent Quartz crystal, which showed R proportional to λ^2 for $0.5\ \text{Å} > \lambda > 0.095\ \text{Å}$ ($25\ \text{keV} < h\nu < 1.3\ \text{MeV}$), and Browne's (1952) observation that 'lines well spaced in energy' reflected from both Quartz and Topaz showed the same relative intensities. Jaffe et al. used their spectrometer to examine the Neptunium L X-rays following Americium 241 alpha decay. These L X-rays have energies in the range 13-22 keV, which is outside the range of Lind et al.'s work. Day (1955), on the other hand, used a correction for R, with R proportional to λ. Later he corrected this to R proportional to $\lambda^{1.35}$. His second expression was obtained by comparing the relative intensities of the 84 keV gamma ray, and ~ 50 keV K X-rays emitted in the decay of

Tm 170. As in the case of Jaffe et al., he applied this correction far outside the region in which it was verified.

Cochran (1955) measured the variation of sensitivity of the 20.0 centimetre spectrograph used here, over a wide range of wavelengths. He compared the measured sensitivity with a calculated sensitivity. His calculation evaluated the sensitivity in terms of the number of silver grains per incident photon in the developed emulsion, allowing for the absorption of radiation between the source and the emulsion, and the processes of absorption leading to the formation of developable silver bromide grains in the emulsion. His calculation employed the mean grain number - energy calibration of Zajac and Ross (1949). This calculation was compared with the observed sensitivity, which was obtained by determining the ratio of the blackening in the $K(\alpha_1 + \alpha_2)$ and $K\beta_1$ lines for the K X-rays of some thirteen elements, covering the energy range from 8 keV to 40 keV, and comparing it with the relative intensities measured by Williams (1933) using an ionisation chamber. The calibration was extended to higher energies, by comparing the intensities of the 82 keV gamma ray, and 31 keV K X-rays emitted in the disintegration of Xe 133, with the intensities of the same radiations recorded in a proportional counter by Hughes. The calibration was described in full by Cochran (1955). The final calibration curve adopted by Cochran is shown in Figure 24.

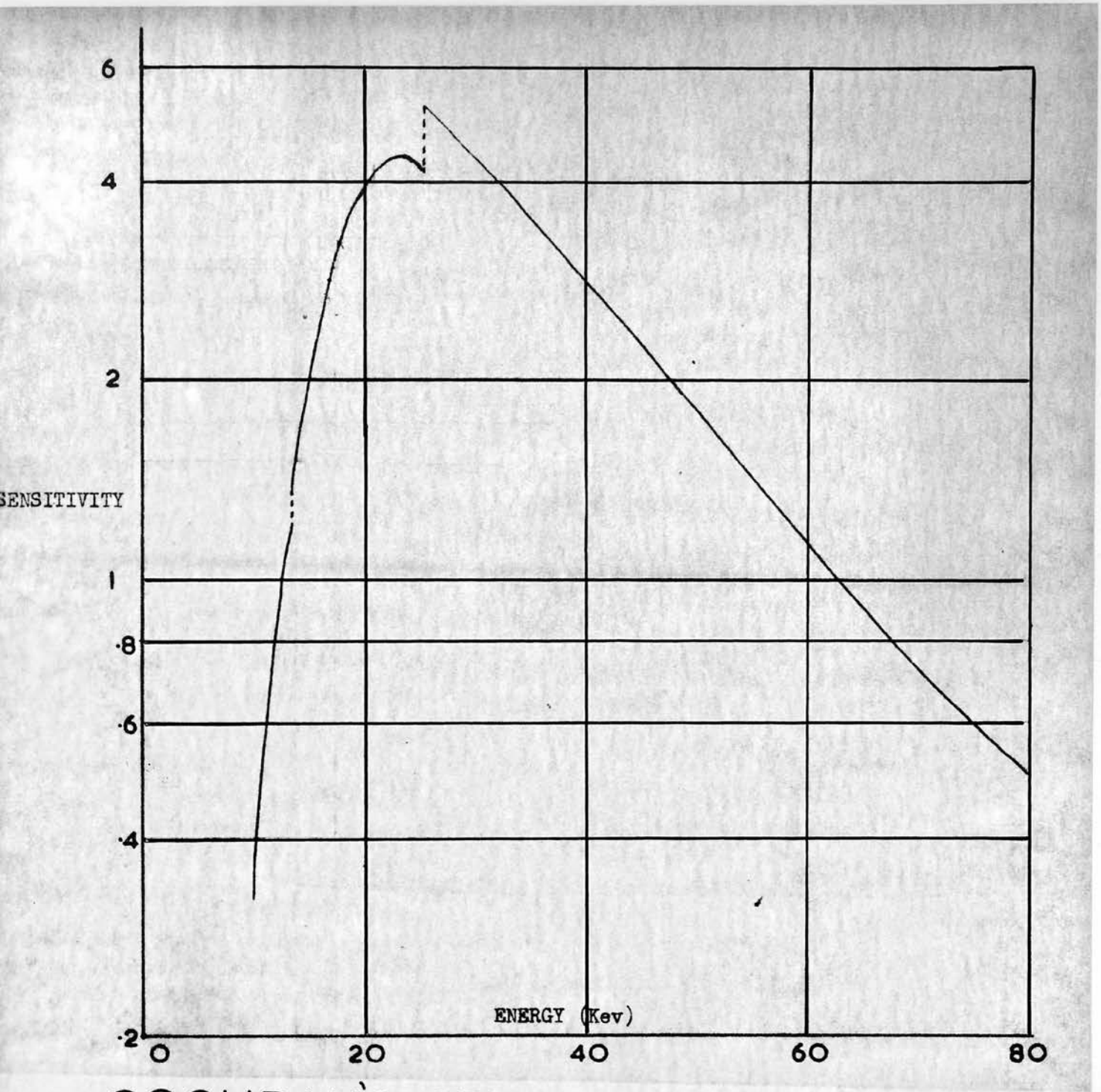

COCHRAN'S SENSITIVITY-ENERGY CURVE FOR THE CURVED CRYSTAL SPECTROGRAPH.

Figure 24

Since Cochran's calculation took no account of the dependence of the sensitivity on crystal reflectivity, the ratio of his observed sensitivity to the calculated sensitivity gave the coefficient of reflection of the (100) planes of the mica crystal. Cochran and Ross (1958) found that for $\lambda < 0.5$ Å ($h\nu > 25$ keV), R is proportional to $\lambda^{1.9}$, which is in reasonable agreement with other experimenters. At lower energies, this relationship no longer holds. Despite the great difficulty of performing measurements at low energies, their results showed conclusively that a constant power law does not hold over the whole range of observation. They concluded that if relative intensity measurements are to be made with such a spectrometer in the wavelength region below 0.5 Å, then it is essential to measure the value of R. The present experiment was carried out under the same conditions as Cochran's direct calibration, and the observed relative intensities were corrected using it.

The Present Experiment.

The Plutonium 238 source, which was used in the present experiment, was obtained from A.E.R.E. Harwell. It consisted of about 150 μgms. of Plutonium painted uniformly on a thin, stainless steel disc, three centimetres in diameter. The source material covered an area, fourteen millimetres in diameter. A small amount of Pu 239, 4.5 per cent by weight, was present in the source.

Since the half life of Pu 239 is approximately 2.4×10^4 years, it contributed only 0.017 per cent of the activity of the 2.6 mC source. Hence no correction was required for the presence of the impurity. The steel source tray was covered with a uniform protective covering of polyvinyl formar, of superficial density 247 μgms./cm.^{2}.

Figure 25 shows a horizontal section of the steel collimator, and steel source holding arrangement used in the experiment. Section A could be removed from the larger steel cylinder B. It was sent to Harwell and the steel source tray was inserted in the position shown. This small steel cylinder was then sealed at C with a mica window, of superficial density 2.30 μgms./cm.^{2}. In transit between Harwell and Edinburgh, the mica window was covered by a protective brass screw cap. On arrival in Edinburgh this brass cover was removed, and the steel source holder A was inserted inside the collimator, B. This procedure dispensed with the need to handle the highly toxic Plutonium source.

The midpoint of the Plutonium source was placed at the point (7.55 cms., 22 cms.) relative to the centre of the crystal. This gave full aperture over the complete Uranium L X-ray spectrum, and an exposure of ten weeks was given. The Ilford G5 emulsion was then processed using the method described in Appendix B,

The quality of the processed plate was not good, and the region near the Uranium L_α lines was spoiled by

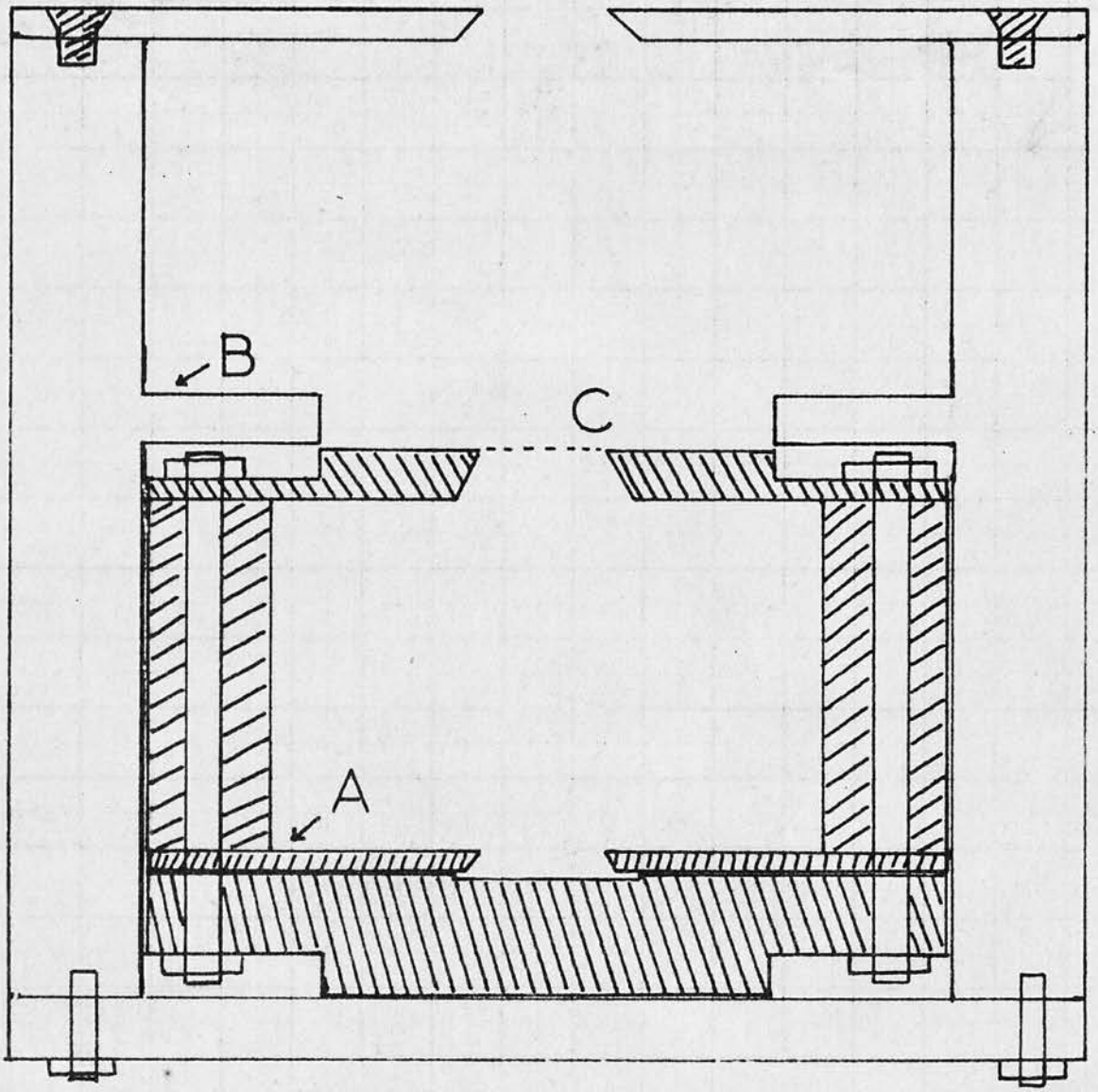

STEEL SOURCE HOLDER &
COLLIMATOR FOR THE Pu238
SOURCE

A -SOURCE HOLDER
B -COLLIMATOR
C -MICA WINDOW

Figure 25

a series of marks, possibly due to radiation from radioactive material in the black paper used to cover the emulsion during the ten week exposure. Some five or six lines were visible to the eye.

The plate was microdensitometered using an automatic recording microdensitometer (Model Mk. III B),* made by Joyce, Loebl and Co. Ltd. A series of six traverses were made at different 'heights' on the plate, and the results were summed. This procedure was necessary because of the large background fluctuations which occur in this type of emulsion. These fluctuations tend to mask or enhance the weaker lines on the plate. The averaging of a series of traverses not only smooths out these fluctuations, but reveals the presence of a true line, since evidence of it appears on every traverse. Figure 26 shows a portion of the summed spectrum, in the region of the Lβ lines.

From the densitometry measurements it was possible to identify the L_{α_1}, L_{α_2}, L_{β_1}, L_{β_2}, L_{β_3}, L_{β_4}, L_{γ_1}, L_{γ_2} and L_{γ_6} lines, some of which were not completely resolved from stronger lines. Several of these lines showed unusual features. The tail of the L_{α_1} line showed an irregular structure which might have been due to satellite lines, but which was more probably a result of the extraneous markings on the plate in this region. The peak marked L_{β_3} in Figure 26 is readily seen to be

---

* See Appendix C.

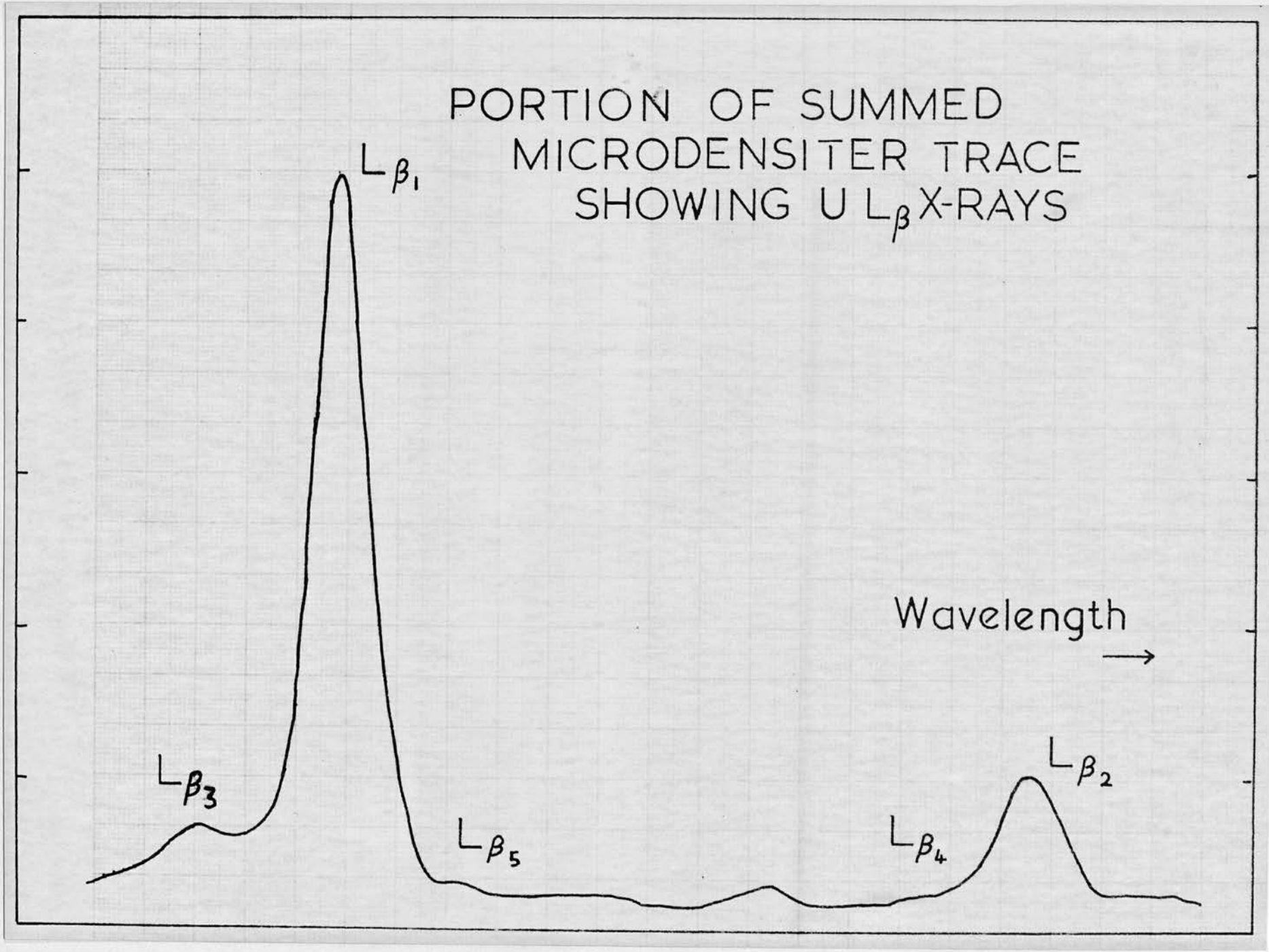
PORTION OF SUMMED
MICRODENSITER TRACE
SHOWING U Lβ X-RAYS
Lβ1
Lβ3
Lβ5
Lβ4
Lβ2
Wavelength
→

Figure 26

very much more intense than L_{β_4}. Both of these lines arise in transitions to the LI shell. Previous measurements by Cochran (1955), Goldberg (1961), Day (1955), and Compton and Allison (1935) show these two lines as having approximately the same intensity. This suggests that some other source of radiation may have contributed to the strength of this line, which lies at wavelength 710.5 x.u. One possible explanation is that the steel of the source tray, or of the source holder and collimating system contained some Molybdenum. Molybdenum is often used as a constituent of steel to increase its hardenability, and reduce its tendency to temper brittleness. The intense bombardment of the alpha particles from the Plutonium source would induce the Molybdenum K_α fluorescent X-rays. The Mo K_{α_1}, and Mo K_{α_2} lines have wavelengths 709.4 x.u. and 713.5 x.u., which straddle the UL_{β_3} wavelength, and they would not be resolved from L_{β_3}. The Mo K_β X-rays would be very much less intense than the K_α lines and might thus escape detection.

The integrated density of each line was converted to intensity using Cochran's calibration, corrected to a path length of 45 centimetres in air, instead of the 60 centimetres used by Cochran. Corrections were applied for the absorption of radiation in the source covering, the mica window, and the source itself. The results are shown in Table 8.

One notable feature of these results is that as we proceed to shorter wavelengths, the relative intensities

TABLE 8

Observed Uranium L X-ray Intensities Following Pu 238 Decay

Line	Transition	Wavelength	Observed Intensity	Corrected Intensity
L_{α_1}	LIII - MV	909 x.u.	66.6	135
L_{α_2}	LIII - MIV	921 x.u.	7.6	19
L_{β_1}	LII - MIV	719 x.u.	100	100
L_{β_2}	LIII - NV	755 x.u.	20.65	24.3
L_{β_5}	LIII - OIV,V	727 x.u.	2.40	2.42
L_{γ_1}	LII - N IV	617 x.u.	16.6	13.1
L_{γ_6}	LII - O IV	594 x.u.	4.4	3.4

TABLE 9

Author	Element	Intensity of L_{β_1} / Total Intensity from LII Shell		Intensity of L_{β_2} / Total Intensity from LIII Shell	
Goldberg (1961)	U(Z = 92)	~~0.7305~~	0.7309	~~0.1843~~	0.1789
Compton & Allison (1935)	U(Z = 92)	~~0.7899~~	0.7851	~~0.1598~~	0.1602
Salguiero et al. (1961)	Pu(Z = 94)	~~0.7935~~	0.7851	~~0.1675~~	0.1663
Barton et al. (1951)	Pu(Z = 94)	~~0.7571~~	0.7498	~~0.1829~~	0.1818
Cochran (1955)	U(Z = 92)	~~0.8244~~	0.8189	~~0.1756~~	0.1740
Day* (1955)	Np(Z = 93)	~~0.7513~~	0.7535	~~0.1760~~	0.1682
Mean Values =		~~0.774 ± 0.026~~	0.771 ± 0.032	~~0.174 ± 0.007~~	0.172 ± 0.009

* Recalculated by Magnusson (1957)

are systematically less than we might expect. This effect, if genuine, suggests an error in the positioning of the source, such that part of the source lies outside the line V_2Q in Figure 22. On checking the calculation of the source position, and checking the positioning of the source no such error could be found.

The value of F_3' was obtained from the intensities in the L_{β_1} and L_{β_2} lines. This method was preferred because the measured intensities of the L_α lines were unreliable. This method also minimises any error introduced by the energy dependent correction, or any other source of energy dependent systematic error.

Table 9 shows the intensities of L_{β_1} relative to the total fluorescence from the LII shell, and of L_{β_2} relative to the total fluorescence from the LIII shell, as measured by several authors. These results indicate that the ratio of the intensities of L_{β_2} and L_{β_1} should be multiplied by 4.44 ± 0.30 to obtain F_3'. The final value of F_3' for Pu 238 decay is thus

$$F_3' = 1.08 \pm 0.08 .$$

From the values of $n_2 + n_3$ following Pu 238 and Pu 240 decay, and the assumption that f_{23} is approximately 0.22, we can obtain a value of

$$F_3' = 1.07 \pm 0.08,$$

for Pu 240 decay.

See note p 103

REFERENCES - CHAPTER 6

1. Bartholomew, G.A., Knowles, J.W. and Lee-Whiting, G.F. (1960), Rep. on Prog. in Physics 23, 453.

2. Barton, G.W. Robinson, E.P. and Perlman, I. (1951), Phys. Rev., 81, 208.

3. Browne, C.I. (1952), Ph.D. Thesis, University of California, UCRL-1764.

4. Cauchois, Y. (1932), Comptes Rendus 195, 1479.

5. Cauchois, Y. (1934), Ann. Phys., Paris, 1, 215.

6. Chupp, E.L., Dumond, J.W.M. and Mark, H. (1958), Rev. Sci. Inst. 29, 1153.

7. Cochran, A.J. (1955), Thesis, University of Edinburgh.

8. Cochran, A.J. and Ross, M.A.S. (1958), Proc. Phys. Soc. 71, 1011.

9. Compton, A.H. and Allison, S.K. (1935), 'X-rays in Theory and Experiment', (Published by D. Van Nostrand Company, Inc., New York).

10. Day, P.P. (1955), Phys. Rev., 97, 689.

11. Day, P.P. (1956), Phys. Rev., 102, 1572.

12. Dilworth, C.C., Occhialini, G. and Vermaesen, L. (1950), Bulletin du Centre de Physique Nucleaire de L'Universite Libre de Bruxelles 13A.

13. Dumond, J.W.M. (1947), Rev. Sci. Inst. 18, 626.

14. Dumond, J.W.M. (1955), In 'β- and γ-Ray Spectroscopy' ed. by K. Siegbahn (Published by North Holland Publishing Co., Amsterdam).

15. Dumond, J.W.M. (1961), Methods of Experimental Physics 5A, pp. 599.- 616, Sec. 2.2.32. (ed. by L. Martin, Academic Press, Inc.)

16. Dumond, J.W.M. and Kirkpatrick, H.A. (1930), Rev. Sci. Inst. 1, 88.

17. Ewan, G.T. (1952), Thesis, University of Edinburgh.

18. Frilley, M. (1929), Ann. Phys., Paris, 11, 483.

19. Goldberg, M. (1961), J. de Phys. 22, 743.

20. Jaffe, H., Passel, T.O., Browne, C.I. and Perlman, I. (1955), Phys. Rev. 97, 142.

21. Kazi, A.H., Rasmussen, N.C. and Mark, H. (1961), Phys. Rev. 123, 1311.

22. Knowles, J.W. (1965), 'Crystal Diffraction Spectroscopy' in α-, β- and γ-Ray Spectroscopy, ed. by K. Siegbahn (Published by North Holland Publishing Co., Amsterdam).

23. Lind, D.A., West, W.J. and Dumond, J.W.M. (1950), Phys. Rev. 77, 475.

24. Rose, D., Ostrander, H., and Hamermesh, B. (1957), Rev. Sci. Inst. 28, 233.

25. Rutherford, E. and Andrade, E.N. da C. (1914), Phil. Mag. 27, 854.

26. Salguiero, L., Ferreira, J.G., Park, J.J.H. and Ross, M.A.S. (1961), Proc. Phys. Soc. 77, 657.

27. Thibaud, J. (1925), Thesis, University of Paris.

28. Williams, J.H. (1933), Phys. Rev. 44, 146.

29. Zajac, B. and Ross, M.A.S. (1949), Nature, Lond., 164, 311.

CHAPTER 7

PROPORTIONAL COUNTER STUDIES

The L X-ray spectra from the Curium 244, Plutonium 238, and Plutonium 240 sources were examined with a proportional counter. The energy resolution was too low to distinguish the individual L X-ray lines, but the L_α, L_β and L_γ groups of lines were clearly resolved in each case. A series of measurements of the relative intensities of the L X-ray groups was made for each of the three sources. From these measurements, and a knowledge of the relative intensities of the L X-ray lines originating in the same subshell, a measure of F_3' was obtained for the three decays studied. These measurements are reported here.

The proportional counter was also used to examine the Neptunium L X-rays, and low energy γ-rays, which are emitted following Americium 241 alpha decay. The relative intensities of the Neptunium L_α, L_β and L_γ X-ray groups, and of the gamma rays observed were measured.

In addition, a hitherto unobserved peak at approximately 9.4 keV was observed in the spectra from the two available sources of Am 241. Several experiments were performed with the object of determining the nature of this peak. These observations led to the tentative conclusion that this peak is due to a 9.4 keV gamma ray associated with the decay of Americium 241, although as yet no completely satisfactory explanation of the place of this gammaray in the decay scheme has been found. The

evidence supporting this conclusion is also reported later in this chapter.

The Proportional Counter

The proportional counter used in these experiments was designed originally for an investigation of the statistical nature of the multiplication process in proportional counters. Consequently, many of the features which were incorporated in its design are of little interest here, and are mentioned but briefly.

Figure 27 shows a vertical section of the counter system. The central portion, the counter itself, was especially designed for ease of assembly. A description of the process of assembling the counter perhaps best serves the purpose of describing the design features of the counter. The process of assembly was as follows.

Initially, the two central ebonite blocks, each of length two inches and diameter 1 7/8 inches, were held rigidly apart by three brass tie rods, as shown in Figure 27. The counter anode, a pure tungsten wire of diameter 0.004 inches, was then threaded through the stainless steel hypodermic needles in the centre of the ebonite blocks, was drawn taut, and the ends were soldered to the brass screws, which held the small brass plates on the outside of the ebonite blocks. This procedure, which allowed easy access to the wire when it was being threaded, ensured that there were no kinks in the anode wire. This was important, since a kink in the wire would

Figure 27

Legend:

A - Ebonite Cylinder to which the Source was attached.

B - Aluminium Window.

C - Removeable Section.

D - Thread to hold Source when placed inside the Counter.

E - Section of Collimator lined with Mo and Al.

F - Counting Region.

G - Copper Cooling Jacket

H - Anti-Coincidence Shield of Plastic Scintillator.

I - Brass Housing.

THE PROPORTIONAL COUNTER

Figure 27

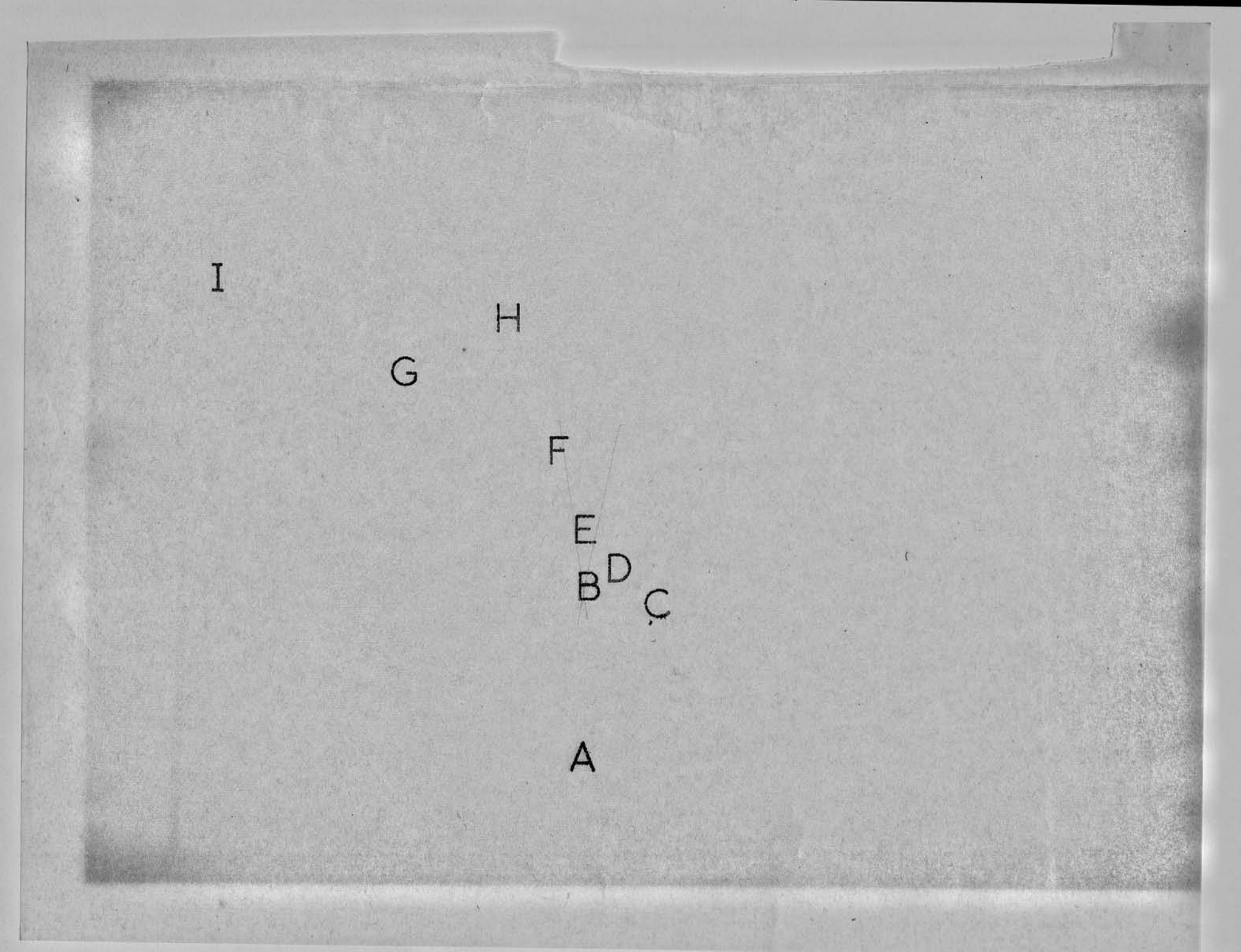
I
H
G
F
E
B
D
C
A

THE PROPORTIONAL COUNTER

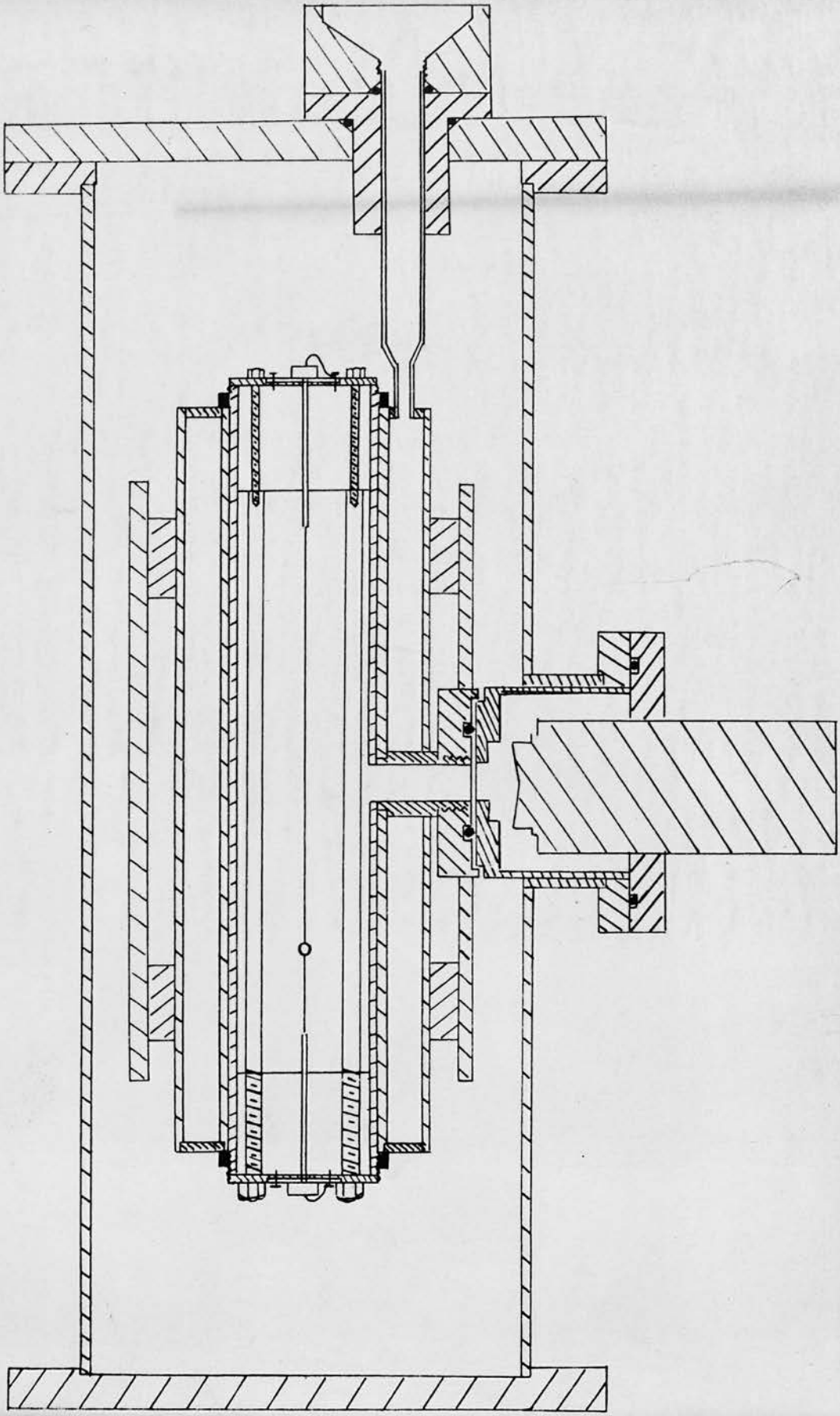

Figure 27

lead to an irregular collecting field, which would spoil the energy resolution of the counter.

Once the anode was in position, the rigid structure, consisting of the ebonite blocks held apart by the tie rods, was placed inside the aluminium cathode, which was a hollow cylinder of length ten inches, internal diameter 1 7/8 inches and external diameter two inches. The ebonite blocks were firmly attached to the cathode by a number of screws, too small to be shown in Figure 27. The brass tie rods were then withdrawn, since they were no longer needed to keep the ebonite blocks rigidly apart. The holes, through which the tie rods had passed, acted as ducts for the gas entering the counter.

The aluminium cathode was then fitted into a copper cooling jacket, which could be maintained at liquid Nitrogen temperature. The lowering of the temperature of the aluminium cathode was to reduce the thermionic emission of electrons from the aluminium. This was important in the experiment on the statistics of the multiplication process, since the thermionic electrons provided a background of single electrons in the counter. This facility was not used in the present series of experiments.

The cooling jacket consisted of two concentric copper cylinders. The inner cylinder, inside which the Aluminium cathode was screwed, was of length ten inches, internal diameter 3 3/16 inches, and external diameter 3 6/16 inches. The space between these cylinders was connected

by two copper tubes to copper funnels outside the brass container. The copper tubes were insulated from the end flange of the brass container by ebonite collars.

This insulation was required, because the cooling jacket was in contact with the aluminium cathode, which was maintained at a high negative potential. The negative high voltage line was firmly connected to both the copper cooling jacket and the aluminium cathode by a knurled ring, which screwed on to the upper end of the aluminium cathode. The other end of this wire was soldered to a brass pin, which was embedded in an ebonite piece set in the upper flange of the brass container. The outer end of this brass pin was connected to the negative high voltage line. The anode wire was connected to earth via a glass-to-metal seal set in the same flange of the brass container.

Outside the cooling jacket, and separated from it by two ebonite insulators of breadth 5/16 inches, was a cylinder of NE102 plastic scintillator, of length 8 inches, internal diameter 4 inches, and external diameter 4½ inches. The photomultiplier tube for this scintillation counter entered the chamber at right angles to the section shown in Figure 27. When the proportional counter was operated in anti-coincidence with this scintillation counter, the background counting rate was considerably reduced. In the experiments described here, this facility was not required.

The complete assembly was housed in a brass cylinder of length 16 inches, internal diameter 5 3/4 inches, and external diameter 6 inches. The end flanges of this container were of thickness ½ inch, and diameter 8 inches.

The Pumping and Filling System

A diagram of the pumping and filling system, which was used with the proportional counter, is shown in Figure 28. The counter was connected as part of a continuous line, which joined it to a tank, which acted as a reservoir of gas, and to a second tank containing a gas purification system. The complete system was evacuated by a rotary pump, and an oil diffusion pump. The subsidiary line, from the counter to the oil diffusion pump, passed through a liquid nitrogen trap, which removed heavy organic molecules from the system.

A mercury manometer, and a McLeod gauge were used to record high and low pressures respectively. The two discharge tubes shown in Figure 28 were used to test for the presence of air in the counter system. If air was present, it was detected by the appearance of the easily recognisable nitrogen band structure in the discharge. It was important that no air was present in the counter, since Oxygen is strongly electronegative, and has a markedly deleterious effect on the gas amplification and energy resolution of the counter.

The most satisfactory way of operating the counter was asfollows. The complete system was first evacuated

FIGURE 28

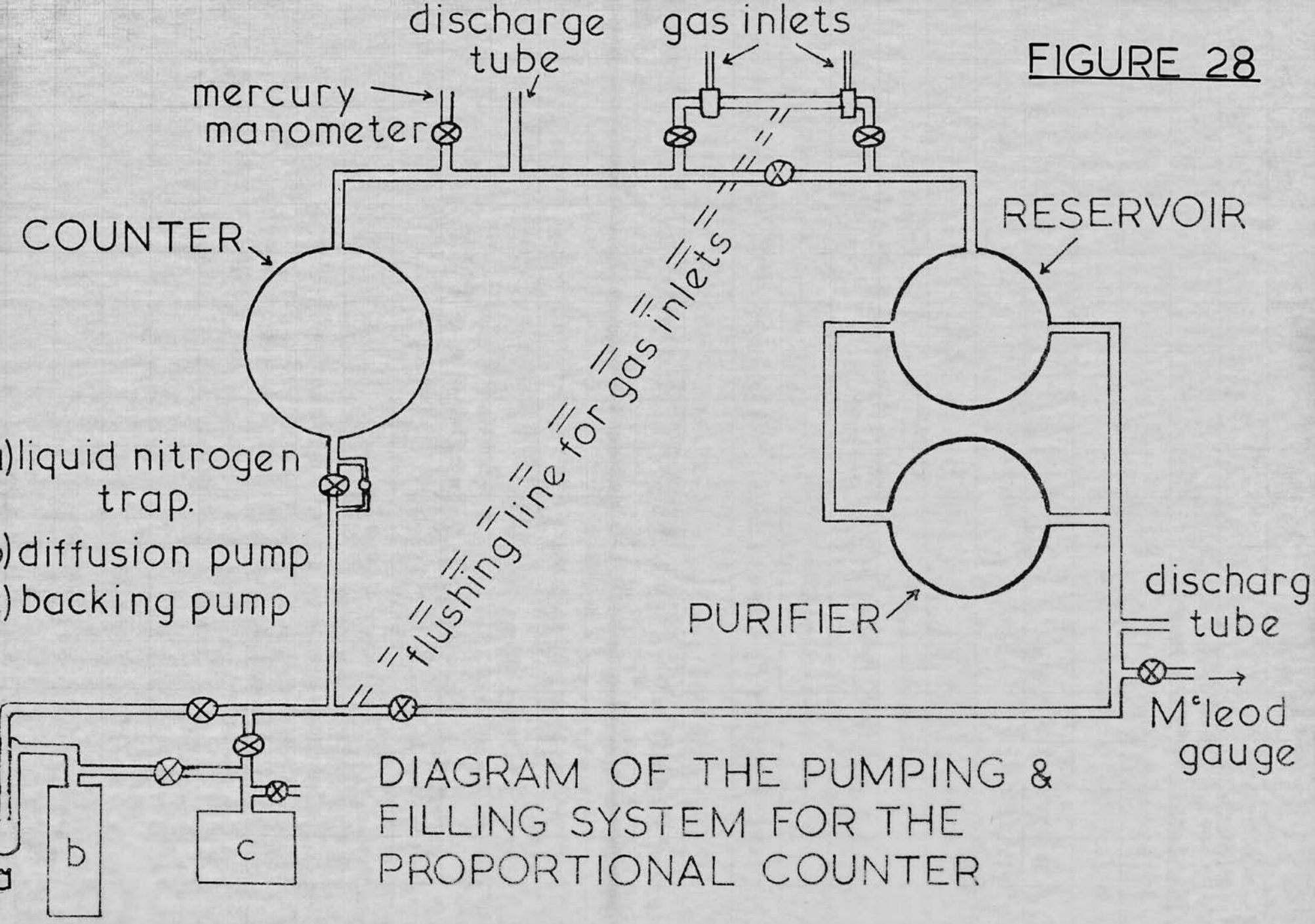

DIAGRAM OF THE PUMPING & FILLING SYSTEM FOR THE PROPORTIONAL COUNTER

and then flushed several times with Argon. It was then filled to the required pressure with the required mixture of Argon and Methane. The direct pumping line, from the backing pump to the gas inlet, ensured that the residual gas left in the inlet was pumped out, before allowing the second gas to enter the system. All of the subsidiary lines were then closed, leaving a constant volume of gas in the system. The purifier, which consisted of calcium turnings heated to between 350° and 400°C by an electrically heated coil, was switched on, and left to run throughout the experiment. All of the gas in the system would be purified by convection, and in this limited sense the counter operated as a flow counter.

It was observed that the gas amplification and energy resolution of the counter improved markedly over the first two or three hours of operation of the purifier. After this period, the operating characteristics settled down, and remained extremely stable over periods of operation up to several weeks. Accordingly, it was operated in this way throughout the experiments described here.

The Electronics

The counter pulses were taken from the anode and fed into a coupled N568B preamplifier and amplifier system. The pulse height spectra of the pulses from the amplifier were recorded on the Sunvic Ltd. 120 channel pulse height analyser, which was described in Chapter 4. Since only relative intensities were measured with the proportional counter, and the pulse height analyser circuits were designed to record a random sample of all pulses entering it, no 'dead time' corrections were required. The negative high voltage for the Proportional Counter was derived from a Type 200 Power unit, made by Dynatron Ltd.,

Procedure

The Curium and Plutonium sources, which were used in the coincidence experiments to measure F, were also used in this series of experiments. They were deposited on thin aluminium foil, and mounted on brass screw caps. One of the Am 241 sources, which we will call source A, was deposited on the surface of a thin silver strip, which was mounted on a brass screw cap similar to those used with the other sources. The other Am 241 source, source B, was contained in a small glass phial in liquid form. The glass phial was mounted in a lead container with a very thin perspex window.

The Curium and Plutonium sources, and the source A of Americium, could be mounted both inside and outside the counter. In the latter case, the brass screw cap was fitted to the ebonite cylinder marked A in Figure 27. This cylinder was free to move in a horizontal direction, and the source was pushed close to the aluminium window at B. This window, 0.127 mms. thick, prevented the alpha particles from the source entering the sensitive region of the counter. In the former case, with the source inside the counter, the section marked C in Figure 27 was removed and replaced by a blank. The brass screw cap was then fitted inside an ebonite holder, which, in turn, was screwed on the thread at D. In this case, the aluminium source backing prevented the alpha particles from reaching the sensitive volume of the counter. In either case, the collimator at E was lined with a layer of 0.002 inches molybdenum, and a layer of 0.001 inches aluminium, to prevent the induced fluorescent radiation from the Copper jacket reaching the sensitive region of the counter.

See Appendix D

It is essential, when making measurements of relative intensity with a proportional counter, to remove the contribution due to background from the spectrum. When a source was mounted inside the counter, the procedure required to do this was both time consuming and uncertain; since it demanded the emptying of the counter, the removal of the source, and the refilling of

the counter, before recording the background spectrum. As a result, the measurements of relative intensities were all made with the sources placed outside the counter.

With the sources outside the counter, two alternative procedures were used to remove the background from the L X-ray spectra. In the first method, the total counting time was split into thirty minute periods, and the L X-ray spectrum under examination, and the background spectrum were measured on the pulse height analyser in alternate periods. The two sets of measurements were then summed, and the background removed from the L X-ray spectrum. In the second method, the L X-ray spectrum was measured for a given period, after which the background spectrum was measured for the same length of time. No significant difference was observed in the results obtained with the two methods, which attests the stability of the counter when operated in the manner described here.

Results of the Measurements of U + Pu L X-ray Intensities.

For each of the three sources, the measurements of the relative intensities of the L X-rays were repeated five times, using gas pressures of 40, 60, and 80 centimetres of mercury. The gas mixture was ninety per cent argon and ten per cent methane. The counting times were all of the order of two to three hours. A typical proportional counter spectrum showing the Plutonium L X-rays following Curium 244 decay, at a gas pressure of

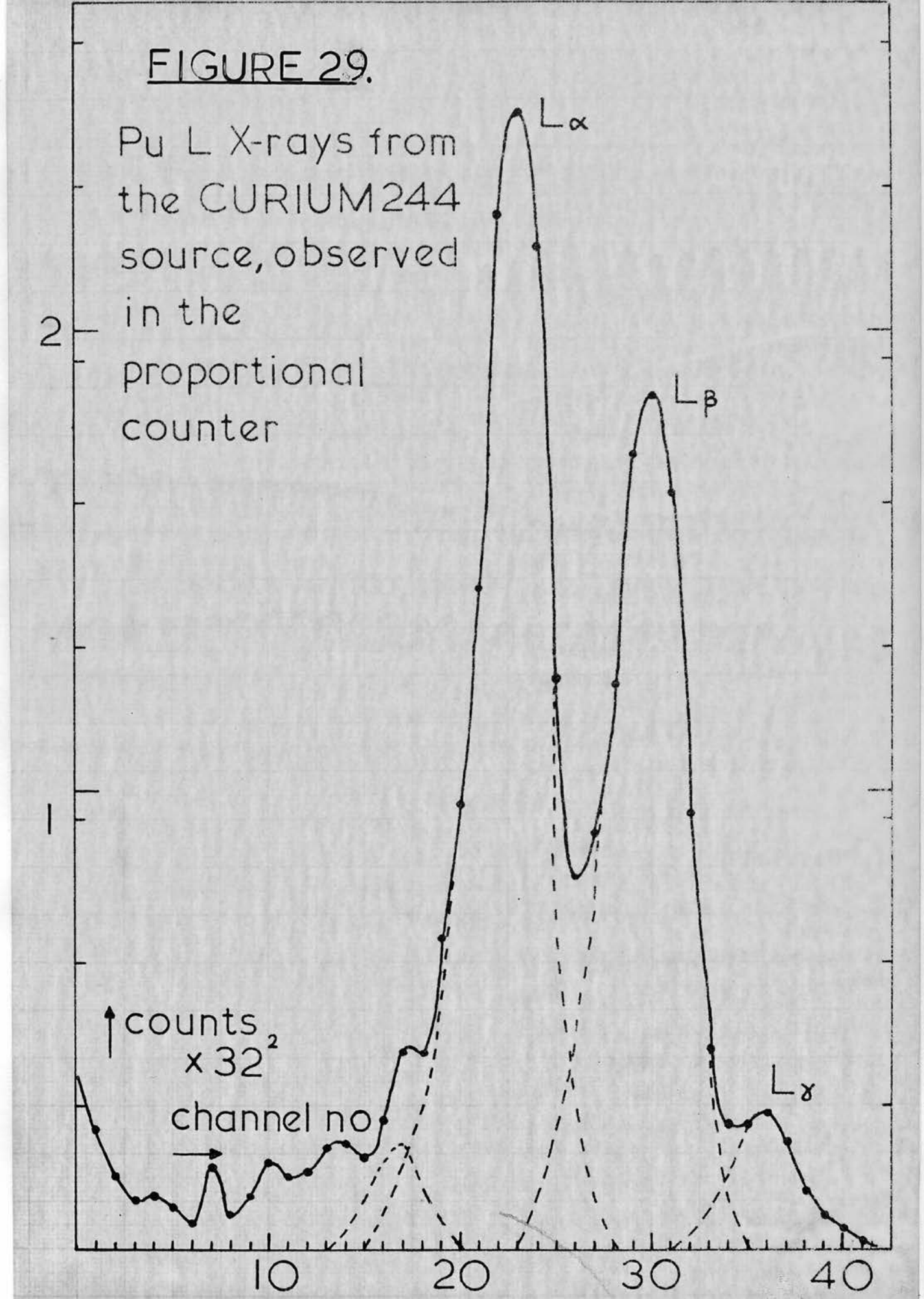
FIGURE 29.
Pu L X-rays from the CURIUM 244 source, observed in the proportional counter
Lα
Lβ
Lγ
2
1
counts x 32²
channel no
10
20
30
40

80 cms. of Mercury, is shown in Figure 29. The spectrum of the background radiation has been removed from the L X-ray spectrum as described in the previous section.

The L_α, L_β, and L_γ groups of X-rays are clearly resolved in the spectrum shown in Figure 29. The peak on the low energy side of the L_α peak, which appeared consistently in all of the observed spectra, is the L_α 'escape' peak. This 'escape' peak arises because almost all of the incident radiation absorbed in the counter gas is absorbed by the photoelectric process in the K shell of Argon. When the argon atom reorganises by an Auger transition, the full energy of the incident quantum is dissipated in the counter. When it reorganises with the emission of an Argon K X-ray, (West and Rothwell (1953) give $\omega_K = 0.11 \pm .01$ for Argon) a large proportion of the Argon K X-rays will escape from the counter. In this case the energy dissipated in the counter equals the incident quantum energy minus the energy of the Argon K X-ray. In the present experiments the intensity of the observed 'escape' peak was approximately five to six per cent of the intensity of the full energy peak. The peaks lower in energy than the L_α 'escape' peak, which are shown in Figure 29, did not occur consistently in all of the observed spectra, and are due to statistical fluctuations in the background in this region.

The measurement of the relative intensities of the L X-ray groups from such recorded spectra proceeded as follows. It was assumed that the shapes of the peaks

observed in the counter were the same as the shape of the peak due to the 59.6 keV gamma ray from Am 241, observed under the same conditions. On this assumption the observed spectrum was analysed into its component peaks, as shown by the dotted lines in Figure 27. The relative intensities of the four peaks were then measured. It is perhaps worth pointing out at this stage that the measure of the relative intensities which was obtained was insensitive to the exact shape chosen for the individual peaks.

The intensity of the 'escape' peak relative to the full energy peak is independent of energy, and depends on the counter geometry alone, at a given gas pressure. Hence the intensity of the L_α 'escape' peak relative to the L_α peak was used to correct the observed intensities of the L_β and L_γ peaks. The observed intensities were also corrected for the absorption of the L X-rays between the source and the sensitive region of the counter, and for the variation of the counter sensitivity with energy. The absorption correction was made using the known absorption coefficients and superficial densities of the materials between the source and the counter. The sensitivity correction was made using the known photoelectric absorption coefficients of Methane and Argon. In making both these corrections it was assumed that the relative intensities of the observed L X-rays were approximately the same as for the Plutonium L X-rays emitted following Curium 242 alpha decay, as observed by Salguiero et al.

(1961). Again this correction is insensitive to variation of the relative intensities of the individual L X-ray lines.

The results of the measurements of the relative intensities of the Uranium and Plutonium L X-ray groups emitted in Curium 244, Plutonium 240, and Plutonium 238 decay are shown in Tables 10, 11, and 12 respectively. Both the observed and the corrected results are shown. The tables also show the corrections applied to the measured intensities at the three gas pressures which were used. The mean values of the intensities, relative to the intensity of L_β, are given in column 10 of the Tables.

From these results, and a knowledge of the intensity in the L_α lines relative to the total intensity in the lines originating in the LIII shell, we can obtain values of F_3' for these three decays. Table 13 shows measured values of this ratio due to several authors. A mean value of 0.750 ± 0.008 was obtained from the values shown in Table 13. On the assumption that all of the ionisation occurs in the LII and LIII subshells, this ratio, together with the measured relative intensities of L_α, L_β, and L_γ yields the values of F_3' shown in Table 14.

Now $$F_3' = \frac{\omega_3(n_3 + f_{13}n_1 + f_{23}(n_2 + f_{12}n_1))}{\omega_2(n_2 + f_{12}n_1)} .$$

Unsatisfactory method X

Hence a knowledge of n_1, n_2, and m_3 for any two isotopes, allows us to obtain a value of F_3' for one isotope from

TABLE 10.

Relative Intensities of Plutonium L X-rays Following Cm 244 Decay, Measured with the Proportional Counter.

Gas Pressure	40 cms.			60 cms.			80 cms.		
	C Factor	(U) C	(U) C	C Factor	(U) C	(U) C	C Factor	(U) C	Mean Values
L_α	0.616	(1.403) 0.850	(1.379) 0.836	0.625	(1.016)* 0.635	(1.653) 1.0330	0.641	(1.444) 0.925	0.856 ± 0.093
L_β	1.0	1.0	1.0	1.0	1.0	1.0	1.0	1.0	1.0
L_γ	1.509	(0.148) 0.223	(0.116) 0.175	1.566	(0.209) 0.327	(0.110) 0.172	1.293	(0.165) 0.213	0.220 ± 0.039

U = Uncorrected.

C = Corrected.

TABLE 11.

Relative Intensities of the Uranium L X-rays Following Pu 240 Decay, measured with the Proportional Counter

Gas Pressure	40 cms.			60 cms.			80 cms.		
	C Factor	(U) C	(U) C	C Factor	(U) C	(U) C	C Factor	(U) C	Mean Values
L_α	0.686	(1.197) 0.821	(1.173) 0.805	0.693	(0.970) 0.672	(1.164) 0.806	0.677	(1.144) 0.775	0.776 ± 0.040
L_β	1.0	1.0	1.0	1.0	1.0	1.0	1.0	1.0	1.0
L_γ	1.541	(0.126) 0.194	(0.133) 0.205	1.521	(0.096) 0.146	(0.118) 0.180	1.434	(0.170) 0.244	0.194 ± 0.023

U = Uncorrected.
C = Corrected.

TABLE 12

Relative Intensities of Uranium L X-rays Following Pu 238 Decay, Measured with the Proportional Counter

Gas Pressure	40 cms.			60 cms.			80 cms.		
	C Factor	(U) C	(U) C	C Factor	(U) C	(U) C	C Factor	(U) C	Mean Values
L_α	0.686	(1.235) 0.847	(1.155) 0.794	0.693	(1.170) 0.810	(1.134) 0.785	0.677	(1.070) 0.725	0.792 ± 0.028
L_β	1.0	1.0	1.0	1.0	1.0	1.0	1.0	1.0	1.0
L_γ	1.541	(0.123) 0.190	(0.070) 0.108	1.521	(0.132) 0.201	(0.179) 0.272	1.434	(0.130) 0.188	0.192 ± 0.034

U = Uncorrected.

C = Corrected.

TABLE 13

Intensity of $L_{\alpha_1} + L_{\alpha_2}$ / Total Intensity of Lines from the LIII Shell	Element	Author
~~0.7605~~ 0.7383	Uranium (Z = 92)	Goldberg (1961)
~~0.7545~~ 0.7297	Thorium (Z = 90)	Goldberg (1961)
~~0.7652~~ 0.7673	Uranium (Z = 92)	Compton & Allison (1935)
~~0.7441~~ 0.7391	Plutonium (Z = 94)	Salguiero et al. (1961)
~~0.7381~~ 0.7338	Plutonium (Z = 94)	Barton et al. (1951)
~~0.7671~~ 0.7564	Uranium (Z = 92)	Cochran (1955)
~~0.7517~~ 0.7534	Neptunium (Z = 93)	Day* (1955)

Mean Value = ~~0.750 ± 0.008~~ 0.745 ± 0.043

* Recalculated by Magnuson (1957).

TABLE 14

Measured Values of F_3'

	F_3' from Proportional Counter Measurements	F_3' from Curved Crystal Measurements	Other Measurements	Final Values
Pu 238 - U 234 (1.092)	1.14 ± 0.10	1.08 ± 0.08	0.854[d]	1.11 ± .07
Pu 240 - U 236 (1.063)	1.11 ± 0.10	1.07 ± 0.08[c]	0.843[d]	1.09 ± .07
Cm 244 - Pu 240 (1.17)	1.22 ± 0.17	1.17 ± 0.06[c]	1.096[d]	1.19 ± .06
Cm 242 - Pu 238	1.16 ± 0.17[a]	1.12 ± 0.06[b]	1.043[d] 1.27[e]	1.13 ± .06

a - Derived from the value for Cm 244 Decay, measured with the Proportional Counter.

b - Measured by Salguiero et al. (1961) with the Curved Crystal Spectrograph.

c - Derived from the values for Pu 238 and Cm 242 Decay, measured with the Curved Crystal Spectrograph.

d - Derived from Listengarten's (1961) calculated fluorescence yields.

e - Measured by Barton et al. (1951) with a Curved Crystal Spectrometer.

a measured value of F_3' for the other. The second column in Table 14 shows the value of F_3' for Cm 242 decay derived from the measured F_3' for Cm 244 decay, using the values of n_1, n_2 and n_3 given in Chapter 8. The values of n_1, n_2 and n_3 are based on Sliv and Band's (1958) calculated internal conversion coefficients, and the measured intensities of the alpha particle groups populating the excited states of the daughter nuclei.

Similarly, column 3 shows the values of F_3' for Pu 240, and Cm 244 decay derived from the direct measurements of F_3' for Pu 238, and Cm 242 decay, which were made by the present author, and by Salguiero et al. (1961) with the curved crystal spectrograph.

Column 4 shows the values of F_3' for the same decays, derived from Listengarten's (1961) calculated fluorescence and Auger yields, and the same values of n_1, n_2 and n_3. In all four cases, the values derived from Listengarten's yields are lower than the measured values shown in columns 2 and 3. Since his values of ω_3 are in reasonable agreement with the few measurements which have been made, this suggests that his values of ω_2 are too high. We will return to this point in Chapter 8.

The two sets of measurements presented here, made with the proportional counter and the curved crystal spectrograph, are in good agreement. Accordingly, the final values of F_3' adopted for use in the calculation of the fluorescence yields of Uranium and Plutonium are

shown in column 5. These values are weighted means of the measurements shown in columns 2 and 3.

A Digression - Some Measurements on the Electromagnetic Radiation from Am 241 Decay

Americium 241 is an alpha emitter, with a measured half life of 458 years. Since it was one of the first of the Transuranic isotopes to be produced isotopically pure in large amount, both the alpha particle and gamma ray spectra have been examined by many workers (Beling et al. (1952), Day (1955), Jaffe et al. (1955), Baranov and Shylagin (1956), Hollander et al. (1956), Rasmussen et al. (1957), Rosenblum et al. (1957), Hoffmann and Dropesky (1958), Samoilov (1959), Wolfson and Park (1964) and Michaelis (1965)), and the main details of the decay scheme are now well established. Figure 30 is a partial level scheme showing the intensities of the alpha particle groups, which populate the low lying excited states of Neptunium 237.

The low energy electromagnetic radiation from Am 241 was examined with the proportional counter described above, and the relative intensities of the radiations observed were measured. Typical examples of the spectra recorded, in the ranges 2-30 keV and 5-60 keV, are shown in Figures 31 and 32 respectively. Figure 33 shows a spectrum taken with source A, placed inside the counter.

The procedure used in the measurement of relative intensities, and the corrections applied to the observed

FIGURE 30

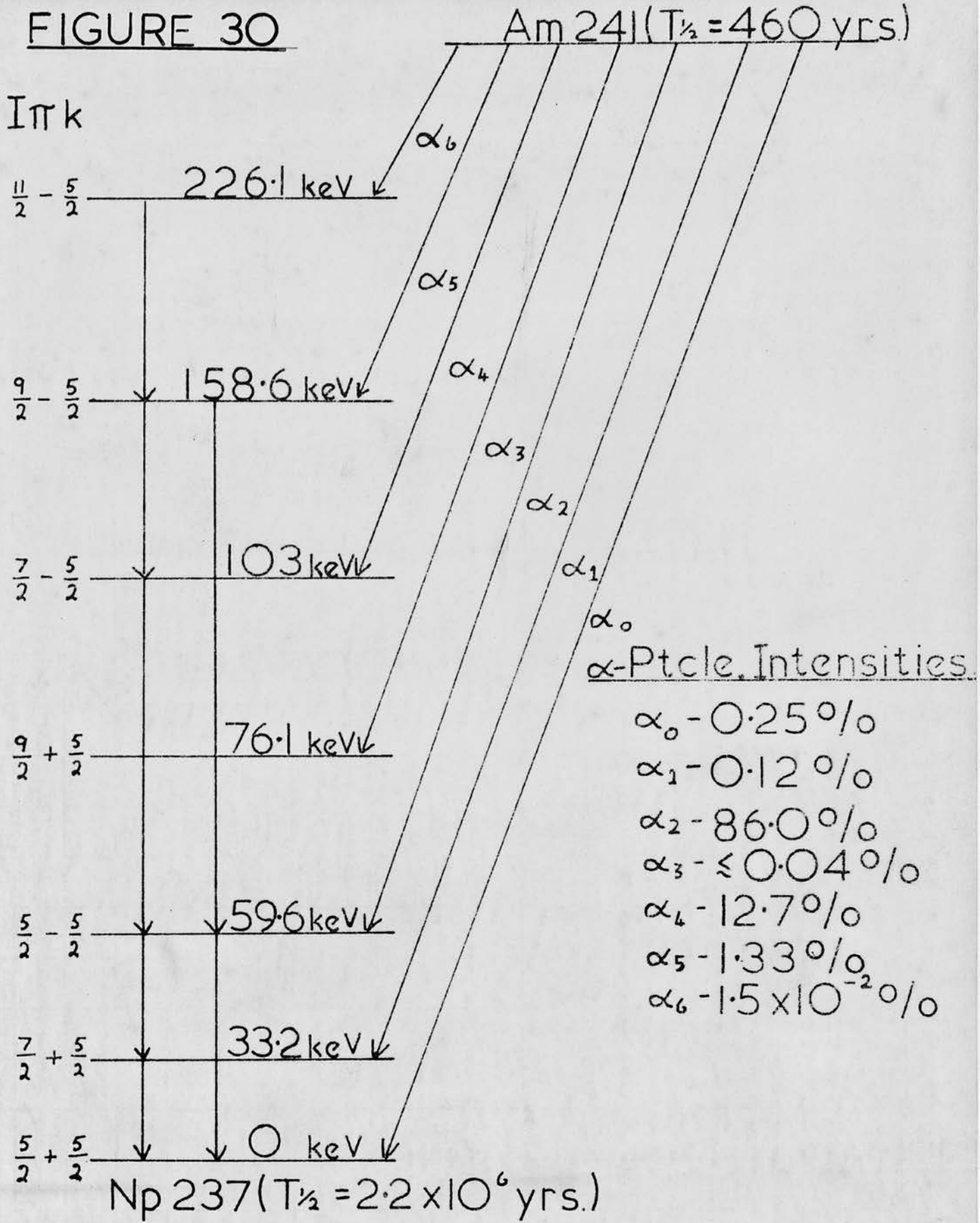

α-Ptcle. Intensities.

α_0 - 0·25 %
α_1 - 0·12 %
α_2 - 86·0 %
α_3 - ≲ 0·04 %
α_4 - 12·7 %
α_5 - 1·33 %
α_6 - 1.5×10^{-2} %

Partial level scheme of Np 237. Alpha group intensities are due to Baranov et.al.(1962)

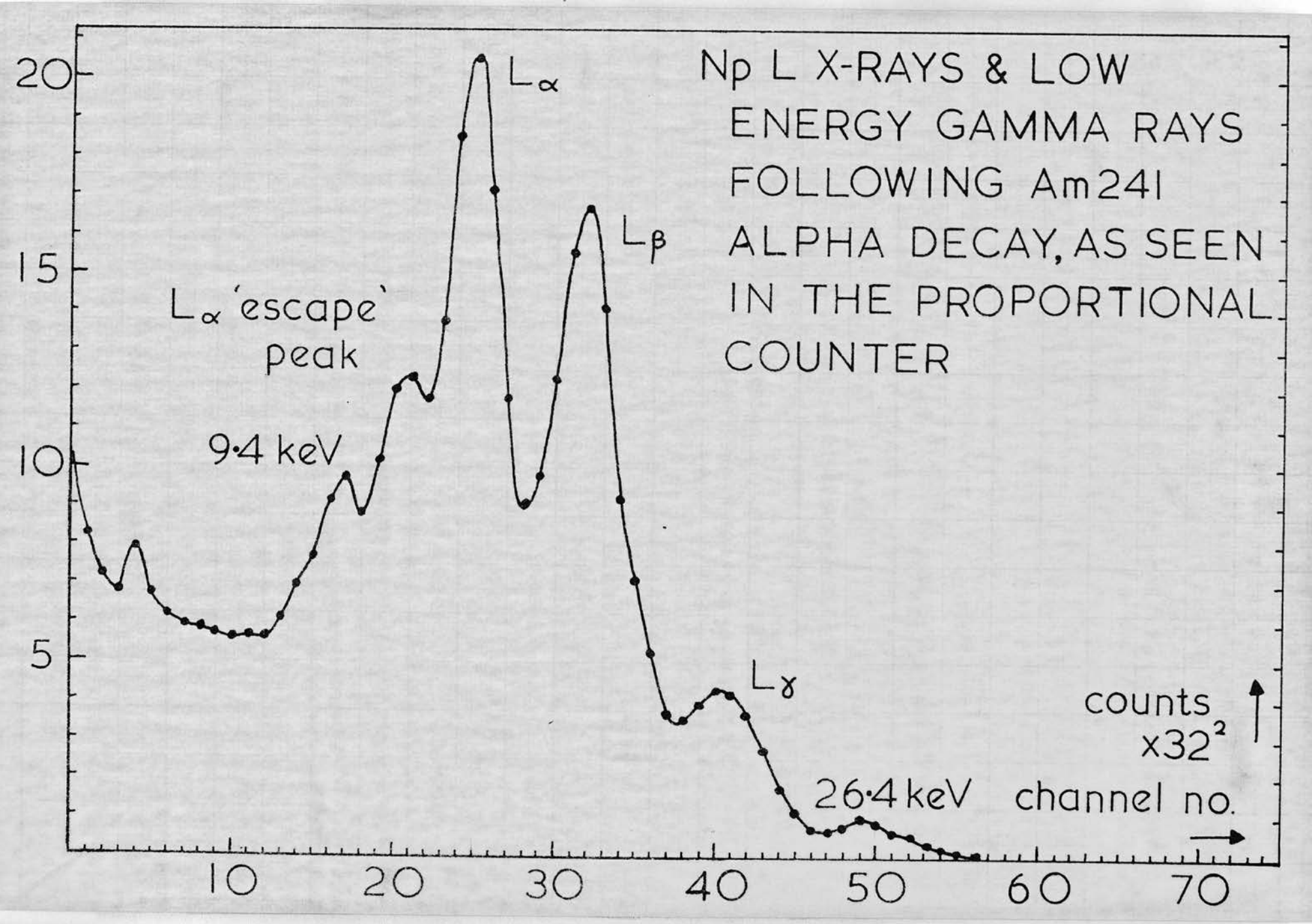
Np L X-RAYS & LOW ENERGY GAMMA RAYS FOLLOWING Am241 ALPHA DECAY, AS SEEN IN THE PROPORTIONAL COUNTER
Lα
Lβ
Lγ
Lα 'escape' peak
9·4 keV
26·4 keV
counts x32²
channel no.
20
15
10
5
10
20
30
40
50
60
70

FIGURE 31.

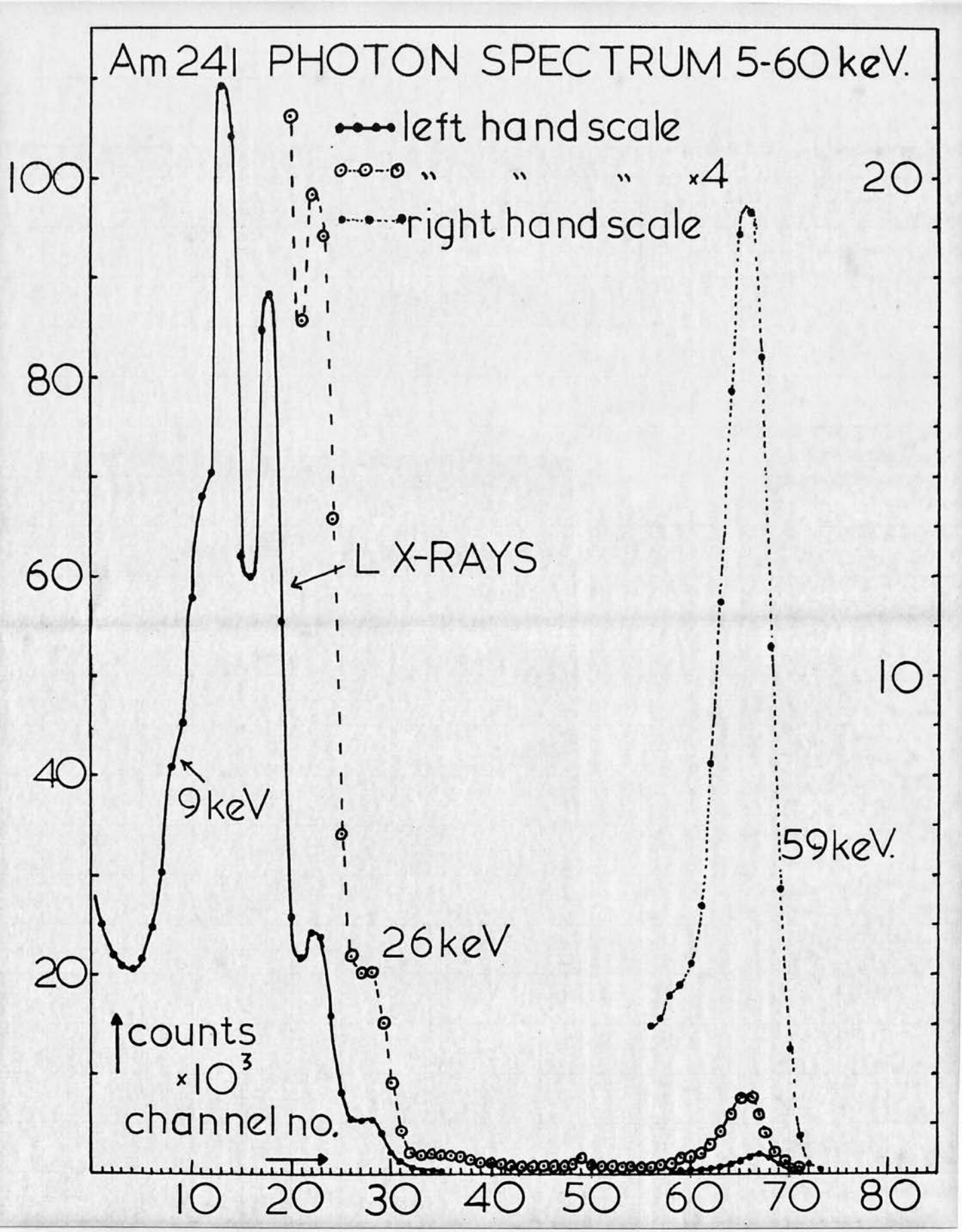
Am 241 PHOTON SPECTRUM 5-60 keV.
left hand scale
" " " ×4
right hand scale
L X-RAYS
9keV
26keV
59keV.
counts
×10³
channel no.
100
80
60
40
20
20
10
10 20 30 40 50 60 70 80

Figure 32

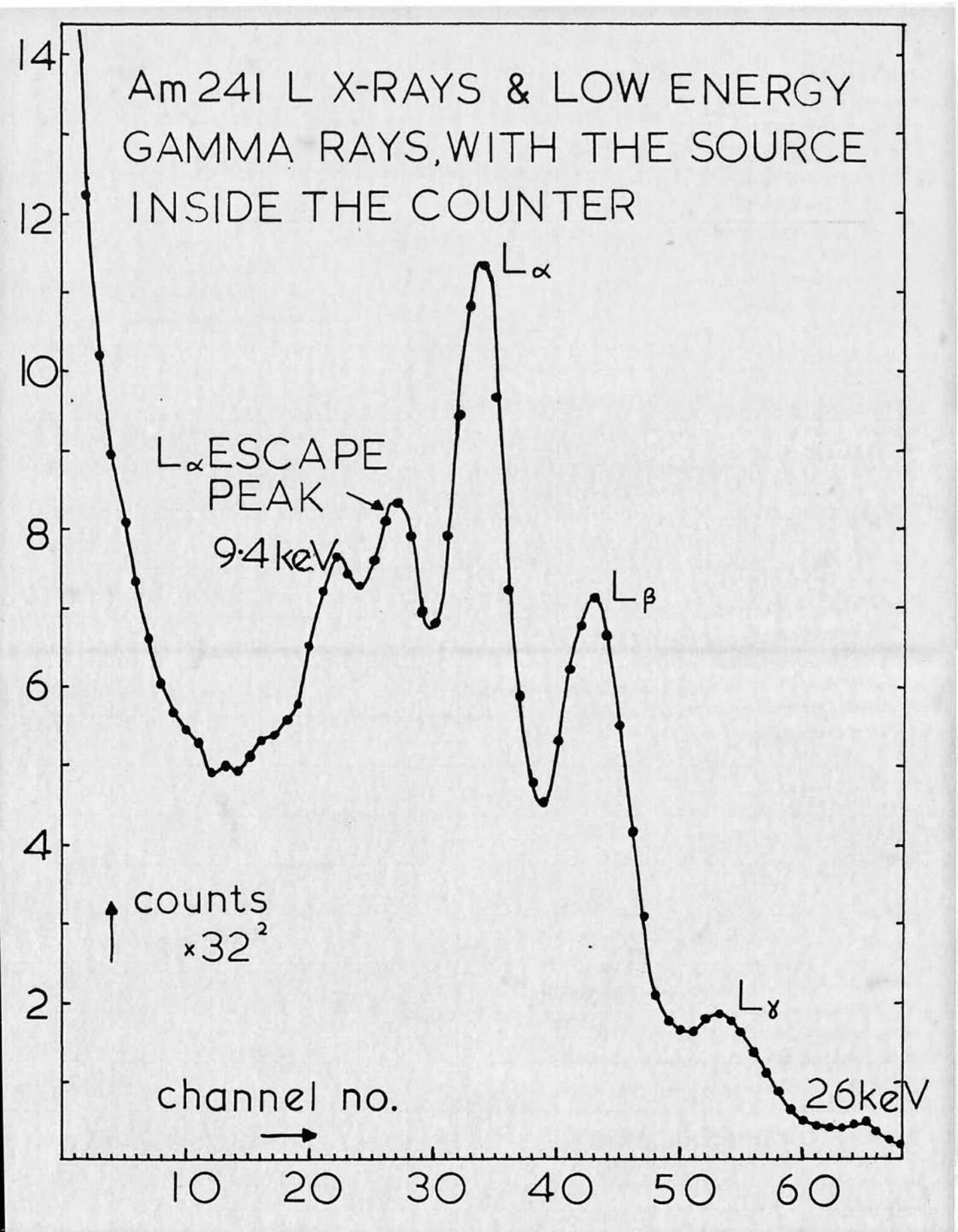
Am 241 L X-RAYS & LOW ENERGY GAMMA RAYS, WITH THE SOURCE INSIDE THE COUNTER
Lα
Lα ESCAPE PEAK
9·4keV
Lβ
Lγ
26keV
counts ×32²
channel no.
14
12
10
8
6
4
2
10
20
30
40
50
60

Figure 33

intensities, were as for the Plutonium and Curium sources, with the addition of a correction for the "wall effect" due to the higher energies of some of the gamma rays involved.

The main process of absorption of radiation in the counter is photoelectric absorption in the K shell of Argon, and the "wall effect" is due to the escape of some of the photoelectrons from the gas into the counter wall. Hence the observed intensity of any radiation must be corrected for the fraction of photoelectrons lost from the gas. West et al. (1952) have examined this effect, and they showed that there is no broadening of the full energy peak due to the "wall effect". The escape of the photoelectron into the wall causes a large diminution of the pulse size, which removes the pulse completely from the region of the peak. At the same time, the diminished pulses add to the background in the counter, and we get an accumulation of pulses at low energies, which must be removed from the spectrum before making the measurements of relative intensities.

The corrections for the "wall effect" were made using the experimental correction curves of West et al. (1952). They measured the efficiency of detection with and without the "wall effect" at various energies, by measuring the counting rate in the full energy peak, with and without a magnetic field of 6000 Gauss parallel to the anode of their cylindrical counter. They assumed that the number of escaped photoelectrons is negligible in the

latter case. West et al.'s measurements were made with a counter of 5 centimetres diameter. The counter used in the present experiments had a diameter of 4.76 centimetres, and the corrections were derived from West et al.'s correction curves on the assumption, that the fraction of counts lost from the full energy peak is a function of the range of the photoelectron, relative to the diameter of the counter.

In all of the spectra which were recorded, it was possible to discern peaks at 9.4, 11, 13.5, 17, 21, 26.4 and 59.6 keV. In addition, if the counting time was long enough, a peak was observed at about 33 keV. The measured intensities of these radiations, relative to the peak at 17 keV, are shown in Table 15. Most of these features of the spectra are readily explained, and have been observed by many authors.

The peaks at 13.5, 17 and 21 keV are the Neptunium L_α, L_β and L_γ X-ray groups, and the peak at 11 keV is composed of the L_α escape peak, and the $L\ell$ X-ray line. The prominent peaks at 26.4 keV, and 59.6 keV are due to two gamma rays, both of which de-excite the heavily populated energy level at 59.6 keV, which is shown in Figure 30. This leaves the peaks which were observed at 9.4 keV and 33 keV. They are not so readily explained.

From the decay scheme shown in Figure 30, it is readily seen that we might expect to observe a gamma ray of 33.2 keV energy, and indeed several workers have observed such a gamma ray. However, the transition

TABLE 15 *

Relative Intensities of the Electromagnetic Radiations Observed in Am 241 Decay

Energy of Radiation	9.4 keV	L_α	L_β	L_γ	26.4 keV	33 keV	59.6 keV
Source B	0.053	0.606 ± 0.009	1.0	0.236 ± 0.014	0.134 ± 0.006	0.079 ± 0.047	1.573 ± 0.061
Source A	0.082	0.589 ± 0.019	1.0	0.479 ± 0.030	0.203 ± 0.022	0.071 ± 0.012	1.748 ± 0.070
Final Result	0.066	0.599 ± 0.013	1.0	0.236 ± 0.014	0.134 ± 0.006	0.075 ± 0.022	1.644 ± 0.086

Notes. (1) All of the Intensities are quoted relative to the intensity of the Np L_β group.

(2) The Intensity quoted for the 9.4 keV peak is an upper limit only.

(3) The final result gives the mean of all the measurements made, except in the case of the L_γ and 26.4 keV peaks. For these radiations, the mean of the measurements made with Source B has been adopted.

* See Appendix D – (b)

de-exciting the $^{7}/_{2}+$ first excited level of the ground state rotational band has E2-M1 polarity, and would be very heavily converted. Day (1955), Jaffe et al. (1955) and Beling et al. (1952) have set limits of 0.002, 0.008 and 0.0005 33.2 keV photons per alpha particle respectively. If we assume that 0.379 60 keV photons are emitted per alpha particle, then the intensity of the 33 keV peak observed here was 0.017 photons per alpha particle, which exceeds all of these limits. Browne (1952) observed a gamma ray at 33 keV, but on purifying his source further, he found that it disappeared. He concluded that the radiation had been due to the fluorescent K_{α} X-rays of Lanthanum, which had been induced by the bombardment of a small amount of Lanthanum, present as an impurity in the source. The present author believes that the same explanation holds here. Lanthanum is a common impurity in Americium, since it is used as a carrier in isolating this element. Only a small amount would be required to produce the K_{α} peak observed in the proportional counter, under bombardment from the alpha particles and gamma rays of the Americium. The K_{β} X-rays which would also be produced, would be very much weaker in intensity, and would probably escape detection.

Finally there is the peak which was observed at 9.4 keV. The intensity quoted for this peak is an upper limit, since it is difficult to measure accurately the intensity of a low energy radiation, when superimposed on

the tail of a more intense peak. This peak has not previously been observed in either the gamma ray or conversion electron spectrum, and there are several possible explanations of its origin.

Firstly it may be due to the fluorescent excitation of the K- or L-X-rays of an element which is present in the source as an impurity. If so, the same element must be present in sources A and B in the same abundance, since the 9.4 keV peak was observed in equal intensity in the spectra from both sources. If it is due to the K X-rays of an impurity, then Gallium is the most likely element since the K_α X-rays of Gallium have 9.25 keV energy. Gallium (Z = 31) is not a common impurity in Americium, and neither are any of its neighbours in the Periodic Table. It is unlikely that it would occur as an impurity in two sources of Americium prepared at several years interval. If, on the other hand, it is due to the L X-rays of an impurity, we would expect to have observed the K X-rays from the same element at about 70 keV. No such peak was observed in the spectrum.

Secondly, this peak may be due to the fluorescent excitation of K X-rays from some material used in the construction of the proportional counter. Brass, copper, ebonite, and aluminium were the main constituents of the counter. Brass contains copper and zinc, and the K_α X-rays of these elements have energies 8.05 keV and 8.64 keV respectively. Accordingly, to test the possibility that the peak at 9.4 keV was due to them, pieces of zinc

and copper were placed between the source and the counter. In each case the fluorescent K X-rays were induced. They appeared superimposed on the normal Am 241 spectrum, but at a lower energy than the 9.4 keV peak, which also appeared in the same intensity as before. A typical example of such a spectrum appears in Fig. 34, showing the copper and zinc fluorescent K X-ray peaks from a sample of the counter brass, which are superimposed on the Am 241 gamma ray spectrum. Similar experiments were carried out with all of the materials used in the construction of the counter, with the same negative result.

A third possible explanation is that the radiation of energy 9.4 keV may be emitted by a radioactive impurity, which is present in the source. This explanation is again open to the objection that the impurity must be present in equal abundance in both sources. In addition we might also expect to see some further evidence of its presence. The alpha particle spectrum from source A was examined with a semiconductor alpha detector at one per cent resolution, and no alpha emitting impurity was observed. The gamma ray spectra of both sources were also examined with a NaI scintillation counter, and again no evidence of any radioactive impurity was found. This explanation cannot be completely ruled out without further experiment, but it is unlikely to be correct, since an examination of the Isotopes Review of Strominger et al. (1958), fails to reveal many isotopes emitting

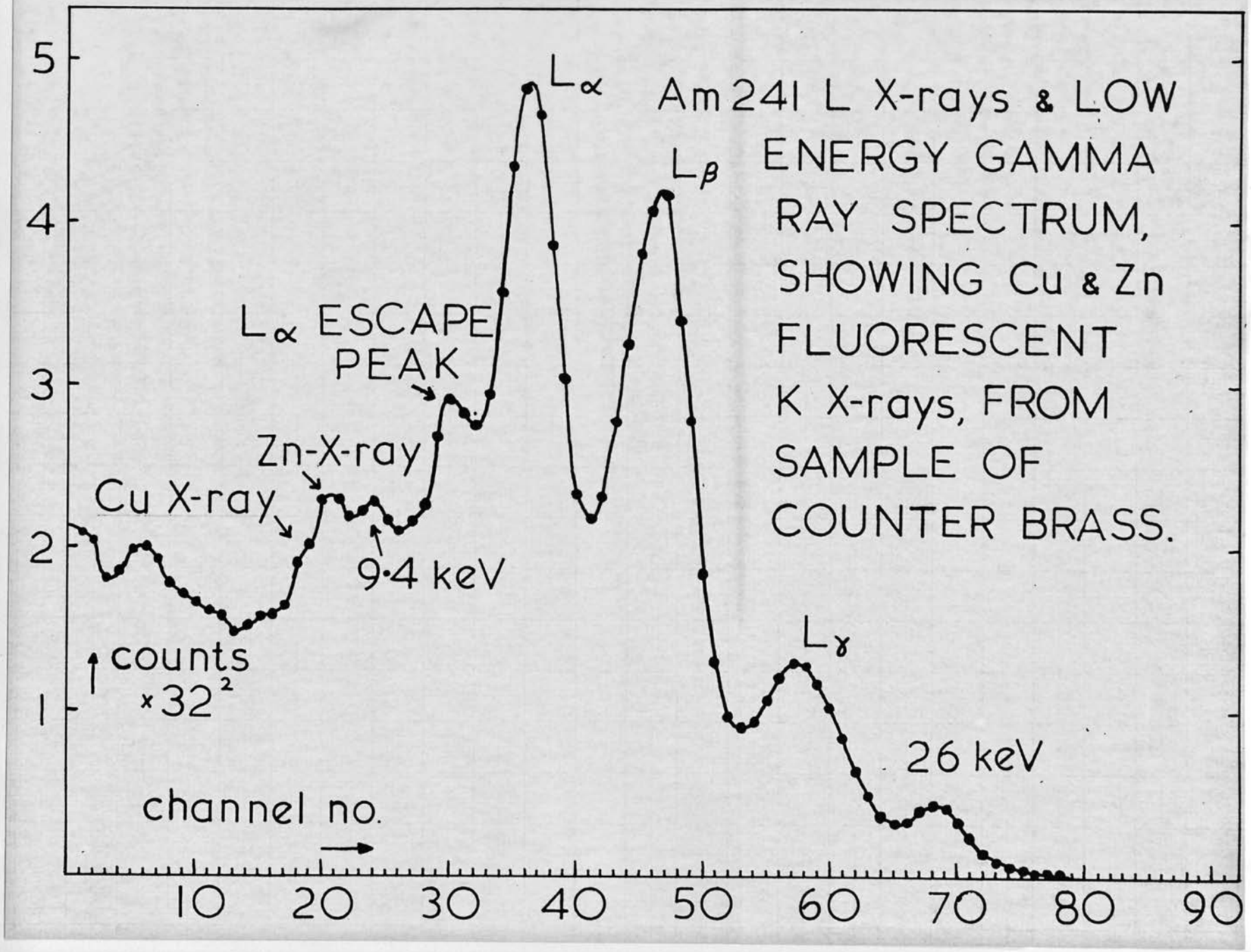
Am 241 L X-rays & LOW ENERGY GAMMA RAY SPECTRUM, SHOWING Cu & Zn FLUORESCENT K X-rays, FROM SAMPLE OF COUNTER BRASS.
Lα
Lβ
Lγ
Lα ESCAPE PEAK
Zn-X-ray
Cu X-ray
9·4 keV
26 keV
counts ×32²
channel no.
1
2
3
4
5
10
20
30
40
50
60
70
80
90

Figure 34

photons with the energy in question, and with the necessary half life of at least five or six years.

Finally, the 9.4 keV peak may be due to a gamma ray emitted in a transition in Neptunium 237. In the opinion of the present author this is the explanation which best fits the facts which are at present available. If it is a gamma ray emitted following Americium 241 decay, then two questions automatically follow. Why has it not been observed before? What part does it play in the decay scheme?

The answer to the first question is relatively straightforward. In previous investigations of the gamma ray or conversion electron spectra, either the conditions were unfavourable for the observation of this transition, or the experimenter was not concerned with this region of the spectrum. Beling et al. (1952) and Magnusson (1957) examined the gamma ray spectrum with proportional counters. The former used a counter filled with Krypton. Since the K X-rays of Krypton have an energy of 12.6 keV the Np L_γ 'escape peak' would occur at about 8.7 keV. Between this and the normal L_α peak, the small peak at 9.4 keV would be lost. Magnusson used an Argon filled counter made of brass. As a result, we observe a very intense peak in his spectrum due to the copper and zinc K fluorescence X-rays. This peak 'swamps' the region of interest and would make it impossible for him to have observed the small peak at 9.4 keV. Three authors (Cochran (1955), Jaffe et al. (1955) and Day (1955)) have examined the X-ray and γ-ray

spectrum in high resolution with a curved crystal spectrograph. It would have been possible for all of them to observe the peak, despite the heavy absorption of such low energy radiation between the source and the detection systen. However none of them had any reason to examine this portion of the spectrum, and there is no evidence to suggest that they did. A transition of energy 9.4 keV does not have sufficient energy to be internally converted in the L shell, and hence it would only be converted in the M and higher shells. This means that the energies of the conversion electrons are such that they fall in the same region as the Auger electrons. Several people (Turner (1955), Baranov and Shylagin (1956), Hollander et al. (1956), Rosenblum et al. (1957), Samoilov (1959), Wolfson and Park (1964)) have examined the conversion electron spectrum from Am 241, but only Wolfson and Park have examined it with sufficient resolution to distinguish between the M shell conversion electrons of a 9.4 keV transition and the Auger electrons. Unfortunately Wolfson and Park were not interested in this region of the spectrum, and they only examined the region between 20 and 95 keV.

The second question is not so readily answered. The partial level scheme shown in Figure 30 reveals two low lying groups of levels. One group, with levels at 0, 33.2, and 76.1 keV, forms a rotational band built on the $\frac{3}{2}+$ ground state. This group is sparsely populated

in Am 241 alpha decay, and the fourth and fifth members, which we might expect at 128.6 keV ($\frac{11}{2}$ +), and 190.6 keV ($\frac{13}{2}$+), are not developed at all. The second group forms a rotational band, which is built on the $^5/_2$ - state at 59.6 keV. This hand has levels at 103, 158, 225, 307, and 395 KeV, with spins up to $\frac{15}{2}$ -. No evidence has been found of a $\frac{3}{2}$ - member of this hand at 29 keV, which would not anyway be expected theoretically. It is readily seen that the energies of these levels, whether hypothetical or not, are not such as to explain a transition of 9.4 keV energy.

Thus the 9.4 keV transition does not occur between the levels which form part of these two low lying rotational bands, and we must turn to the higher enervy levels in Neptunium 237. Figure 35 shows a fuller version of the Np 237 level scheme, as given by Michaelis (1965). A transition between the levels shown at 360 keV and 369 keV would have the correct energy to fit the observed gamma ray. However several factors militate against this solution. The level at 369 keV is thought by Baranov and Shylagin (1956), and by Michaelis (1965) to be the $\frac{5}{2}$ + member of a $\frac{1}{2}$+ rotational band. The level at 360 keV is thought to be a single hole excitation with spin $\frac{3}{2}$ +, which theory predicts in this region. A transition between these levels would then have M1 polarity, and would be heavily converted in the M shell. Since the 369 keV state is only directly populated in 1.2 x 10^{-3} alpha particle decays, the

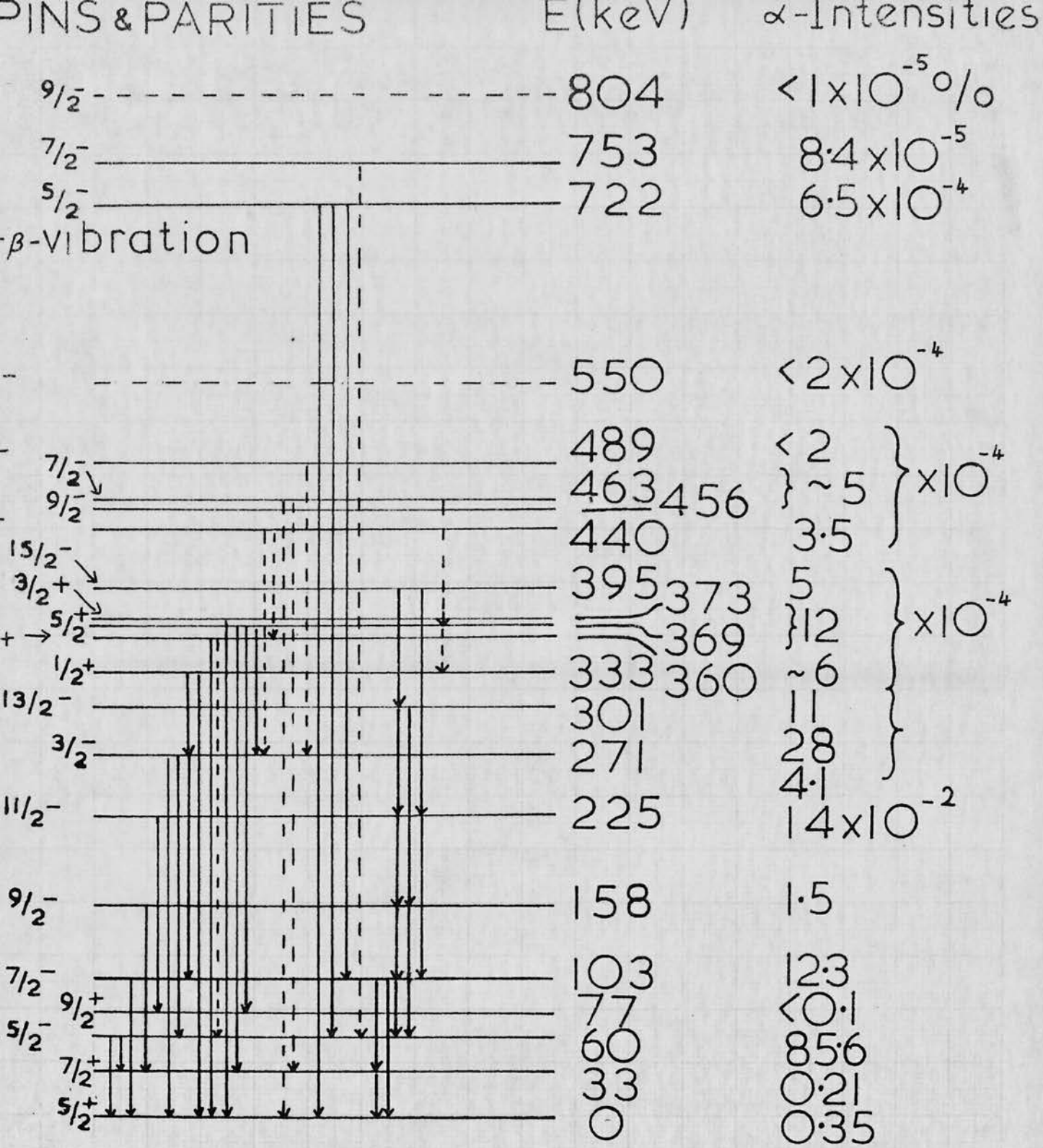

PARTIAL LEVEL SCHEME FOR Np237, SHOWING THE RELATIVE INTENSITIES OF Am241 α-Ptcles., ACCORDING TO MICHAELIS (1965).

FIGURE 35.

intensity of the gamma ray would have to be several orders of magnitude less than the upper limit given here. It is of course possible that the parities assigned to one of these levels by Michaelis is wrong, in which case we would have an E1 transition which would proceed mainly by gamma emission. The upper limit of the gamma ray intensity given here is 1.35×10^{-2} 9.4 keV photons per alpha particle, if we assume an intensity of 0.379 59.6 keV photons per alpha particle. If this is an overestimate by a factor of ten, and if the parity of the 360 keV level is odd not even, then this might explain the gamma ray reported here.

To sum up, the origin of the 9.4 keV peak is not clear. In the author's opinion it is probably a gamma ray emitted in Am 241 decay, but it would require gamma-gamma coincidence experiments involving this gamma ray to confirm or deny this hypothesis, and if it is correct to define its part in the decay scheme.

The Measured Relative Intensities of the Am 241 Radiations

The measured relative intensities, of the electromagnetic radiations which were observed in Am241 decay, were given in Table 15. The table shows separately the relative intensities measured with sources A and B. In both cases the results shown are the means of a large number of measurements on recorded spectra, at gas pressures of 40, 60, and 80 centimetres of Mercury

pressure. The two sets of measurements agree reasonably well, with the exception of the intensities of the Np L_γ X-rays, and of the 26.4 keV gamma ray. In both cases the intensity measured with source A is considerably higher. The reason is not hard to find.

Source A consists of a strip of Silver, with Americium diffused into the surface. Under bombardment by the alpha particles and gamma rays of Americium, the silver fluorescent K X-rays will be induced. Now, the silver K_α- and K_β- X-rays have energies of 22.2 keV and 25.2 keV respectively. In the proportional counter these radiations would not be resolved from the peaks at 21 keV and 26.4 keV. If we assume that source B gives the correct relative intensities for the peaks at 21 keV and 26.4 keV, and subtract them from the values obtained with source A, we are left with relative intensities of 0.258 and 0.069 for the silver K_α and K_β X-rays. The ratio of these two intensities gives $K_\alpha/K_\beta = 3.895 \pm 2.0$, which agrees with $K_\alpha/K_{\beta_1} + K_{\beta_2} = 4.25$, the value measured by Williams (1933), and confirms our hypothesis.

Table 15 also shows the final values adopted for the relative intensities of the radiations emitted in Am 241 decay. For the L_γ X-rays and the 26.4 keV gamma ray, the mean of the values obtained with source B was adopted. For the other radiations, the mean of all the measurements made with both sources was adopted.

In Table 16 these adopted values are compared directly with other measurements of the same quantities. This

TABLE 16 †

Comparison of the Measured Intensities of the Am 241 Electromagnetic Radiations

Energy / Author	L_α	L_β	L_γ	26.4 keV	33.2 keV	59.6 keV	$I(L)/I(60)$
Present Results	0.599 ±0.013	1.0	0.236 ±0.014	0.134 ±0.006	0.075 ±0.022	1.644 ±0.086	1.11 ± 0.07
Magnusson (1957)	0.733	1.0	0.270	0.133	-	1.757	1.14
Beling et al. (1952)	0.572	1.0	0.277	0.123	-	1.786	1.035 ± 0.096
Jaffe et al. (1955)	0.486	1.0	0.438	-	-	-	
	0.607	1.0	0.357	-	-	-	
Cochran (1955)	1.51	1.0	0.256	-	-	-	
Day (1955)	0.551	1.0	0.264	0.154	0.0094	1.88	0.964
Day (1956)	0.556	1.0	0.252	0.151	0.008	2.02	

Notes. (1) Intensities are quoted relative to the Np L_β group.

(2) The second set of results attributed to Jaffe et al. was obtained from the first, on the assumption that the reflectivity of their curved crystal is proportional to the wavelength of the incident electromagnetic radiation.

Amended Values.

Magnusson (1957)	0.776	1.0	0.272	0.133	—	1.96	1.047.
Day * (1957)	0.601	1.0	0.266	0.154	—	2.05	0.911

* Recalculated by Magnusson (1957)

† See Appendix D – (b)

Table also includes the measured values of I(L)/I(60), which is the ratio of the total intensity of the L X-rays to the intensity of the 59.6 keV gamma ray. Two sets of measurements are given in the Table opposite the name of Jaffe et al. The first set are those given by Jaffe et al. on the assumption that the reflectivity of their curved crystal spectrograph varies as $1/E^2$. The second set are the same results modified by Cochran (1955), on the assumption that the reflectivity varies as $1/E$. The second set are in much better agreement with the other values in the Table.

An examination of the results shown in Table 16 shows that the values presented here are in good agreement with most of the previous measurements, but that they markedly disagree with the original measurements of Jaffe et al., and with the measurements of Cochran. The former disagreement is partially dispelled by Cochran's amendment of the reflectivity correction. To recapitulate from Chapter 6, "If relative intensity measurements are to be made with such a spectrometer in the wavelength region below 0.5Å, then it is essential to measure the value of R." Any residual disagreement with the results of Jaffe et al. would probably be corrected by a knowledge of the correct variation of reflectivity of their crystal. Cochran's results disagree violently not only with the results presented here, but with all of the results shown in the Table. His value of L_α/L_β is more than twice that of any of the other values shown, and there is

little doubt that it is in error. It is possible that his source was wrongly positioned relative to the curved crystal, which would result in a large energy dependent error in the observed relative intensities.

The Fluorescence Yields of Neptunium

From the measured relative intensities of the electromagnetic radiations observed in Am 241 decay, together with measurements of the conversion electron and Auger electron intensities which have appeared in the literature, we can obtain a measure of the L shell fluorescence, Auger, and Coster-Kronig yields of Neptunium ($Z = 93$).

The mean L shell fluorescence yield $\bar{\omega}_L$ may be written in terms of measured quantities as

$$\bar{\omega}_L = \frac{I_L}{I_{60}\,\alpha_L} \cdot \frac{N_{60}}{N_L} \qquad (7.1),$$

where I_L and I_{60} are the intensities of the L X-rays and 60 keV gamma rays emitted in Am 241 decay; α_L is the L shell conversion coefficient of the 60 keV gamma ray; N_L and N_{60} are the intensities of all L conversion electrons, and of L conversion electrons due to the 60 keV transition respectively, in arbitrary units.

The mean of the measurements shown in Table 16 shows

I_L/I_{60} = 1.058 ± 0.040. Samoilov (1957) has made the most complete examination of the conversion electron spectrum and his results are in reasonable agreement with other workers except for the LI: LII : LIII conversion ratios for the 60 keV transition. For this transition he finds LI : LII : LIII = 0.64 : 1.0 : 0.357, compared with the values 0.502 : 1.0 : 0.285, which are the means of the results due to some six authors quoted by Wolfson and Park (1964). Using Samoilov's results we obtain N_{60}/N_L = 0.497. Correcting them to take account of the discrepancy noted in his measurements for the 59.6 keV transition we get N_{60}/N_L = 0.478. Jaffe et al. (1955) have measured α_L as 0.72 ± 0.007. This value was obtained from measurements of the transmission of their β-spectrometer, and of the alpha particle counting rate. They also assumed that 0.40 60 keV photons are emitted per alpha disintegration. On correcting this last value to 0.379 60 keV photons per alpha particle we obtain α_L = 0.76.

On inserting these values in equation (7.1) we obtain $\bar{\omega}_L$ = 0.665, a value greatly in excess of the few direct measurements previously made in this region. In the opinion of the author the reason for this discrepancy lies in the value adopted for α_L, which Jaffe et al. obtained indirectly from a series of measurements. The other values inserted in equation (7.1) were measured directly, and are either the means of several measurements, or are in reasonable agreement with other available

measurements of the same quantities. Accordingly, it was decided to obtain an estimate of the value of α_L from other sources.

The total conversion coefficient of the 59.6 keV gamma ray can be written as

$$\alpha_T = \frac{59.6e^-}{59.6\gamma} \qquad (7.2)$$

where 59.6γ and $59.6e^-$ represent the intensities per alpha disintegration of the 59.6 keV gamma rays, and conversion electrons from all shells respectively. This notation will be used to represent intensities throughout this section of the thesis. A subscript attached to the e^-, e.g. e^-_L, will indicate the shell in which conversion has taken place.

Equation (7.2) may be rewritten as*

$$\alpha_T = \frac{\text{Population of the 59.6 keV state} - 59.6\gamma - 26.4e^- - 26.4\gamma}{59.6\gamma} \qquad (7.3)$$

59.6γ has been measured by both Beling et al. (1952) and Magnusson (1957). They found $59.6\gamma = 0.40 \pm 0.015$ and 0.359 respectively. The mean of these measurements, $59.6\gamma = 0.379$, has been adopted here. Turner (1952) has measured $26.4\ e^-_{M+N} = 0.023$. This value can be combined with Samoilov's measurement of $e^-/e^-_{M+N} = 3.15$ for the same transition, to give $26.4\ e^- = 0.0725$. 26.4γ was measured here as 0.0316.

If we ignore the weak gamma transitions from levels

* See Appendix D – (a).

higher than the $^{9}/_{2}$-level at 158.6 keV we can write:

$$\text{Population of the 60 keV state} = 0.86 + 43.4\gamma + 43.4e^{-} + 99.0\gamma + 99.0e^{-} \qquad (7.4).$$

Jaffe et al. have measured $43.4\ e_L^- = 0.091$, which can be combined with the value $e_L^-/e^- = 0.78$, measured by Passel (1954) for the 44 keV transition in Cm 242 decay, to give $43.4e^- = 0.118$. The ratio $43.4\gamma/59.6\gamma$ has been measured as 0.006 by Day (1955). Using $59.6\gamma = 0.379$ we obtain $43.4\gamma = 0.0023$. Jaffe et al. have also measured $99e_L^- = 0.00099$ and $99\gamma = 0.0006$. On combining the former value with $e^-/e_L^- = 1.3$, which was measured by Passel for the 102 keV transition in Cm 242 decay, we obtain $99.0e^- = 0.0013$. From these measurements we obtain a value of 0.9822 for the population of the 60 keV level.

Substituting in equation (7.3) we obtain

$$\alpha_T = \frac{0.9822 - 0.379 - 0.0729 - 0.0316}{0.379}$$

$$= 1.317 \ ,$$

which we can combine with $\alpha_L/\alpha_T = 0.78$ to give $\alpha_L = 1.028$.

We may now return to equation (7.1). On substituting the values $N_L/N_{60} = 0.478$, $I_L/I_{60} = 1.058$, and $\alpha_L = 1.028$ we obtain $\bar{\omega}_L = 0.4925$, which is in much better agreement with the other values previously measured in this region of the Periodic Table.

Using this value of $\bar{\omega}_L$ we can also obtain a measure of the individual fluorescence and Auger yields of the L subshells. If we define X_1, X_2, and X_3 as the number of X-ray quanta from the LI, LII, and LIII subshells per primary vacancy created in the L shell; and A_1, A_2, and A_3 as the number of Auger electrons from the LI, LII, and LIII subshells per primary vacancy created in the L shell, then we may write

$$\left.\begin{aligned} X_1 + X_2 + X_3 &= \bar{\omega}_L \\ A_1 + A_2 + A_3 &= \bar{a}_L \\ n_1 + n_2 + n_3 &= 1 \end{aligned}\right\} \qquad (7.5)$$

$$\left.\begin{aligned} X_1 &= \omega_1 n_1 \\ X_2 &= \omega_2(n_2 + f_{12} n_1) \\ X_3 &= \omega_3(n_3 + f_{13}n_1 + f_{23}(n_2 + f_{12}n_1)) \end{aligned}\right\} \qquad (7.6)$$

$$\left.\begin{aligned} A_1 &= a_1 n_1 \\ A_2 &= a_2(n_2 + f_{12}n_1) \\ A_3 &= a_3(n_3 + f_{13}n_1 + f_{23}(n_2 + f_{12}n_1)) \end{aligned}\right\} \qquad (7.7)$$

$$\left.\begin{aligned} \bar{\omega}_L + \bar{a}_L &= 1 \\ \omega_1 + f_{12} + f_{13} + a_1 &= 1 \\ \omega_2 + f_{23} + a_2 &= 1 \\ \omega_3 + a_3 &= 1 \end{aligned}\right\} \qquad (7.8)$$

We have already found $\bar{\omega}_L = 0.4925$, so that $\bar{a}_L = 0.5075$. From a knowledge of the quantities n_1, n_2, n_3, X_1, X_2, X_3, A_1, A_2, and A_3 we can obtain the individual L subshell yields from equations (7.5), (7.6), (7.7) and (7.8). We are also required to make the assumption that $f_{12} = 0.1$.

Some six or seven authors (Turner (1952), Hollander et al. (1956), Rosenblum et al. (1957), Samoilov (1957), Wolfson and Park (1964) have examined the conversion electron spectrum from Am 241. Their results are not all equally reliable, and they have not all used sufficiently high resolution to distinguish clearly between the many peaks present in the complex electron spectrum. ~~Accordingly it was decided to use the results of Wolfson and Park, and of Samoilov to obtain the values of n_1, n_2, and n_3, and to use the results of the other workers to correct their values when they deviate markedly from the norm.~~ Samoilov's measurements were much more extensive than those of Wolfson and Park, but the latter were made at much higher resolution. Thus Wolfson and Park were able to examine the spectrum in greater detail. The values of n_1, n_2, and n_3 were derived from Wolfson and Park's measurements, using Samoilov's data for the low energy transitions not examined. The resulting values were $n_1 = 0.356$, $n_2 = 0.453$, and $n_3 = 0.191$.

The values* of X_1, X_2, and X_3 were obtained from the measured ratios $L_\alpha : L_\beta : L_\gamma = 0.599 : 1.0 : 0.236$, which were presented earlier in this chapter, together

* See Appendix D – (c) & (d).

with a knowledge of the fractions of photons from the LI, LII, and LIII shells which appear in the L_β group. The fractions* of LI, and LII photons were taken as 0.7316, and 0.7674 respectively, the means of the values given by Day (1955), Cochran (1955), Compton and Allison (1935), Barton et al. (1951), Salgueiro et al. (1961) and Goldberg (1961). It follows from the results shown in Table 13 that the fraction of photons from the LIII shell appearing in L_β is 0.250. This value was adopted here. Using these values we obtain $X_1 : X_2 : X_3 = 1.0 : 5.49 : 4.94$. From the value $\bar{\omega}_L = 0.4925$ we find $X_1 = 0.043$, $X_2 = 0.236$ and $X_3 = 0.2125$.

Only one measurement of the Auger electron intensities from the three L subshells was available. Akalayev et al. (1964) found $A_1 : A_2 : A_3 = 11 : 15 : 35$. They have published very few experimental details, and it is impossible to assess how reliable these values are. Combining them with the value $\bar{a}_L = 0.5075$, we obtain $A_1 = 0.092$, $A_2 = 0.125$, and $A_3 = 0.291$.

We now have all of the information required to obtain the desired subshell yields. On substituting the values which we have found in equations (7.5) - (7.8), we obtain the values shown in column 2 of Table 17. This Table also shows the values of the same quantities which are given by Listengarten (1961), and by Akalayev et al. (1964).

The results presented here are in much better agreement with Listengarten's results than with those of Akalayev et al. The latter group obtained their values

* See Appendix D – (c)

TABLE 17 *

L Shell Fluorescence Yields of Neptunium (Z = 93)

	Present Results	Listengarten (1961)	Akalayev et al. (1964)
ω_1	0.12 ± 0.02	0.28 ± 0.06	0.19 ± 0.04
ω_2	0.48 ± 0.08	0.51 ± 0.10	0.78 ± 0.19
ω_3	0.424 or 0.422 ± 0.07	0.47 ± 0.10	0.57 ± 0.12
a_1	0.26 ± 0.05	$0.15 \pm {0.19 \atop 0.15}$	0.16 ± 0.03
a_2	0.26 ± 0.08	0.30 ± 0.18	0.20 ± 0.06
a_3	0.576 or 0.578 ± 0.07	0.53 ± 0.10	0.43 ± 0.09
f_{12}	0.1	0.1	0.1
f_{13}	0.52 ± 0.07	0.47 ± 0.09	0.55 ± 0.09
f_{23}	0.26 ± 0.10	0.20 ± 0.08	$0.02 \pm {0.05 \atop 0.02}$
$\bar{\omega}_L$	0.49 ± 0.07	0.56	0.66 ± 0.08

Notes:

(1) The value of $f_{12} = 0.1$ was assumed by the present author, and by Akalayev et al.

(2) $\bar{\omega}_L$ was calculated from Listengarten's individual yields using $n_1 = 0.356$, $n_2 = 0.453$ and $n_3 = 0.191$.

(2) In column 2 two values of ω_3 and a_3 are given because these two quantities can be obtained in two ways from the information available.

* See Appendix D – (d).

from an analysis similar to that employed here. Their final values of $\omega_3 = 0.57$ and $\omega_2 = 0.78$, are much higher than the present values, and very much higher than any previous measurement would lead one to expect. The reason for this disagreement lies mainly in the values $\bar{\omega}_L = 0.66$, and $n_1 = 0.374$ which they adopted. The present author believes that the former value is erroneous, and that the fault lies in the adoption of Jaffe et al.'s (1955) value of $\alpha_L = 0.72$ for the L shell conversion coefficient of the 59.6 keV transition. Their values of n_1, n_2, and n_3 were obtained entirely from the conversion electron measurements of Samoilov (1959). The present author has already pointed out that Samoilov's measurement of the ratio of LI/LII conversion for the 59.6 keV transition is some thirty per cent higher than that of any other author. This discrepancy is the main factor in producing the high value of n_1 which was finally adopted by Akalayev et al.

Within the quoted uncertainties the present values of the LII and LIII shell yields of Neptunium agree reasonably well with those of Listengarten. We again note that $\omega_2 = 0.48$ is somewhat lower than Listengarten's value, $\omega_2 = 0.51$; a point which we will return to later. For the LI shell yields, the agreement is not as good, and in particular the values of ω_1 are very different. It is the larger value of ω_1, which is the prime cause of the higher value of $\bar{\omega}_L$ obtained from

Listengarten's fluorescence yields using the values of n_1, n_2, and n_3 obtained earlier.

It is worth pointing out at this juncture that the large uncertainties attached to the present values result from the cumulative nature of experimental error. They are the natural consequence of any form of analysis such as the present one, and emphasise the advantages of the experimental approach described in Chapter 3, which is the main subject of this thesis.

REFERENCES - CHAPTER 7

1. Akalayev, G.G., Vartanov, N.A. and Samoilov, P.S. (1964), Isvestiya Akad. Nauk SSSR, Ser. Fiz. 28, 1260.

2. Baranov, S.A. and Shylagin, K.N. (1956), J. Exp. i. Teor. Fiz. (U.S.S.R.), 3, 200.

3. Barton, G.W., Robinson, H.P. and Perlman, I. (1951), Phys. Rev. 81, 208.

4. Beling, J.K., Newton, J.O. and Rose, B. (1952), Phys. Rev. 87, 670.

5. Browne, C.I. (1952), Ph.D., University of California, UCRL - 1764.

6. Cochran, A.J. (1955), Ph.D. Thesis, University of Edinburgh.

7. Compton, A.H. and Allison, S.K. (1935), 'X-rays in Theory and Experiment', (Published by D. Van Nostrand Company, Inc., New York).

8. Day, P.P. (1955), Phys. Rev. 97, 689.

9. Goldberg, M. (1961), J. Phys. Rad. 22, 743.

10. Hoffman, D.C. and Dropesky, B.J. (1958), Phys. Rev. 109, 1282.

11. Hollander, J.M., Smith, W.G. and Rasmussen, J.O. (1956), Phys. Rev. 102, 1372.

12. Jaffe, H., Passel, T.O., Browne, C.I. and Perlman, I. (1955), Phys. Rev. 97, 142.

13. Listengarten, M.A. (1961), Isvestiya Nauk Akad. SSSR, Ser. Fiz. 24, 1041.

14. Magnusson, L.B. (1957), Phys. Rev. 107, 161.

15. Michaelis, W. (1965), Z. Physik 186, 42.

16. Rasmussen, J.O., Canavan, F.L. and Hollander, J.M. (1957), Phys. Rev. 107, 141.

17. Rosenblum, S., Valadares, M. and Milsted, J. (1957), J. phys. Rad. 18, 609.

18. Salguiero, L., Ferreira, J.G., Park, J.J.H. and Ross, M.A.S., (1961), Proc. Phys. Soc. 77, 657.

19. Samoilov, P.S. (1959), Isvestiya Akad. Nauk SSSR, Ser. Fiz. 23, 1416.

20. Sliv, L.A. and Band, I.M. (1956), Leningrad Physico-Technical Institute Report (Translation: 1958, Reports 57ICCKI, 58ICCLI, Physics Department, University of Illinois).

21. Strominger, D., Hollander, J.M. and Seaborg, E.T., (1958), Rev. Mod. Phys. 30, 585.

22. Turner, J.F. (1955), Phil. Mag. 46, 687.

23. West, D., Dawson, J.K. and Mandleberg, C.J. (1952), Phil. Mag. 43, 875.

24. West, D. and Rothwell, P. (1953), Phil. Mag. Suppl. 2, 411.

25. Williams, J.H. (1933), Phys. Rev. 44, 146.

26. Wolfson, J.L. and Park, J.J.H. (1964), Can. J. Phys. 42, 1387.

CHAPTER 8

THE LII SHELL YIELDS OF URANIUM AND PLUTONIUM

In Chapter 3 it was shown that the LII shell fluorescence yields of Uranium and Plutonium could be obtained from measurements of the five quantities ω_3, I, C_3', F, and F_3' for the three decays Pu 238, Pu 240, and Cm 244. In Chapters 4 and 5 measurements of F for these three decays were described; followed in Chapters 6 and 7 by the description of measurements of F_3' for the same isotopes. In the present chapter, values of the remaining three quantities, drawn from the literature, will be discussed. The LII shell yields of Uranium and Plutonium will then be derived by substitution of the measured quantities in equations (3.3) and (3.4). Finally, the significance of the measured values will be discussed.

ω_3 :- Very few measurements of ω_3 exist for elements in this region of the Periodic Table. Stephenson (1937) has made direct measurements of the LIII shell yields of Thorium (Z = 90) and Uranium (Z = 92). He obtained $\omega_3 = 0.42$ for Thorium, and $\omega_3 = 0.44$ for Uranium. Listengarten (1961) has estimated the values of ω_3 for all elements between Z = 47 and Z = 98 from the calculated radiation widths, and the measured total effective line widths. He obtained $\omega_3 = 0.46 \pm 0.05$ for Uranium, and $\omega_3 = 0.48 \pm 0.05$ for Plutonium.

The values finally adopted here were those of Burhop (1955). Burhop's values were based on Küstner and Arends' (1935) direct measurements of ω_3 for seven

elements in the range Z = 73 to Z = 83, and the direct measurements of ω_3 made by Stephenson (1937) for Z = 82, 90, and 92. He fitted this data to a relation of the form

$$\left(\frac{\omega_3}{1-\omega_3}\right)^{1/4} = A + BZ \quad , \qquad (8.1)$$

where A and B are constants. From a least squares fit he obtained the values A = -0.221, and B = + 0.0126 for these constants. For Uranium, equation (8.1) gives $\omega_3 = 0.437 \pm 0.010$, and for Plutonium it gives $\omega_3 = 0.462 \pm 0.010$. These values agree with Listengarten's LIII shell yields within the quoted errors.

Some criticism of the use of Burhop's values may be made on the grounds that they are not based on all of the data now available. No attempt has been made to incorporate the results of Jopson et al. (1964) for some twelve elements in the range Z = 67 to Z = 83, since they have very large uncertainties attached, and do not show a very definite variation with Atomic number. A few measurements for single elements were also ignored, since in general they agree reasonably well with the values obtained from equation (8.1).

C_3' and I for Cm 244 Decay:- Both of these quantities can be obtained from a knowledge of n_1, n_2, and n_3, the numbers of primary ionisations per disintegration in the LI, LII, and LIII subshells. In their turn, values of n_1, n_2, and n_3 can be obtained from measurements of the intensities of the alpha particle groups populating the excited levels of Pu 240, U 234, and U 236, together with a knowledge of the relative intensities of internal

conversion and gamma emission for the transitions de-exciting these excited states.

For Cm 244 decay, Hummel (1956) has made precise measurements of the relative intensities of the states of Pu 240 produced from Cm 244 alpha decay. Hummel used an alpha particle magnetic spectrograph with approximately 8 keV resolution. His work was carefully carried out, and his results are shown in Table 18a. From these results the absolute intensities of the 42.88 keV, 100 keV, and 150 keV transitions are 0.23316, 0.00021, and 0.00004 per alpha disintegration respectively.

With regard to measurements of the relative intensities in conversion and emission of the transitions de-exciting the excited states of Pu 240, the position is much less satisfactory. A single direct measurement of the LII/LIII conversion ratio for the 42.88 keV transition is available. Smith and Hollander (1956) made a rough measurement of this ratio with a β-spectrograph, and concluded that the results were "essentially the same as obtained with Cm 242". Since no other measurements have been made, the calculated conversion coefficients of Sliv and Band (1958) have been adopted. The resulting relative intensities in conversion and emission are shown in Table 18b.

The amount of conversion in the (M + N + O) shells was obtained from the total L conversion, using the measured ratios of L/(L + M + N + O) conversion for the corresponding 44 keV and 102 keV transitions in Pu 238, following Np 238 and Cm 242 decay.

From the values shown in Tables 18a and 18b, $n_1 = 0.00337$, $n_2 = 0.09652$, and $n_3 = 0.08015$ for Cm 244

TABLE 18

a) Relative Intensities of the Alpha particle groups emitted in Cm. 244 Decay

Alpha Particle Group	Decay Energy to Ground State	Abundance	Author
α_0	0 keV	0.767	Hummel (1956)
α_1	42.9 keV	0.233	"
α_2	142.2 keV	0.00017	"
α_3	292 keV	0.00004	"

b) Relative Intensities in conversion and emission of Transitions in Pu 240

Energy	K	LI	LII	LIII	(M+N+O)	Y	Total
150 keV	0.1892	0.0981	1.1420	0.6318	0.556	1.0	3.6171
100 keV	-	0.3711	7.596	4.788	3.775	1.0	17.530
42.9 keV	-	13.42	384.5	319.40	211.85	1.0	930.171

decay. These values take account of the transfer of vacancies from the K- to the L-shells, following the K conversion of the 150 keV transition. The ratios of $K\alpha_2 : K\beta : K\alpha_1$ were obtained from Wapstra et al. (1959), and $\omega_K = 0.96$ was obtained from Listengarten (1961).

In calculating C_3' and I from the values of n_1, n_2, and n_3 we must take account of the non-zero value of n_1. Since the Coster-Kronig transfers f_{12} and f_{13} are approximately 0.1 and 0.5 in this region, most of the vacancies in the LI shell are transferred to the LII and LIII shells. Thus the final values of C_3' and I are given by

$$C_3' = \frac{n_3\left(1 + f_{13}\frac{n_1}{n_3}\right)}{n_2\left(1 + f_{12}\frac{n_1}{n_2}\right)} , \qquad (8.2)$$

$$\text{and } I = n_2 + n_3 + n_1(f_{12} + f_{13}) .$$

On substituting the values of n_1, n_2, and n_3 for Pu 240, following Cm 244 decay, in equations (8.2) we obtain

$$\begin{aligned} I &= 0.1787 \pm 0.005 , \\ \text{and } C_3' &= 0.845 \pm 0.03 \end{aligned} \qquad (8.3)$$

We now have sufficient information on Cm 244 decay to obtain the LII shell yields of Plutonium. On substituting the values

$$\begin{aligned} F &= 0.0942 \pm 0.0012 , & C_3' &= 0.845 \pm 0.03 , \\ F_3' &= 1.19 \pm 0.06, & I &= 0.1787 \pm 0.005 \\ \text{and } \omega_3 &= 0.462 \pm 0.01 , \end{aligned} \qquad (8.4)$$

in equations (3.3) and (3.4) we obtain the Plutonium LII shell yields;

$$\omega_2 = 0.444 \pm 0.025 \ ,$$

$$f_{23} = 0.30 \pm 0.15 \ , \qquad (8.5)$$

$$\text{and } a_2 = 0.26 \pm 0.17 \ .$$

These values are compared with other measures of the same quantities in Table 19. Row 2 of Table 19 also shows the LII shell yields of Plutonium derived from the values given in (8.4), with the present value of F replaced by F = 0.0890, the measured value obtained by Woods Halley and Engelkeimer (1964). Table 19 also shows two sets of LII shell yields, which are ascribed to Salguiero et al. (1961). Row 3 gives their original values for Cm 242 decay, and Row 4 shows their results recalculated on the same basis as the present results for Cm 244 decay, i.e. using Sliv and Band's calculated conversion coefficients, and Burhop's value of ω_3 for Plutonium. Finally, in column 5, Table 19 shows the LII shell yields of Plutonium according to Listengarten (1961).

The four sets of values shown in Table 19 agree within the experimental error, although Listengarten's value of ω_2 is somewhat higher than the others. The agreement with the recalculated values of Salguiero et al.'s results is better than with their original results, which is not altogether surprising, since their values were recalculated on the same basis as the other results presented here. This raises the question of the effect of the

TABLE 19

Comparison of Measured Values of the LII Shell Yields of Plutonium

Author	Decay	ω_2	f_{23}	a_2
Present Results	Cm 244	0.444 ± 0.025	0.30 ± 0.15	0.26 ± 0.17
Woods Halley & Engelkeimer (1964)	Cm 244	0.422 ± 0.025	0.24 ± 0.15	0.34 ± 0.17
Salguiero et al. (1961)	Cm 242	0.413 ± 0.02	0.22 ± 0.08	0.37 ± 0.08
Salguiero et al. (1961)*	Cm 242	0.429 ± 0.02	0.29 ± 0.09	0.28 ± 0.11
Listengarten (1961)	-	0.48 ± 0.10	0.24 ± 0.10	0.28 ± 0.20

* This set of values was derived from Salguiero et al.'s measurements of F and F_3' for Cm 242 decay, together with Sliv and Band's conversion coefficients and Burhop's (1955) value of ω_3.

adoption of the calculated conversion coefficients on the resulting LII shell yields.

Virtually no experimental evidence is available concerning the conversion coefficients of the relevant transitions in Pu 240, U 234, and U 236. As already pointed out, what little there is suggests that they are essentially the same as for the corresponding transitions in Pu 238, following Cm 242 and Np 238 decay. Again this is not surprising since Cm 242 decay is of exactly the same type as the three decays studied here. Salguiero et al. (1961) have summarised the available information on the 44.1 keV transition in Pu 238, and the relevant data, taken from their paper, is shown in Table 20.

From the results shown in Table 20 it is clear that the ratio of LIII/LII conversion for the 44.1 keV transition is somewhat less than Sliv and Band's calculated value. Indeed the mean of the experimental values is some nine per cent less than the calculated value. The strong similarity in the nuclear properties of Cm 242 and the three isotopes studied here, suggests that the calculated values of LIII/LII conversion are likely to be too high for the corresponding transitions in these nuclei. Now it is readily seen from equation (8.2) that C_3' is mainly determined by the ratio of LIII/LII conversion for this transition. Hence if Sliv and Band's calculated values are adopted, the value of C_3' is likely to be too high by some eight per cent. The LII shell yield is

TABLE 20

Relative Intensities in Conversion and Emission of the 44 keV Transition in Pu 238

Author	LI	LII	LIII	(M+N+O)	γ-Ray
Slatis et al. (1954)	-	1.0	0.732	0.530	-
Passel (1954)	0.032	1.0	0.795 ± 0.03	0.538	-
Smith & Hollander (1956)	-	1.0	0.820 ± 0.03	-	-
Sliv & Band (1958)	0.035	1.0	0.857	-	0.003
Experimental Mean Values	-	1.0	0.782 ± 0.03	0.534 ± 0.02	-

Note - (1) The entries in this Table are taken from Salguiero et al. (1961).

(2) The first and second entries were measurements made following Np 238 β^--decay.

(3) The values attributed to Sliv and Band are calculated values.

proportional to $(1 + C_3')$, so that an error of eight per cent in C_3' will lead to an error of some three to three and a half per cent in the final value of ω_2. From this information it must be concluded that the adoption of the theoretical conversion coefficients, in the calculations of C_3' and I for the decays studied here, is likely to lead to a systematic error of about three to three and a half per cent in the values of ω_2 which are obtained. The values of ω_2 will be too high by this amount. Nevertheless in the absence of any direct experimental evidence, it has been thought best to use the calculated conversion coefficients in the knowledge that they may later prove to differ from the true values.

C_3' and I for Pu 238:- Four authors have examined the alpha particle spectrum from Pu 238, and their measurements of the intensities of the alpha particle groups populating the excited states of U 234 are shown in Table 21a. The first three used alpha particle magnetic spectrographs, and the fourth used a semiconductor counter with 20 keV resolution. The four sets of results agree reasonably well, and the mean values of the intensities were adopted. From these results the absolute intensities of the 43.5 keV, 100 keV, and 146 keV transitions are 0.29335, 0.00135, and 0.00005 per alpha disintegration respectively.

Again no measurements of the internal conversion coefficients of the 43.5 keV, 100 keV, and 146 keV

TABLE 21

a) Relative Intensities of the α-Particle Groups emitted in Pu 238 Decay.

Author	α_0	α_1	α_2	α_3
Asaro and Perlman (1954)	0.72	0.28	0.001	0.00005
Goldin et al. (1955)	0.69	0.31	-	-
Kondratyev et al. (1957)	0.711	0.288	0.0013	0.00005
Woods Halley & Engelkeimer (1964)	0.711	0.289	-	-
Selected Values	0.7067	0.292	0.0013	0.00005

b) Relative Intensities in Conversion and Emission of Transitions in U 234.

Transition Energy	K	LI	LII	LIII	(M+N+O)	γ	Total
146 keV	0.2095	0.0776	0.8925	0.5020	0.438	1.0	3.1196
100 keV	-	0.288	6.087	3.968	3.072	1.0	14.415
43.5 keV	-	9.545	284.7	248.5	160.3	1.0	704.037

transitions in U 234 are available. On this account Sliv and Band's calculated conversion coefficients were again adopted, and the relative intensities in conversion and emission of the above mentioned transitions in U 234 are shown in Table 21 b. The conversion coefficients shown in Table 21b, together with the absolute intensities of the transitions, lead to the values $n_1 = 0.00401$, $n_2 = 0.11921$, and $n_3 = 0.10392$ for U 234 following Pu 238 alpha decay. As in the previous case allowance was made for the transfer of ionisation from the K- to the L-shells following the K conversion of the 146 keV transition.

On substituting these values of n_1, n_2, and n_3 in equations (8.2) we obtain

$$\begin{aligned} c_3' &= 0.886 \pm 0.03, \\ \text{and } I &= 0.2255 \pm 0.005 \quad . \end{aligned} \tag{8.6}$$

We now have sufficient information concerning Pu 238 decay to obtain the LII shell yields of Uranium. On substituting the values

$$\begin{aligned} F &= 0.1283 \pm 0.0010 , & c_3' &= 0.886 \pm 0.03, \\ F_3' &= 1.11 \pm 0.07 , & I &= 0.2255 \pm 0.005, \\ & \text{and } \omega_3 = 0.437 \pm 0.010 \end{aligned} \tag{8.7}$$

in the equations (3.3) and (3.4) we obtain

$$\omega_2 = 0.508 \pm 0.03 \quad , \qquad .494$$

$$f_{23} = 0.403 \pm 0.15 \quad , \qquad .334 \qquad (8.8)$$

$$\text{and} \quad a_2 = 0.089 \pm \begin{matrix} 0.18 \\ 0.089 \end{matrix} \quad , \qquad .172$$

for Uranium. These values, together with the values of the same quantities derived from the measurements on Pu 240 decay will be discussed later.

C_3' and I for Pu 240 Decay.

For Pu 240 decay only one measurement has been made of the relative intensities of the alpha particle groups feeding the excited states of U 236. These measurements were made by Goldin et al. (1956) with an alpha particle magnetic spectrograph. Their results are shown in Table 22a. From these measurements the absolute intensities of the 45.28 keV, 105 keV, and 162 keV transitions in U 236 are 0.24477, 0.00092, and 0.00003 per alpha disintegration respectively.

Again there are no experimental measurements of the conversion coefficients of the transitions in U 236, and again it is necessary to have recourse to the calculated conversion coefficients. The adopted conversion coefficients from Sliv and Band's Tables are shown in Table 22b. The values of n_1, n_2, and n_3 for U 236 following Pu 240 alpha decay were obtained from these conversion coefficients, together with the values of the absolute intensities of the three transitions. The values obtained were $n_1 = 0.00332$, $n_2 = 0.10010$, and $n_3 = 0.08554$.

TABLE 22

a) Relative Intensities of the α-Particle Groups emitted in Pu 240 Decay

Alpha Particle Group	Decay Energy to Ground State	Abundance	Author
α_0	0 keV	0.755	Goldin et al. (1956)
α_1	45.28 keV	0.245	"
α_2	151 keV	0.00085	"
α_3	206 keV	0.00007	"

b) Relative Intensities in Conversion and Emission of Transitions in U 236.

Transition Energy	K	LI	LII	LIII	(M+N+O)	γ	Total
45.28 keV	-	8.138	244.80	209.40	137.62	1.0	600.96
105.7 keV	-	0.236	4.6400	3.011	0.223	1.0	11.217
162 keV	0.1989	0.0662	0.6954	0.3745	0.336	1.0	2.5710

On substituting for n_1, n_2, and n_3 in equations (8.2) we find

$$C_3' = 0.868 \pm 0.03 , \quad \text{and} \quad I = 0.1876 \pm 0.005. \tag{8.9}$$

We now have sufficient information to obtain the Uranium LII shell yields from the measurements for Pu 240 decay. On substituting the values

$$F = 0.1041 \pm 0.0007 , \quad C_3' = 0.868 \pm 0.03 ,$$
$$F_3' = 1.09 \pm 0.07 , \quad I = 0.1876 \pm 0.005 , \tag{8.10}$$
$$\text{and} \quad \omega_3 = 0.437 \pm 0.010 ,$$

In equations (3.3) and (3.4) we obtain

$$\omega_2 = 0.496 \pm 0.03 ,$$
$$f_{23} = 0.36 \pm 0.15 , \tag{8.11}$$
$$\text{and} \quad a_2 = 0.14 \pm \begin{matrix} 0.18 \\ 0.14 \end{matrix} .$$

for Uranium.

We now have two sets of results for the LII shell yields of Uranium, and in Table 23 they are compared. Table 23 also shows the LII shell yields of Uranium derived from equations (3.3) and (3.4), using Woods Halley and Engelkeimer's (1964) measurement of F = 0.1060 for U 234 following Pu 238 alpha decay, together with the other values given in (8.7). Listengarten's (1961) values of the LII shell yields of Uranium are also given.

From Table 23 it can be seen that the two sets of

TABLE 23

Comparison of the LII Shell Yields of Uranium

Author	Decay			
Present Results	Pu 240	0.496 ± 0.03	0.36 ± 0.15	$0.14 \pm {}^{0.18}_{0.14}$
Present Results	Pu 238	0.508 ± 0.03	0.40 ± 0.15	$0.089 \, {}^{+0.18}_{-0.14}$
Woods Halley & Engelkeimer (1964)	Pu 238	0.422 ± 0.03	0.18 ± 0.11	0.40 ± 0.14
Listengarten (1961)	-	0.54 ± 0.10	0.11 ± 0.04	0.35 ± 0.14

values presented here are in very good agreement. But these values do not agree with the values obtained from Woods Halley and Engelkeimer's measurement of F for Pu 238 decay, which is not surprising since their value of F is lower than that presented in Chapter 5.by some sixteen per cent. This discrepancy was discussed in Chapter 5, where it was pointed out that Woods Halley and Engelkeimer's value of F for Th 230 decay was also some twenty six per cent lower than that of Booth et al. (1956). Indeed, where their measured values of F can be compared with others, they are always consistently lower.

Listengarten's value of ω_2 for Uranium is again higher than the values presented here. It is perhaps worth noting that for both Uranium and Plutonium, the present values of ω_2 are about seven and a half per cent lower than those of Listengarten. The value of ω_2 for Neptunium, which was presented in Chapter 7 was also some six and a half per cent lower than that given by Listengarten. Taken together, these results suggest that Listengarten's somewhat arbitrary correction of ten per cent to Massey and Burhop's (1936) calculated radiation widths for Z = 92 may be an overestimate.

The present values of f_{23} and a_2 differ markedly from the other values shown in Table 23. However these quantities are strongly dependent on the value found for ω_2, and a small disagreement in the measurement of ω_2 results in a large disagreement in the values of f_{23} and a_2.

Comparison of the LII Shell Yields of Uranium and Plutonium.

An examination of Tables 19 and 23 reveals that the present results show that ω_2 and f_{23} decrease, and a_2 increases as we go from Z = 92 to Z = 94. Thus although these results are not entirely in agreement with Listengarten's semi-empirical values of the LII shell yields, they do confirm his prediction of a cusp in the curve of ω_2 versus Z in the region above Z = 91.

Two main differences between the present results and Listengarten's predictions are apparent. Firstly he predicts that f_{23} should increase from 0.11 ± 0.04 for Uranium to 0.24 ± 0.10 for Plutonium. This compares with the decrease from 0.38 ± 0.15 to 0.30 ± 0.15, observed by the present author. Listengarten's prediction was based on the assumption "that the LII - LIII MIV, MV transitions cause Γ_{23} to increase for $Z > 91$ in the same way as Γ_{13} increases for $Z > 73$." In Chapter 2 it was pointed out that this assumption is unlikely to be correct. In that chapter it was remarked that the absolute Coster-Kronig transition probability is inversely proportional to the distance between the initial electron vacancy and the electron making the transition to fill this vacancy. In the case of f_{23} this distance will be smaller than for the case of f_{13}. In addition it was also pointed out that the absolute transition probability depends strongly on the energy of the ejected Coster-Kronig electron. Figure 3, in Chapter 1, showed

the variation of the energy of the LI - LIII MIV, MV, and LII - LIII MIV, MV Coster-Kronig electrons with Atomic number for the regions Z > 73, and Z > 91 respectively. It is readily seen from Figure 3 that the energy dependence is very different in the two cases. In the latter case, the ejected electron energy is very much higher when the transition first becomes possible. To judge from the electron energies at which the transition probability is a maximum in the other two cases shown in Figure 3, it seems likely that for the LII - LIII MIV, MV transitions the maximum transition probability will occur just when the transition becomes energetically possible, and will thenceforth decrease.

The present values also differ from Listengarten's values in the absolute magnitude of ω_2. This point has been raised several times already. In Chapter 7 it was noted that the values of F_3' predicted for Cm 244, Pu 238, and Pu 240 decay, from Listengarten's values of the L shell fluorescence yields, were much lower than the experimental values. It was suggested there that the values of F_3' were too low because the predicted values of ω_2 were too high. In the present chapter it was noted that the present values of ω_2 for Z = 92, 93, and 94 are lower than Listengarten's values by some six to eight per cent. Indeed, all of the experimental information available in this region suggests that his values of ω_2 are too high.

The LII shell yields derived from Woods Halley and Engelkeimer's measurements of F for Pu 238 and Cm 244 decay, disagree strongly with the present results. For Plutonium there is a reasonable measure of agreement, but for Uranium the results differ considerably from those presented here. Consequently they show an entirely different variation of ω_2 with Z. Their results suggest that there is no cusp in the graph of ω_2 versus Z for $Z > 91$, although there may be a stationary value, and that f_{23} increases only slightly in going from $Z = 92$ to $Z = 94$. The extent of the disagreement between these results and the present results is such that it can only be resolved by further experiment.

The Mean L Shell Fluorescence Yields.

It was explained in Chapter 2 that the mean L shell fluorescence yield, $\bar{\omega}_L$, is not of very great interest, since it is dependent not only on the individual fluorescence and Coster-Kronig yields of the element concerned, but on the mode of excitation employed. However it is a simple matter to obtain the mean L shell fluorescence yields of Uranium and Plutonium following the internal conversion of the low energy electric quadrupole transitions de-exciting the first excited states of U 234, U 236, and Pu 240.

We can write $\bar{\omega}_L = F/I$ in our usual notation. Substituting for the relevant values of F and I from

(8.4), (8.7), and (8.10) we obtain

$$\bar{\omega}_L = 0.530 \pm 0.02 \text{ for Pu 240, following Cm 244 } \alpha\text{-decay,}$$
$$\bar{\omega}_L = 0.571 \pm 0.02 \text{ for U 234, following Pu 238 } \alpha\text{-decay,} \quad (8.12)$$
and
$$\bar{\omega}_L = 0.554 \pm 0.02 \text{ for U 236, following Pu 240 } \alpha\text{-decay.}$$

In Conclusion

The LII shell fluorescence, Auger, and Coster-Kronig yields of Uranium and Plutonium have been measured as precisely as possible using the method outlined in Chapter 3. The results obtained confirm Listengarten's (1961) prediction that the LII shell fluorescence yield decreases for $Z > 91$, due to the onset of the LII - LIII MIV, MV Coster-Kronig transitions at $Z = 91$, and $Z = 94$. At the same time the present results show that the Coster-Kronig transfer yield, f_{23}, decreases as we go from $Z = 92$ to $Z = 94$, which disagrees with Listengarten's predictions. The present results suggest that f_{23} has a maximum for Z just greater than 91, and then decreases for higher values of Z.

The present results have been compared with the few other measurements of the LII shell yields of Uranium and Plutonium which are available. For Plutonium it was seen that the measured values agree reasonably well, but for Uranium they disagree strongly. In particular the present results differ markedly from those derived from the measurements of Woods Halley and Engelkeimer (1964).

Only further experiment will show which are correct.

In deriving values of C_3' and I to be used in determining the required LII shell yields it was found necessary to adopt Sliv and Band's (1958) calculated internal conversion coefficients for transitions in U 234, U 238, and Pu 240, since no experimental measurements had been made. In the present chapter the error introduced by the adoption of the calculated values was discussed, and from a comparison of the experimental and calculated values of the internal conversion coefficients for the similar case of Cm 244 decay, it was concluded that the final values of ω_2 are likely to be too high by some three to three and a half per cent. Precise measurements of the intensities of the conversion electrons emitted in the decays studied would improve the present results.

In 1955 it was possible for Ross et al. to say that "Further evidence on the fluorescence yields would clearly be of value." Ten years later, there has been little progress in this field. If measurements of the fluorescence yields are to be sufficiently reliable to be used as a basis for further experimentation on other phenomena such as electron capture and internal conversion a great deal of work requires to be done. The present results are a small step forward.

REFERENCES - CHAPTER 8

1. Asaro, F. and Perlman, I. (1954), Phys. Rev. 94, 381.

2. Burhop, E.S. (1955), J. Phys. Rad. 16, 625.

3. Goldin, L.L., Novikova, G.I. and Tretyakov, E.F. (1955), Conference of the USSR Academy of Sciences on Peaceful Uses of Atomic Energy.

4. Goldin, L.L., Novikova, G.I. and Tretyakov, E.F. (1956), Phys. Rev. 103, 1004.

5. Hummel, J.P. (1956), Ph.D. Thesis, University of California, UCRL Report - 3456.

6. Jopson, R.C., Khan, J.M., Mark, H., Swift, C.D. and Williamson, M.A., (1964), Phys. Rev. 133A, 381.

7. Kondratyev, L.N., Novikova, G.I., Dedov, V.B. and Goldin, L.L. (1957), Isvestiya Akad. Nauk SSSR, Ser Fiz. 21, 907.

8. Kustner, H. and Arends, E. (1935), Ann. Phys., Lpz., 22, 443.

9. Listengarten, M.A. (1961), Isvestiya Akad. Nauk SSSR, Ser. Fiz. 24, 1041.

10. Massey, N.S. and Burhop, E.S. (1936), Proc. Camb. Phil. Soc. 32, 461.

11. Passel, T.O. (1954), Thesis, University of California Laboratory Report No. 2528.

12. Salguiero, L., Ferreira, J.G., Park, J.J.H. and Ross, M.A.S. (1961), Proc. Phys. Soc. 77, 657.

13. Slatis, H., Rasmussen, J.O. and Atterling, H. (1954), Phys. Rev. 93, 646.

14. Sliv, L.A. and Band, I.M. (1956), Leningrad Physico-Technical Institute Report (Translation: 1958, Reports 57 ICCKI, 58 ICCLI, Physics Department, University of Illinois.)

15. Smith, W.G. and Hollander, J.M. (1956), Phys. Rev. 101, 746.

16. Stephenson, R.J. (1937), Phys. Rev. 51, 637.

17. Wapstra, G.J., Njigh, A.H. and Van Lieshout, R, (1959), Nuclear Spectroscopy Tables (Published by North Holland Publishing Co., Amsterdam).

18. Woods Halley, J.W. and Engelkeimer, D. (1964), Phys. Rev. 134A, 24.

APPENDIX A

Previous Measurements of LI Shell Fluorescence Yields for Z > 73.

Element	Kustner & Arends (1935)	Paschke (1963)	Kinsey (1948)	Roos (1960)	Listengarten (1961)	Akalayev et al. (1964)	Present Results
Ta (73)	.284		.17	.28	.17		
W (74)	.305						
Re (75)			.11		.13		
Os (76)							
Ir (77)	.370		.10				
Pt (78)	.392			.35			
Au (79)	.410		.09	.36			
Hg (80)		.08	.09		.11		
Tl (81)							
Pb (82)	.475			.37			
Bi (83)	.487				.12		
Th (90)					.21		
U (92)					.26		
Np (93)					.28	.19	.12

Previous Measurements of LII Shell Fluorescence Yields for Z > 73.

Element	Kustner & Arends (1935)	Kinsey (1948)	Listengarten (1961)	Jopson et al. (1964)	Salguiero et al. (1961)	Roos (1960)	Haynes & Achor (1955)	Ross et al. (1955)	Present Results	Nall et al. (1960)	Woods Halley et al. (1964)	Paschke (1963)
Ta (73)	.326	.31	.31	.37		.23						
W (74)	.311	.33	.33									
Re (75)												
Os (76)												
Ir (77)	.281	.37										
Pt (78)	.274			.46		.31						
Au (79)	.272	.39		.50		.27						
Hg (80)			.40	.58		.24	.42			.32		.26
Tl (81)		.43		.57								
Pb (82)	.264			.50								
Bi (83)	.255	.46	.46	.51				.32				
Th (90)		.56	.56									
Pa (91)												
U (92)		.59	.54						.508 .496		.422	
Np (93)			.51									
Pu (94)			.48		.413				.444		.422	

Previous Measurements of LIII Shell Fluorescence Yields for Z > 73.

Element	Kustner & Arends (1935)	Stephenson (1937)	Kinsey (1948)	Roos (1960)	Haynes & Achor (1960)	Winkenbach (1958)	Jopson et al. (1964)	Paschke (1963)	Akalayev et al. (1964)	Listengarten (1961)	Present Result	Risch (1958)
Ta (73)	.191		.18	.23			.25			.204		
W (74)	.201									.215		
Re (75)			.20							.224		
Os (76)										.236		
Ir (77)	.244		.23							.252		
Pt (78)	.262			.275			.31			.264		
Au (79)	.276		.25	.32			.31	.24		.275		
Hg (80)					.34		.32			.30		
Tl (81)			.27			.33	.37			.324		
Pb (82)	.337	.32		.35			.35			.348		
Bi (83)	.367		.30				.37			.364		.41
Th (90)		.42	.39							.436		
Pa (91)										.44		
U (92)		.44	.41							.46		
Np (93)									.57	.47	.424	
Pu (94)										.48		

REFERENCES - APPENDIX A

1. Akalayev, G.G., Vartanov, N.A. & Samoilov, P.S. (1964), Isvestiya Akad. Nauk SSSR., Ser. Fiz. 28, 1260).

2. Haynes, S.K. & Achor, W.T. (1955), J. Phys. Rad. 16, 635.

3. Jopson, R.C., Khan, J.N., Mark, H., Swift, C.D. & Williamson, M.A. (1964), Phys. Rev. 133A, 381.

4. Kinsey, B.B. (1948), Can. J. Res. 26A, 404.

5. Küstner, H. & Arends, E. (1935), Ann. Phys. Lpz. 22, 443.

6. Listengarten, M.A. (1961), Isvestiya Akad. Nauk SSSR, Ser. Fiz. 24, 1041.

7. Nall, J.C., Baird, Q.L. & Haynes, S.K. (1960), Phys. Rev. 118, 1278.

8. Paschke, R. (1963), Z. Physik 176, 143.

9. Risch, K. (1958), Z. Physik 150, 87.

10. Roos, C.E. (1960), Quoted by Robinson, B.L. & Fink, R.W., (1960), Rev. Mod. Phys. 32, 117.

11. Ross, M.A.S., Cochran, A.J., Hughes, J. & Feather, N. (1955), Proc. Phys. Soc. 68, 612.

12. Salguiero, L. Ferreira, J.G., Park, J.J.H. & Ross, M.A.S. (1961), Proc. Phys. Soc. 77, 657.

13. Stephenson, R.J. (1937), Phys. Rev. 51, 637.

14. Winkenbach, H. (1958), Z. Physik 152, 387.

15. Woods Halley, J. & Engelkeimer, D. (1964), Phys. Rev. 134A, 24.

APPENDIX B

The Processing of the Ilford G5 Emulsions.

It is important in the use of nuclear emulsions of 200 micron thickness that the plate is developed evenly throughout its depth. The method used to achieve this is known as Temperature Development.

The principle of this method is very simple. It is based on the large difference in the activity of the developer at low and high temperatures. The plate is first immersed in a bath of cold developer (4 - 5°C). In this stage the developer penetrates the emulsion, but there is little or no image formation. The temperature is then raised to 21°C, and the image is formed. The development is finally checked by lowering the temperature, and immersing the plate in a stop bath. After a short period in the stop bath the plate is washed and transferred to the fixing solution. After about 24 hours the fixing is complete, and the fixing bath is slowly diluted. The washing continues until no residual hypo can be detected in a sample of the wash water by the Potassium Permanganate test. (A drop of dilute $KMnO_4$ disappears in a solution containing a trace of hypo).

The sequence of operations which has to be carried out are shown in Table 24.

Table 24

Stage	Procedure	Time
1	Developing solution cooled to 4-5°C.	30 mins.
2	Plate immersed in cold developer	30 mins.
3	Temperature of Developer raised to 21°C	30-35 mins.
4	Plate transferred to the Stop Bath	15 mins.
5	Plate washed and transferred to the Fixing Solution	-
6	Plate immersed in Fixing Solution	24 hrs.
7	Plate washed slowly. Washing continues until no residual Hypo can be detected in a sample of the wash water	-

During stage 4 a brown stain due to an opaque layer of silver forms on the surface of the emulsion. It is best removed by rubbing the surface lightly with a finger. At all stages the plate must be kept horizontal to prevent the emulsion slipping from the glass backing.

The solutions used by the present author to process the 200μ thick G5 emulsions in the experiments described in Chapter 6 were as follows.

Solution A.

Crystalline Sodium Sulphite	25 gms.
(or non-crystalline Sodium Sulphite)	12.5 gms.
Elon (or Metol)	3 gms.
Distilled water to	1000 ccs.

Solution B.

Anhydrous Sodium Carbonate	50 gms.
" " Bicarbonate	50 gms.
Distilled water to	1000 ccs.

Stop Bath

Sodium Bisulphite	5 gms.
Distilled water to	100 ccs.

Fixing Solution

Sodium Thiosulphate	300 gms.
Distilled water to	1000 ccs.

Solution A was prepared immediately before use, and solution B was prepared once a fortnight. These two solutions constitute the developer, and are only added together just before use.

APPENDIX C

The Operation of the Microdensitometer.

In previous experiments with the Curved Crystal Spectrograph the recorded γ- and X-ray spectra were scanned using a Hilger and Watts non-recording microphotometer. Cochran (1955) examined the relationship between the microphotometer readings and the quantity he called 'blackening' of the plate, i.e. the number of developed grains produced on the plate by a given radiation. He assumed; (i) That the number of grains developed in an exposure of time t to radiation of a given energy is proportional to t. (ii) That the light transmitted through the plate is given by $I = I_o e^{-c_2 n}$, where I_o is the transmitted intensity at a clear part of the plate. Cochran was unable to prove that both of these assumptions were correct. But he was able to show that if one of them was correct, then the other was also valid.

In the experiment described in Chapter 6 the Ilford G5 emulsion was microdensitometered using an automatic recording microdensitometer (Model Mk. IIIB), made by Joyce, Loebl and Co. This instrument was designed to record photographic densities linearly using a method of comparison with a standard wedge. If relative intensities were to be measured with the Curved Crystal spectrograph, then it was incumbent upon the present

author to show that the readings recorded on the microdensitometer were linearly related to the intensity of the incident radiation.

As in Cochran's case it was not possible to show that the microdensitometer operated correctly, without also assuming that the photographic density (D) is proportional to the exposure (E). D is defined as $\text{Log}_{10} I_o/I$, where I_o and I are the incident and transmitted intensities of a beam of light falling on the plate. Previous work suggests that D is not proportional to E for Densities greater than 2D.

An emulsion was exposed to a collimated beam of heterogeneous X-rays from an X-ray tube operated at 40 kV. A series of exposures of 3 seconds, 5 seconds, 7½ seconds, 10 secs., and 30 seconds were given. The plate was then developed using the procedure outlined in Appendix B. The plate was microdensitometered, and it was found that the 30 seconds exposure was too dense to give a reading on the instrument, since the upper limit of the instrument available was 1.6D. The Areas under the other four recorded peaks were plotted against the time of exposure to give the graph shown in Figure 36. Within the experimental uncertainties this graph shows a linear relationship between D and the exposure. It must of course be emphasised that this only shows that D is proportional to E provided we assume that the microdensitometer gives a deflection proportional to Photographic Density.

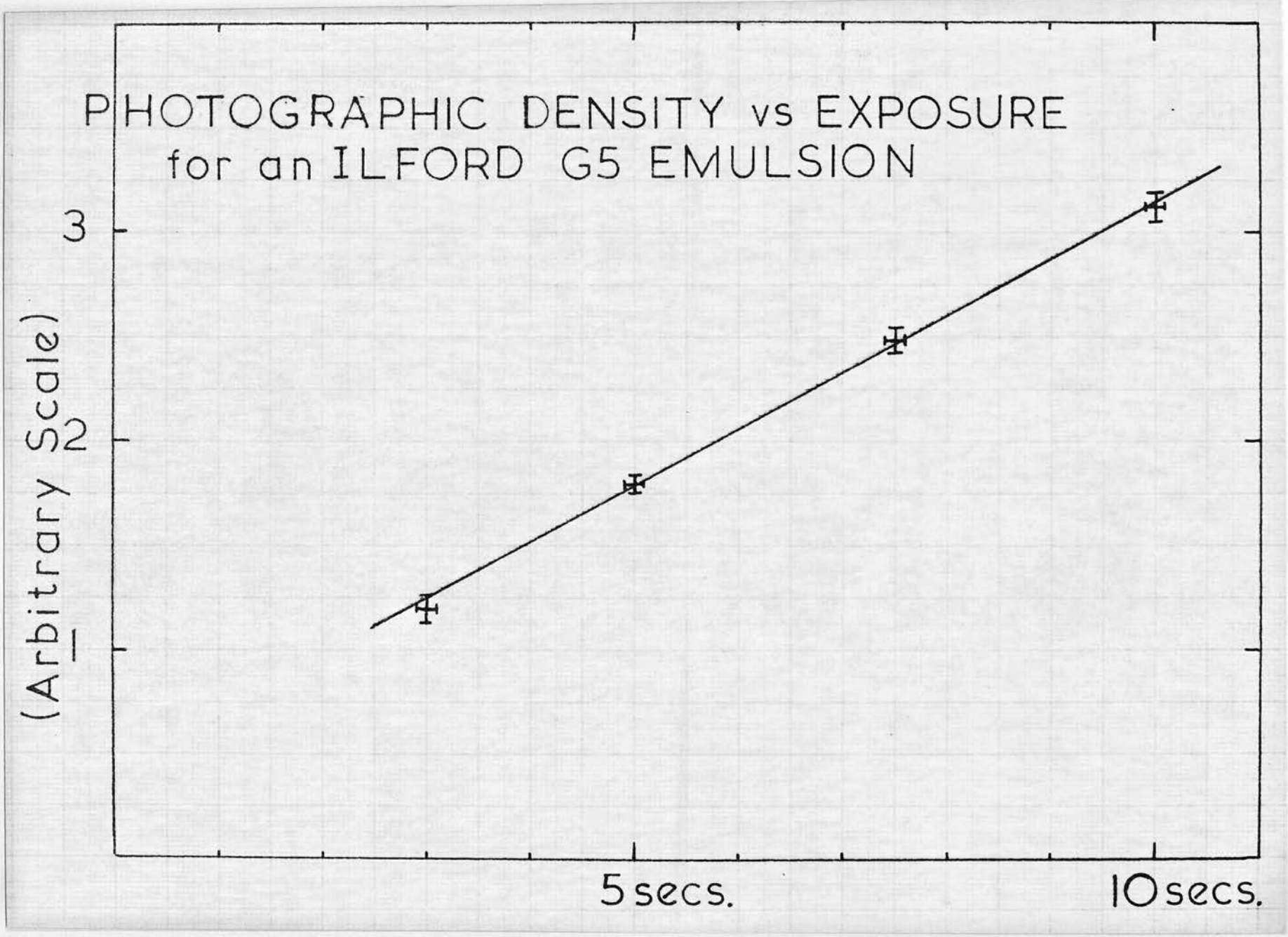
PHOTOGRAPHIC DENSITY vs EXPOSURE
for an ILFORD G5 EMULSION
(Arbitrary Scale)
3
2
5 secs.
10 secs.

FIGURE 36.

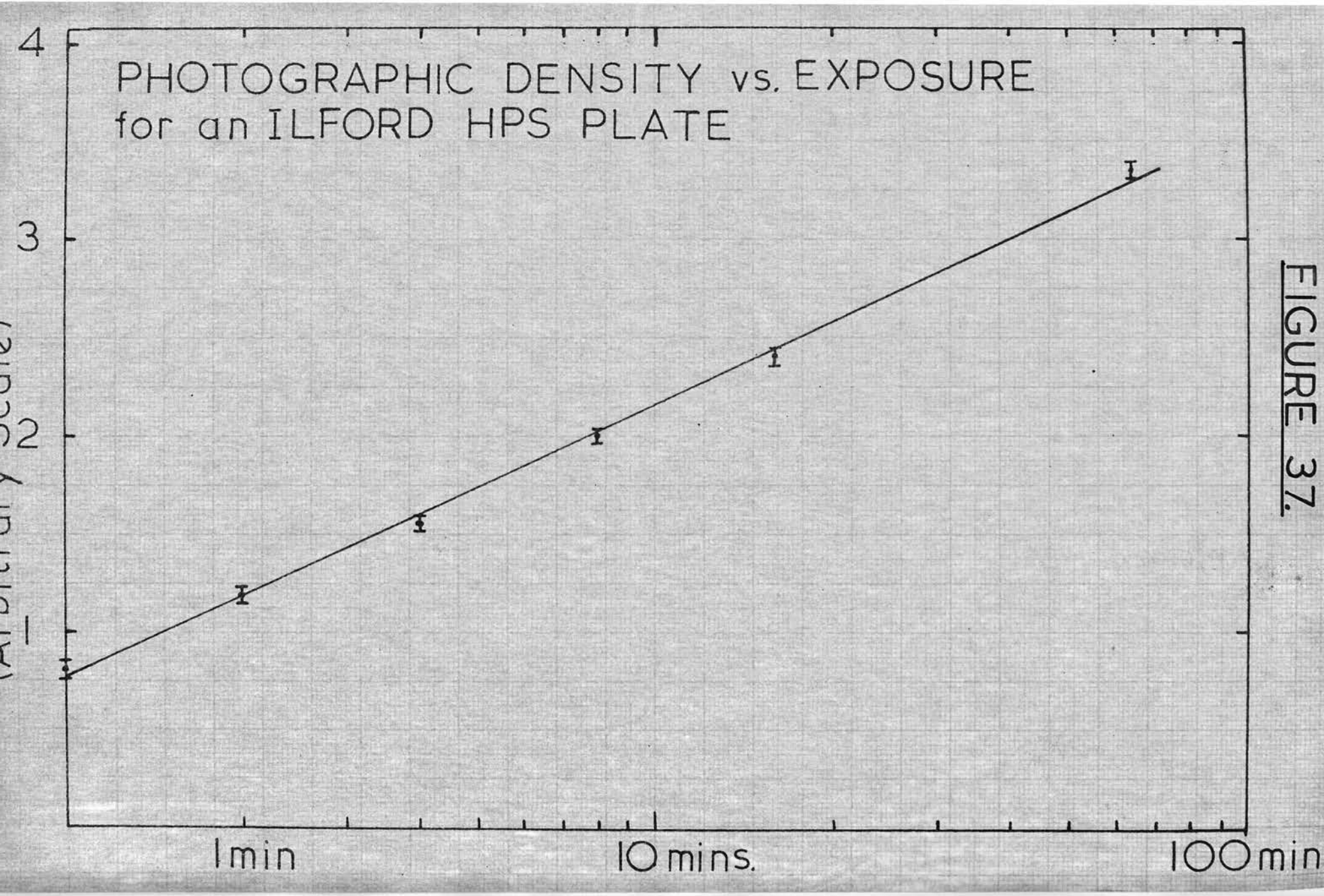
PHOTOGRAPHIC DENSITY vs. EXPOSURE
for an ILFORD HPS PLATE
4
3
2
1
1min
10 mins.
100 min

FIGURE 37.

As a further test of the instrument an Ilford HPS panchromatic photographic plate was exposed to the Cadmium-Mercury line spectrum on a prism spectrograph. A series of exposures of 1 min., 2 mins., 4 mins. 8 mins., 16 mins., and 64 mins., were given. The line at 4047 $\mathring{A}$ wavelength in the Mercury spectrum showed a suitable range of density, and the exposures of this line were microdensitometered. The photographic densities recorded were then graphed against the exposure times. The resulting graph is shown in Figure 37. This graph shows clearly that D is proportional to Log_{10}(Exposure) for the photographic plate. Again it must be pointed out that because the expected relationship between D and E was obtained, it does not prove that the instrument records Densities linearly. It proves only that it records densities linearly provided the Density on the photographic plate is proportional to the logarithm of the Exposure.

ACKNOWLEDGEMENTS

It is my pleasure to thank the many people who have assisted me in the course of the experiments described here.

In particular, I should like to acknowledge the interest and advice given by Professor N. Feather, F.R.S. and by Dr. M.A.S. Ross, who has supervised this research and taken an active interest in it.

Thanks are due to Mr. A. Headridge and the members of the workshop staff for their unfailing assistance.

Thanks are also due to Mr. C. McAnna for his invaluable advice and assistance with electronics.

I am also indebted to Mr. W. Wilson for patiently complying with my many requests for materials and information.

Finally I should like to acknowledge the help and assistance of many of my colleagues in the Department of Natural Philosophy. In particular I should like to thank Dr. J. Byrne and Mr. J. Kyles for many helpful discussions on several aspects of Nuclear and Atomic Physics. I should also like to thank Mr. F Shaikh for his collaboration in the measurements described in Chapter 7, and Mr. K.G. Stewart for his advice on the subject of Microdensitometry.

Appendix D

APPENDIX D

a) A simpler and more effective method of obtaining the total internal conversion coefficient (α_T) of the 59.6 keV transition in Np 237 is as follows.

In the notation of page 119 we may rewrite equation (7.3) in the form

$$\alpha_T = \frac{\text{Population of the 59.6 keV state} - 59.6\,\gamma - 33.0\,\gamma - 33.0e^-}{59.6\,\gamma} \qquad \ldots\ldots\ldots(7.3')$$

The population of the 59.6 keV state is given in the text as 0.9822. The most recent measurement of 59.6 γ is that of Magnusson (1957). His measurements were carefully carried out and we may readily adopt his value of 59.6 γ = 0.359. The 33.2 keV transition has E2-M1 polarity, and in consequence it is very heavily converted. The results given in Table 16 indicate that it occurs in fewer than 0.0025 disintegrations. Accordingly we may neglect 33.0 γ.

From the measurements of Samoilov (1957) we find that the intensity in conversion of the 33.2 keV transition relative to the 59.6 keV conversion intensity is 0.3350. This ratio, together with the expression

$59.6e^-$ = Population of the 59.6 keV state - 59.6 γ - $33.0e^-$,

leads to the value $33.0e^-$ = 0.1558.

On/

On substituting the above values in equation (7.3') we obtain

$$\alpha_T = 1.305$$

b) The measured relative intensities of the Np L X-rays and low energy gamma rays, which are presented in Tables 15 and 16, are in error due to the presence in the recorded spectra of an unknown amount of Molybdenum fluorescent K X-radiation. The collimator (E) of the proportional counter, shown in figure 27, was lined with molybdenum and aluminium. Under direct irradiation by the gamma rays of Np237 the molybdenum K X-rays will be induced, and will be detected in the counter. The energy of the molybdenum K X-rays is approximately 17.5 keV. Hence this radiation will contribute almost entirely to the Np Lβ X-ray group.

c) The ratios $X_1 : X_2 : X_3$ are readily obtained from the measured relative intensities of the L_α, L_β, and L_γ X-ray groups using the equations

$$L_\alpha = aX_3$$
$$L_\beta = (1-a)X_3 + b\,X_2 + c\,X_1$$
$$L_\gamma = (1-b)X_2 + (1-c)X_1$$

where L_α, L_β, and L_γ represent the relative intensities of the Np L X-ray groups, and a is the fraction of photons from the L_{III} shell entering the L_α group, b is the fraction of photons from the L_{II} shell entering the L_β group, and c is the fraction of photons from the L_I shell entering the L_β group. The best available values of the constants a, b, and c, the means of the measurements of Day (1957),/

(1957), Compton and Allison (1935), Jaffe et al (1955), Goldberg (1961), Salguiero et al (1961), Barton et al (1951), and Cochran (1955) are a = 0.782, b = 0.753, and c = 0.682.

d) The measured relative intensities, $L_\alpha : L_\beta : L_\gamma$, which were given in Table 15 are in error due to the presence of an unknown amount of molybdenum fluorescent K X-radiation in the recorded spectra. Hence the values of $X_1 : X_2 : X_3$ derived from these measurements are also in error by an unknown amount. In consequence the L shell fluorescence yields of Neptunium, which were derived using these values of $X_1 : X_2 : X_3$ and were presented in Table 17, are also in error to an unknown extent.